Západočeská Univerzita v Plzni
Fakulta Aplikovaných Věd
Katedra Matematiky

Rough modely frakcionální stochastické volatility

diplomová práce

Plzeň, 2021 Jan Matas

ZÁPADOČESKÁ UNIVERZITA V PLZNI

Fakulta aplikovaných věd

Akademický rok: 2020/2021

ZADÁNÍ DIPLOMOVÉ PRÁCE

(projektu, uměleckého díla, uměleckého výkonu)

Jméno a příjmení:	**Bc. Jan MATAS**
Osobní číslo:	**A20N0010P**
Studijní program:	**N0541A170005 Matematika a finanční studia**
Studijní obor:	**Matematika a finanční studia**
Téma práce:	**Rough modely frakcionální stochastické volatility**
Zadávající katedra:	**Fakulta aplikovaných věd**

Zásady pro vypracování

1. Zpracovat podrobnou rešerši rough modelů frakcionalní stochastické volatility.
2. Popsat matematické vlastnosti těchto modelů a postupů jejich simulace, oceňování a kalibrace.
3. Bude-li to možné, stávající postupy simulace, oceňování a kalibrace vylepšit a nebo navrhnout nové.
4. Implementovat tyto postupy ve vhodném SW.
5. Provést srovnání jednotlivých modelů za použití reálných dat.

Rozsah diplomové práce: **cca 45 stran**
Rozsah grafických prací: **dle potřeby**
Forma zpracování diplomové práce: **tištěná**
Jazyk zpracování: **Angličtina**

Seznam doporučené literatury:

- Bergomi, L. (2016). Stochastic Volatility Modeling. Chapman and Hall/CRC Financial Mathematics Series. Chapman and Hall/CRC, Boca Raton. ISBN 978-1-4822-4407-6.
- Bayer, C., Friz, P., and Gatheral, J. (2016). Pricing under rough volatility. Quant. Finance 16(6), 887904. ISSN 1469-7688. doi: 10.1080/14697688.2015.1099717.
- Gatheral, J., Jaisson, T., and Rosenbaum, M. (2018). Volatility is rough. Quant. Finance 18(6), 933949. ISSN 1469-7688. doi: 10.1080/14697688.2017.1393551.
- McCrickerd, R. and Pakkanen, M. S. (2018). Turbocharging Monte Carlo pricing for the rough Bergomi model. Quant. Finance. ISSN 1469-7688. doi: 10.1080/14697688.2018.1459812.

Vedoucí diplomové práce: **Ing. Jan Pospíšil, Ph.D.**
Katedra matematiky

Datum zadání diplomové práce: **1. října 2020**
Termín odevzdání diplomové práce: **21. května 2021**

L.S.

Doc. Dr. Ing. Vlasta Radová
děkanka

Doc. Ing. Marek Brandner, Ph.D.
děkan

V Plzni dne 1. října 2020

Abstrakt

Rough modely frakcionální stochastické volatility jsou slibně se rozvíjejícím oborem výzkumu v oblasti oceňování finančních derivátů. První část této práce je úvodem do problematiky oceňování opcí a rough modelů frakcionální stochastické volatility. Druhá část se skládá ze dvou článků na téma simulace a robustnosti studovaných modelů.

První článek *On simulation of rough Volterra stochastic volatility models* zkoumá metody simulací zmíněných modelů. Porovnáváme Choleského metodu, hybridní schéma, a rDonsker schéma podle jejich přesnosti a časové náročnosti. Dále uvádíme některé nedostatky metody redukce rozptylu zvané turbocharging a navrhujeme modifikace metody a několik dalších doporučení ohledně simulování zkoumaných modelů pro účely oceňování opcí.

Ve druhém článku *Robustness and sensitivity analyses of rough Volterra stochastic volatility models* se zabýváme citlivostní studovaných modelů na změny v opční struktuře opčních dat. Empeirická studie se skládá z vizuálních a statistických metod pomocí kterých studujeme přítomnost závislostí mezi odhady parametrů, variabilitu a míru chyb modelových cen opcí odhadnutých pomocí kalibrování daného modelu na bootstrapované data sety, které simulují zmíněné změny v opční struktuře dat.

Klíčová slova: rough model frakcionální volatility; rough Bergomi model; Volterra process; kalibrace; Monte Carlo simulace; hybridní schéma

University of West Bohemia in Pilsen
Faculty of Applied Sciences
Department of Mathematics

Rough Fractional Stochastic Volatility Models

master's thesis

Plzeň, 2021 Jan Matas

Declaration

I hereby declare that I am the sole author of this master's thesis and that I have not used any sources other than those listed in the bibliography and identified as references.

Plzeň, June 26, 2021

. . . . . .

Signature

Acknowledgments

I would like to express my sincere gratitude to the supervisor of this thesis, Ing. Jan Pospíšil, Ph.D. I appreciate his scientific guidance, remarks and his patience during my work on the thesis. I learned a lot from our numerous consultations.

I also thank my family for supporting me throughout writing this thesis, during my studies and my life in general. This accomplishment would not have been possible without them.

This thesis was partially supported by the GAČR Grant GA18-16680S *Rough Models of Fractional Stochastic Volatility*.

Computational resources were supplied by the project "e-Infrastruktura CZ" (e-INFRA LM2018140) provided within the program Projects of Large Research, Development and Innovations Infrastructures

Abstract

Rough fractional stochastic volatility models are a progressive and promising field of research in derivative pricing. In the first part of this thesis, we give an introduction to option pricing and we outline the motivation that led to the development of the rough fractional stochastic volatility models. The second part consists of two papers on the simulation and the robustness of these models.

The first paper *On simulation of rough Volterra stochastic volatility models* examines the simulation of the studied models. It compares the Cholesky method, the hybrid scheme, and the rDonsker scheme in terms of accuracy and time efficiency. Then, we show the obstacles of the so-called turbocharging technique of variance reduction used for Monte Carlo simulation pricing. Finally, we suggest a modification of the turbocharging technique and give several recommendations for simulating the models especially when used for pricing options.

In the second paper *Robustness and sensitivity analyses of rough Volterra stochastic volatility models*, we study the sensitivity of the models to the changes in the option data structure. In our empirical study, we use visual as well as statistical methods to analyze patterns, variation, and errors in model prices estimated by calibrating a given model to bootstrapped data sets that simulate the changes in the option structure.

Keywords: rough fractional stochastic volatility; rough Bergomi model; Volterra process; calibration; Monte Carlo simulation; turbocharged Hybrid scheme

Contents

Chapter 1

Introduction

Option pricing is a part of mathematical finance and financial engineering that evolved from the increasing needs of market participants in early 1960s. During that period, financial derivatives were becoming more and more popular for hedging risk of investments. The reason for that was probably the sudden downswing of stock prices in 1962, also known as the Flash Crash. The experience of severe losses fueled the further development of financial products for the sake of insuring portfolios by hedging its risk level.

Hedging the risk of an investment means to assure that the position in an asset, e.g., a stock, is insensitive to the volatility of its spot price, or at least, protected from sudden price drops over a given period of time. The simplest way to insure a position in a stock is to pair each share with put option on that given stock. If we want the position to be immune to, say, more than a 10% drop, we must buy options with the strike of 90% of the current spot price (current market price) of the stock. When the stock price falls more than 10% at the end of the life of the option contracts, we exercise them. The profit from doing so will thus cover the loss from the stock position.

However, financial derivatives are not a recent invention as it might seem. There are signs of contracts, similar to today's financial derivatives, that were in use in the ancient times usually for trading of agricultural products outside the main harvest season [38]. Since then, the growth of national economies and businesses caused popularity of derivatives to increase and hence, the theory of pricing of financial contracts began to shape itself.

The first application of advanced mathematics to a problem in finance is credited to a French mathematician L. Bachelier. In his Ph.D. thesis named *Theory of Speculation* [3], which was published in 1900, he presents a revolutionary idea to model stock price movements by a scaled random walk. Unfortunately, it was not fully appreciated for a long time. Nonetheless, the idea was later revisited, as we will see.

Meanwhile, substantial progress was made in the probability theory and stochastic analysis. For mathematical finance, the development of the mathematical description of the Brownian motion, in which, among others, A. Einstein and N. Wiener participated, proved to of great importance. Another important milestone was the formulation of

the basis of stochastic calculus, pioneered by a Japanese mathematician K. Itô. This laid the foundations for modern mathematical finance.
Surprisingly, the mentioned idea of L. Bachelier was revisited as late as in early 1970s by P. Samuelson [39]. For the model of random stock price moves, the formerly proposed scaled random walk was replaced by its limit case – the Brownian motion which was at that time already a anchored by a solid theory. The model of a stock price evolution is the geometric Brownian motion that we can express as an stochastic differential equation of the form

$$\mathrm{d}S_t = \mu S_t \mathrm{d}t + \sigma S_t \mathrm{d}W_t, \tag{1.1}$$

where S_0 it the initial value of the process S_t, coefficients μ and σ are called drift and diffusion (or volatility term) respectively, and W_t is the Brownian motion. While the drift conveys the trend of a stock price over time, the diffusion affects the amplitude of noise around the trend.
The breakthrough was made by Black, Scholes, and Merton [10, 34] in 1973, when they introduced a model that is now referred to as the *Black-Scholes* or the *Black-Scholes-Merton* (BSM) model that, among other, assumes a constant volatility in (1.1). The big advantage of the model was, and still is, that we know its analytic solution and hence, the price of a derivative and its sensitivity to the model parameters (Greeks) can be computed immediately via a closed-form solution formulas. In fact, the BSM model sets the entire framework for derivative pricing.
Nonetheless, the BSM model has also drawbacks. Relative simplicity and elegance are bought out by many assumptions that simplifies the reality too much. One of the most criticized one has been the assumption of constant volatility. We explain this issue further in Subsection 2.6.1. As a potential solution to that issue, non-constant volatility was suggested. Apparent expansion is to take a deterministic function of time instead of a constant, i.e., $\sigma = \sigma(t)$. However, it is usually a difficult task to find a suitable formula for $\sigma(t)$. A more fruitful improvement was suggested by Dupire [17] in 1994. His idea was to replace constant volatility by a function of time and the underlying stock price, $\sigma = \sigma(t, S_t)$. Models including such a volatility function are today referred to as *local volatility* models. Those models can be quickly calibrated to an exact fit to market data; however, such models sometimes tend to suffer from overfitting and the resulting surface of a fitted model may not be arbitrage-free. Nonetheless, the class of local volatility models became a premonition for stochastic volatility models.
The idea of *stochastic volatility* models is to consider the volatility of the underlying stock to be modeled by another stochastic process, i.e., $\sigma = \sigma(t, \omega) = \sigma_t$. This approach was originally proposed by Hull and White [27] in 1987. They used the SDE (1.1) as a stock price model but added another SDE to model the volatility of the stock. Later, in 1993, Heston in [24] introduced a semi-closed-form solution formula for a model where volatility is modeled by a stochastic process with mean reversion. His main idea was to reduce the model partial differential equation into ordinary differential equation by the Fourier transform, solve it, and then transform it back by the inverse Fourier transform. However, the obtained formula cannot be expressed only using elementary functions

hence such results are usually referred to as semi-closed solution formulas. Heston's approach was then further generalized by adding a jump-diffusion dynamic by Bates [4] in 1996 and letting the parameters depend on time [35], [19].
Although many SV models have been proposed so far, none of them can be considered as the ultimately best one. On different datasets, different models may appear better than others. Moreover, there are still more or less serious inaccuracies of those models describing the reality. For example, [16] and [1] listed empirical observations of volatility that are sometimes called the *stylized facts* about volatility. A particularly important stylized facts is the long memory property. Based on that, Comte and Renault [14] in 1998 pioneered the fractional stochastic volatility (FSV) model where the volatility process is driven by the fractional Brownian motion with the Hurst parameter $H > 1/2$, assuming it possesses long memory. This idea was further studied in [13].
However, in 2014, Gatheral, Jaisson, and Rosenbaum published a pre-print[1] paper named Volatility is Rough [21] that argues that volatility does not possess long memory. This claim is based on the estimation of the Hurst parameter from several financial time-series by a new methodology proposed in the paper. The main result was that $H \approx 0.14$ was estimated for major stock indexes (similar results of $H \in [0.05, 0.25]$ were obtained for more than 2000 equities in [6]). Based on that, they proposed a new model named rough FSV (RFSV), which is a modification of FSV when $H < 1/2$, and later, Bayer, Friz, and Gatheral [5] introduced rough Bergomi (rBergomi) model – a generalization of the Bergomi model [8]. In Subsection 2.6.2, we will introduce the αRFSV model that unifies the two models as Merino et al. suggested in [32].

[1] officially published as [22] in 2018.

Chapter 2

Path to rough fractional stochastic volatility models

This chapter aims to give an introduction to option pricing and outline the motivation and historical development that led to formulation of the rough fractional stochastic volatility models.

2.1 Introduction to options

An *option* is a financial derivative. It means that it is a contract between two parties whose value depends on an underlying asset or an underlying instrument. The owner of an option holds the right, but not the obligation, to buy or sell the underlying asset at a specified strike price K prior to or on a specified date T. There are many types of options that can be classified into two groups: vanilla options and exotic options. Vanilla options are the most basic European and American, put and call options, usually traded at exchanges as standardized contracts. On the other hand, exotic options are complex instruments tailored to the specific needs of a buyer and they are traded solely over-the-counter.
We will focus only on *European options*, and more precisely, on European options whose underlying asset is a stock that does not pay a dividend. We do so because this type of option is the easiest to price and therefore, it is usually used as the first step to build a model. Then, the model can be further expanded to cover a stock paying a dividend, to price an American option, etc.
The difference between a European and an American option is that a European option can be exercised only at its maturity T, as opposed to an American option that can be exercised at any time prior to and including the date T. Because an American option possesses an additional feature its value is considered bigger than in case of a European option.
The holder's payoff of a European call option, i.e., an option providing the right to buy, at T is given by $(S_T - K)^+ = \max(S_T - K, 0)$, where S_T is the price of the underlying

stock at time T. That means that if the stock price at time T is greater than the strike K, the holder exercises the option with a profit of $S_T - K$ and if the stock price is equal to or less than the strike, the holder does not exercise the option and their profit is 0. The payoff of a European put option, i.e., an option with the right to sell, is $(K - S_T)^+$.
The price of a European option at time t can be broken down into two components. The first one is the option's *intrinsic value* at time t which is simply the corresponding payoff at time t that we described in the previous paragraph. If the payoff is positive, we say that the option is *in-the-money* (ITM). If the strike equals to the spot price of the stock, we say the option is *at-the-money* (ATM), and finally, when the payoff of the option is zero and the option is not ATM, we say the option is *out-of-the-money* (OTM). The second component of the price of an option is the so-called *time value*. It is, in fact, the difference between the market price and the intrinsic value. Hence, we can think of the time value as the amount which an investor is willing to pay above the intrinsic value (or how much he discounts the price, if the time value is negative). Therefore, the time value reflects investors' believe of the future movements of the underlying stock. However, as less time is left to expiration, uncertainty of the final payoff of the option is decreasing and thus the time value converges to zero.
To determine the price of an option, so-called *arbitrage-free argument* is widely used. The idea is that an arbitrage opportunity cannot be expected to be found in a liquid financial market. An *arbitrage* is a trading strategy such that one starts with zero capital and at some point later in time, there is certainty that no money is lost and positive probability of profit. There are several types of an arbitrage but all of them exploits combinations of long and short positions. Being in a long position (being long) on an asset means buying and holding an asset. Conversely, being in a short position (being short) means that the speculator borrows an asset and sells it. After some time, they buys the asset back and returns it to the lender while they retains the difference between the selling and buying price.
One simple example of an arbitrage is a geographical arbitrage. Having two similar markets with difference spot (current market) prices for the same asset, one can buy the asset at the under-priced market and sell it at the over-priced market at the same time. The result is making money with (theoretically) no capital and no risk. In option markets, different types of arbitrages can occur. Two examples are a calendar arbitrage and a butterfly arbitrage. The former one is an options arbitrage strategy that takes advantage of discrepancies in extrinsic values across two identical options that differ only in their maturities. A butterfly arbitrage is similar but instead of exploiting mispricing in maturities it operates with two identical options that vary only in the strike price. More about option arbitrages can be find in [20].
Having a call and a put option with strike K and maturity T, both on the same stock S, which does not pay a dividend, and provided that we know the price of one of them, we can calculate the price of the second one. This relation is called the *put-call parity* and it states that

$$C_t - P_t = S_t - K \cdot \mathrm{e}^{-r(T-t)},$$

where C_t, P_t represent the prices of call and put options respectively, S_t denotes the

stock price at time t, and r is the risk-free interest rate.
Now, when we understand the basics of European call and put options on a stock, and as we previously stated that those are of our main concern in this thesis, we refer to them simply as call and put options. Moreover, it should be clear now, that its prices depend on the price of the underlying stock, which is however very difficult to predict. In fact, we are going to treat it as random and we are going to model its evolution by a stochastic process. Therefore, in the following section, we are going to set up the necessary theoretic probability background. Nonetheless, we introduce only the most important terms for us and we do not aim to be exhaustive as it would exceed the scope of this thesis. For more detailed overview, we recommend [40] or [11].

2.2 Probability background

Let the triplet $(\Omega, \mathcal{F}, \mathbb{P})$ be a *complete probability space*, where Ω is a sample space, i.e., the set of all possible outcomes, $\mathcal{F}$ is a σ-algebra that represents the set of events, and $\mathbb{P}$ is a probability measure. A probability space is complete, if for all sets $B \in \mathcal{F}$ with $\mathbb{P}(B) = 0$ and for every $A \subset B$ holds that $A \in \mathcal{F}$.
If a set $A \in \mathcal{F}$ satisfies $\mathcal{P}(A) = 1$, we say that the event A occurs *almost surely* (a.s.). Moreover, the Borel σ-algebra on $\mathbb{R}$, denoted by $\mathcal{B}$, is the σ-algebra generated by the collection of all open intervals in $\mathbb{R}$ thus containing all the intervals.

Definition 1. A real-valued *random variable* X on Ω is a mapping $X : \Omega \to \mathbb{R}$ such that

$$X^{-1}(A) = \{X \in A\} = \{\omega \in \Omega : X(\omega) \in A\}$$

is an even in $\mathcal{F}$ for every $A \in \mathcal{B}$.

It means, that a random variable is a function that assigns a union of intervals to an event from σ-algebra $\mathcal{F}$. Equivalently, we say that X is *$\mathcal{F}$-measurable*. Thus, we can operate with real intervals (Borel sets), instead of operating with actual events of $\mathcal{F}$ which can be arbitrary objects. Then, the probability distribution of X is the probability measure μ_X that assigns to each Borel set B the mass $\mu_X(B) = \mathbb{P}\{X \in B\}$. Nevertheless, we usually write simply $\mathbb{P}(X \in B)$.
Now, we define the expected value, conditional expected value, and the variance of a random variable.

Definition 2. Let X be a random variable. The *expected value* (or expectation) of $X = X(\omega)$ is defined as the following Lebesgue integral

$$\mathbb{E}[X] = \int_\Omega X(\omega) \mathrm{d}\mathbb{P}(\omega),$$

whenever the integral exists.

Definition 3. Let $\mathcal{G} \subset \mathcal{F}$ be a σ-algebra, and let X be a random variable. The *conditional expectation* of X given $\mathcal{G}$, denoted $\mathbb{E}[X|\mathcal{G}]$, is any random variable that is $\mathcal{G}$-measurable and satisfies

$$\int_A \mathbb{E}[X|\mathcal{G}](\omega)\mathrm{d}\mathbb{P}(\omega) = \int_A X(\omega)\mathrm{d}\mathbb{P}(\omega) \quad \text{for all } A \in \mathcal{G},$$

whenever the integral exists.

Definition 4. Let X be a random variable whose expected value is defined. The *variance* of X is defined as

$$\mathrm{Var}[X] = \mathbb{E}\left[(X - \mathbb{E}X)^2\right].$$

Because $(X - \mathbb{E}X)^2$ is non-negative, $\mathrm{Var}[X]$ is always defined, although it may be infinite. The *standard deviation* of X is $\sqrt{\mathrm{Var}[X]}$.
In the following part, we define a stochastic process and associated terms, necessary for the theory of option pricing.

Definition 5. A *filtration* $\{\mathcal{F}_t, t \geq 0\}$ is a collection of σ-algebras in $\mathcal{F}$ such that if $s \leq t$, then $\mathcal{F}_s \subseteq \mathcal{F}_t$).

A filtration contains the information whether an $E \in \mathcal{F}$ has already happened at time t. In financial modeling, we can think of a filtration as a model of flow of public information.

Definition 6. A *stochastic process* (also random process) on $(\Omega, \mathcal{F}, \mathcal{P})$ is an indexed collection of random variables $\{X_t, t \in \mathbb{T}\}$.

If the set of indexes is discrete, e.g., $\mathbb{T} = \mathbb{N}$, the process X_t is called *discrete-time* and analogically, if it the set is continuous, e.g.,$\mathbb{T} = \mathbb{R}$, we call X_t a *continuous-time* process. We will be concerned mainly with the latter case, when $\mathbb{T} = [0, \inf)$. Additionally, as random variables X_t are, in fact, functions of $\omega \in \Omega$, we can understand a stochastic process as a function of two variables, i.e., $X_t = X(\omega, t)$. If we fix a specific value of t, we obtain a single random variable. Otherwise, if we fix a particular ω, we obtain a deterministic function of t, which we call a *sample path* or a *trajectory*.
Moreover, we will be interested only in processes that cannot "look into the future" as such property is natural for applications in finance. The following definition formalizes the idea.

Definition 7. Let $\mathcal{F}_t$ be a filtration of $\mathcal{F}$. We say that a stochastic process X_t is *adapted* to the filtration $\mathcal{F}_t$ if X_t is $\mathcal{F}_t$-measurable.

If a process X_t is adapted to the $\mathcal{F}_t$, it cannot reveal more information at time t than the σ-algebra $\mathcal{F}_t$ allows.
Now, we introduce martingales and Markov processes, fundamental types of processes for option pricing modeling. For the following definitions, let $\mathcal{F}_t$ be a filtration of $\mathcal{F}$ and consider a process adapted to $\mathcal{F}_t$ as adapted.

Definition 8. We say that an adapted stochastic process $\{M_t, 0 \leq t < \infty\}$ is a

- *martingale*, if $\mathbb{E}[M_t|\mathcal{F}_s] = M_s$ holds a.s. for all $0 \leq s \leq t < \infty$,
- *sub-martingale*, if $\mathbb{E}[M_t|\mathcal{F}_s] \geq M_s$ holds a.s. for all $0 \leq s \leq t < \infty$,
- *super-martingale*, if $\mathbb{E}[M_t|\mathcal{F}_s] \leq M_s$ holds a.s. for all $0 \leq s \leq t < \infty$.

We can think of a martingale process as a model of a fair game (coin flip). No matter how genius our betting and stopping strategies are, the expectation of the game is still constant (as long as we cannot look into the future, i.e., as long as the process is adapted). In case of a sub or super-martingale, there is a tendency to fall or rise respectively. A more general group of processes are called semi-martingales that we define soon after introducing necessary terms.

Definition 9. A *stopping time* τ with respect to the filtration $\mathcal{F}_t$ is a random variable taking values from $[0, \infty)$ or inf and satisfying

$$\{\tau \leq t\} \in \mathcal{F}_t \text{ for all } t \geq 0.$$

The definition above says that a positive real random variable can be considered a stopping time if the decision to stop is based on the information available at time t contained in the filtration $\mathcal{F}_t$.

Definition 10. Let τ be a stopping time w.r.t. $\mathcal{F}_t$ and let $\{X_t, t \geq 0\}$ be a stochastic process. Then a *stopped process* $\{X_t^\tau, t \geq 0\}$ is defined by

$$X_t^\tau = X_{\min\{t,\tau\}} = \begin{cases} X_t, & t < \tau, \\ X_\tau, & t \geq \tau. \end{cases} \tag{2.1}$$

Simply put, a stopped process X_t^τ is equivalent to the process X_t until the time τ. For $t \geq \tau$, the stopped process remains constant with the value of X_τ.

Definition 11. An adapted stochastic process $\{L_t, 0 \leq t < \infty\}$ is called a *local martingale* if there exists a sequence of stopping times $\{\tau_n\}_{n=1}^\infty$ such that

- $\{\tau_n\}$ is an increasing sequence a.s.: $\mathbb{P}(\tau_k < \tau_{k+1}) = 1$,
- $\{\tau_n\}$ diverges a.s.: $\mathbb{P}\left(\lim_{n\to\infty} \tau_n = \infty\right) = 1$,
- the stopped process $\{L_t^{\tau_n}, 0 \leq t < \infty\}$ is a martingale for every $n \in \mathbb{N}$.

Definition 12. A stochastic process $\{X_t, t \geq 0\}$ is said to be *continuous a.s.* at t_0 if

$$\mathbb{P}\left(\left\{\omega \in \Omega : \lim_{t\to t_0} |X_t(\omega) - X_{t_0}(\omega)| = 0\right\}\right) = 1. \tag{2.2}$$

Additionally, we say that the process X_t is *right-continuous a.s.* at t_0, resp. *left-continuous a.s.* at t_0, if the limit in (2.2) is right-sided, resp. left-sided.

Definition 13. Suppose that $\{X_t, t \geq 0\}$ is a stochastic process. The *total variation* of the process X on interval $[a, b] \subset [0, \infty)$ is the random variable $V_a^b(X)$, defined as

$$V_a^b(X) = \lim_{\|\mathcal{P}\| \to 0} \sum_{k=1}^{n} \left| X_{t_k} - X_{t_{k-1}} \right|,$$

where $\mathcal{P} = \{t_0, t_1, \ldots, t_n\}$, such that $a = t_0 < t_1 < \ldots < t_n = b$, is a partition of the interval $[a, b]$ whose norm is defined as $\|\mathcal{P}\| = \sup_{i=1,\ldots,n} \{t_i - t_{i-1}\}$.

Definition 14. We say that a process $\{X_t, t \geq 0\}$ has *bounded variation* on interval $[a, b] \subset [0, \infty)$, if there exists a finite number $M > 0$ such that $V_a^b(X) < M$.

Definition 15. We say that an adapted stochastic process $\{X_t, 0 \leq t < \infty\}$ is a *semi-martingale* if it can be decomposed as

$$X_t = L_t + A_t,$$

where $\{L_t, 0 \leq t < \infty\}$ is a local martingale on $\mathcal{F}_t$ and A_t is a càdlàg[1] process, adapted to $\mathcal{F}_t$, that has locally bounded variation.

Remark 16. Every càdlàg martingale, super-martingale, and sub-martingale is a semi-martingale.

Martingales are the crucial objects for option pricing. Based on the theory of risk-neutral pricing, which operates with martingales, a powerful pricing formula (2.17) can be derived. We briefly discuss the whole framework in Section 2.6.
Another important property of a stochastic process is the Markovian property.

Definition 17. Let $\{X_t, 0 \leq t < \infty\}$ be an adapted stochastic process. Suppose that for all $0 \leq s \leq t < \infty$ and for every non-negative, Borel-measurable function f, there exists another Borel-measurable function g such that

$$\mathbb{E}[f(X_t)|\mathcal{F}_s] = g(X_s). \tag{2.3}$$

Then, we say that the process X_t is a *Markov process*. We also refer to Equation (2.3) as the *Markovian property*.

The future value of a Markov process (and thus also its expectation) depends only on the present value and not on the past values. The reason, why the Markovian property is important in option pricing is stated in the following Remark which we borrow from Shreve [40, Corollary 6.3.2].

Remark 18. Solution to stochastic differential equations are Markov processes.

In the following sections we introduce the Brownian motion as an example of a stochastic process used in finance modeling and we summarize the main results of stochastic calculus. We then define the fractional Brownian motion and employ all the previous theory in the section Models 2.6.

[1] from French: "continue à droite, limite à gauche" meaning right continuous with left limits.

2.3 Brownian motion

The Brownian motion (Bm), sometimes also refer to as the Wiener process, is the fundamental object in stochastic analysis. It is named after R. Brown who observed an irregular motion of pollen particles suspended in water in 1827. Later, L. Bachelier discovered that the Bm is the limit object of discrete random walk in his thesis [3] named *The Theory of Speculation* which was likely the first attempt to apply advanced mathematics to a problem in finance. Also, Albert Einstein contributed to the mathematical description of the Bm by his paper [18] published in 1905. Ultimately, a rigorous mathematical description of the Brownian motion was formulated by Norbert Wiener in his later papers, e.g., [41]. This is why the Bm is also called the Wiener process. His work was further expanded and simplified by other mathematicians including Kolmogorov and Lévy. Now, the Bm is widely used in modeling of physical phenomena, in engineering, and in mathematical finance.

Definition 19. The *Brownian motion* $\{W_t, t \geq 0\}$ is a real-valued stochastic process adapted to the filtration $\mathcal{F}_t$ that has stationary independent Gaussian increments and whose trajectories are continuous a.s. In other words,

- $B_0 = 0$ a.s.,
- $W_t(\omega)$ is continuous a.s.,
- For $s \leq t$, the increment $W_t - W_s$ follows the normal distribution $N(0, t-s)$ and it is independent of $\mathcal{F}_s$.

Remark 20. The Brownian motion is a martingale and it is a Markov process.

To show that the Brownian motion is a martingale, we only need to exploit the zero mean property of its increments.

$$\mathbb{E}[W_t|\mathcal{F}_s] = \mathbb{E}[W_t - W_s + W_s|\mathcal{F}_s] = \mathbb{E}[W_t - W_s|\mathcal{F}_s] + \mathbb{E}[W_s|\mathcal{F}_s] = W_s.$$

The proof of Markovianity of the Bm is more complicated. See, for example, [40, Theorem 3.5.1].
In finance, the Brownian motion is used, for example, in a model of the evolution of a stock price. It can be used to drive processes to model volatility as well. However, we will later introduce models that use fractional Brownian motion to model volatility.

2.4 Introduction to stochastic calculus

In this section, we introduce the stochastic calculus (also known as the Itô's calculus), the analogy of the standard calculus that operates with stochastic processes. The theory was pioneered by K. Itô during 1950's and 1960' by defining the stochastic integral and introducing the identity to find the differential of a time-dependent function of a

stochastic process. This later led to the prolific field of stochastic differential equations (SDEs) and its application in finance.
The stochastic integral is usually defined in two steps: first for simple processes and then the definition is extended for non-simple processes. Let $\mathcal{P} = \{t_0, t_1, \ldots, t_n\}$ where $0 = t_0 \leq t_1 \leq \ldots \leq t_n = T$ be a *partition* of interval $[0, T]$. A process $\{\Delta_t, 0 \leq t \leq T\}$ is called a *simple process*, if it is constant in t on each sub-interval $[t_j, t_{j+1})$. For a simple process Δ_t and $t_k \leq t \leq t_{k+1}$, the stochastic integral I_t is defined by

$$I_t = \int_0^t \Delta_s \mathrm{d}W_s = \sum_{j=0}^{k-1} \Delta_{t_j}(W_{t_{j+1}} - W_{t_j}) + \Delta_{t_k}(W_t - W_{t_k}).$$

In the second step, we generalize the stochastic integral I_T for processes that are allowed to vary continuously and also to jump.

Definition 21. Let $\{W_t, 0 \leq t \leq T\}$ be the Brownian motion adapted to the filtration $\mathcal{F}_t$ and let $\{\Delta_t, 0 \leq t \leq T\}$ be an $\mathcal{F}_t$-adapted càdlàg stochastic process, which is continuous a.s. such that

$$\mathbb{E}\left[\int_0^T \Delta_t^2 \mathrm{d}t\right] < \infty. \tag{2.4}$$

Next, let $\mathcal{P} = \{t_0, t_1, \ldots, t_n\}$ where $0 = t_0 < t_1 < \ldots < t_n = T$ be a partition of the interval $[0, T]$. The *stochastic integral* (or the *Itô's integral*) of the process Δ_t is defined by the formula

$$I_t = \int_0^t \Delta_s \mathrm{d}W_s = \lim_{n\to\infty} \int_0^t \Delta_s^n \mathrm{d}W_s, \quad 0 \leq t \leq T, \tag{2.5}$$

where $\{\Delta^n\}_{n=1}^{\infty}$ is a sequence of simple processes that converge to Δ. In this case, we understand convergence as

$$\lim_{n\to\infty} \mathbb{E}\left[\int_0^T |\Delta_t^n - \Delta_t|^2 \, \mathrm{d}t\right] = 0.$$

Now, we define a stochastic differential equation (SDE) and an Itô process.

Definition 22. Let $\mathcal{F}_t$ be the filtration that is generated by the Brownian motion W_t, let T be a positive constant, let $\mu : \mathbb{R} \times [0, T] \to \mathbb{R}$ and $\sigma : \mathbb{R} \times [0, T] \to \mathbb{R}$ be measurable functions, and let X_0 be an $\mathcal{F}_0$-measurable random variable. A *stochastic differential equation* is then defined by

$$\mathrm{d}X_t = \mu(X_t, t)\mathrm{d}t + \sigma(X_t, t)\mathrm{d}W_t, \quad t \in [0, T], \tag{2.6}$$

which with an initial condition

$$X_0 = x_0 \in \mathbb{R} \tag{2.7}$$

forms am initial value problem.
Moreover, if $\int_0^T \mu(X_t, t)\mathrm{d}t < \infty$ and $\int_0^T \sigma^2(X_t, t)\mathrm{d}t < \infty$ then a continuous $\mathcal{F}_t$-adapted process X_t satisfying

$$X_t = x_0 + \int_0^t \mu(X_s, s)\mathrm{d}s + \int_0^t \sigma_s \mathrm{d}W_s, \quad t \in [0, T], \tag{2.8}$$

is said to be a (strong) solution to SDE (2.6) with condition (2.7).

A process X_t written as (2.8) is called an *Itô process* (in differential form is given by (2.6)). It is worth to note that the first integral on the right-hand side of (2.8) is the Lebesgue integral and the second one is the stochastic integral.
Having the stochastic integral and SDE defined, we now formulate another analogy to the standard calculus – a chain rule for stochastic differentials that is referred to as *Itô 's formula*. By $\mathcal{C}^{1,2}([0,T)\times\mathbb{R})$, we denote the space of function whose first time derivative and second space derivatives are continuous on $[0,T]\times\mathbb{R}$.

Theorem 23. *Let $V \in \mathcal{C}^{1,2}([0,T)\times\mathbb{R})$ and let $\{X_t, 0 \le t \le T\}$ be an Itô process. Then the process $Y_t = V(t, X_t)$ has a stochastic differential*

$$\mathrm{d}Y_t = \frac{\partial V}{\partial t}(t, X_t)\mathrm{d}t + \frac{\partial V}{\partial x}(t, X_t)\mathrm{d}X_t + \frac{1}{2}\frac{\partial^2 V}{\partial x^2}(t, X_t)(\mathrm{d}X_t)^2 \tag{2.9}$$

The proof of Theorem 23 can be found for example in [28].
Itô's formula is an useful tool of the stochastic calculus. To be able to carry out calculations, we also remind a few practical heuristics to manipulate with stochastic differentials. The well-known rules are:

$$\begin{aligned} \mathrm{d}t \cdot \mathrm{d}t = \mathrm{d}t \cdot \mathrm{d}W_t = 0, \\ \mathrm{d}W_t \cdot \mathrm{d}W_t = \mathrm{d}t. \end{aligned} \tag{2.10}$$

In the following example, we see how the Itô 's formula together with the heuristics above can be used to solve an SDE.

Example 24. Consider a stock with spot price $S_0 > 0$, whose price is modeled by the SDE in the form

$$\mathrm{d}S_t = \mu S_t \mathrm{d}t + \sigma S_t \mathrm{d}W_t, \quad t \ge 0, \tag{2.11}$$

where $\mu \in \mathbb{R}$ is called the *drift* that conveys the trend of the stock price evolution, and $\sigma > 0$ is called the *diffusion* that models the noise around the trend.
Taking the substitution $Y_t = \log(S_t)$, we can us the Itô's formula to find the differential of Y_t. In this case, $V(t,x) = V(x) = \log(x)$. Then, we have

$$\mathrm{d}Y_t = \mathrm{d}(\log S_t) = 0 \cdot dt + \frac{1}{S_t}\mathrm{d}S_t - \frac{1}{2}\frac{1}{S_t^2}(\mathrm{d}S_t)^2.$$

Substituting the differential $\mathrm{d}S_t$ from (2.11), we get

$$\mathrm{d}(\log S_t) = \frac{\mu dt + \sigma S_t \mathrm{d}W_t}{S_t} - \frac{(\mu S_t \mathrm{d}t + \sigma S_t \mathrm{d}W_t)^2}{2S_t^2}.$$

Expanding the quadratic expression and using the rules (2.10) results in

$$\mathrm{d}(\log S_t) = \mu \mathrm{d}t + \sigma \mathrm{d}W_t - \frac{1}{2}\sigma^2 \mathrm{d}t.$$

Now, we integrate both sides:

$$\int_0^t \mathrm{d}(\log S_u)\mathrm{d}u = \int_0^t \mu \mathrm{d}u + \int_0^t \sigma \mathrm{d}W_u - \int_0^t \frac{1}{2}\sigma^2 \mathrm{d}u$$

which results in

$$\log S_t - \log S_0 = \mu t + \sigma \mathrm{d}W_t - \frac{1}{2}\sigma^2 t.$$

After simplification, we can express the solution as

$$S_t = S_0 \exp\left\{\left(\mu - \frac{1}{2}\sigma^2\right)t + \sigma W_t\right\}, \quad t \geq 0. \tag{2.12}$$

We refer to the resulting process (2.12) as the *geometric Brownian motion* and we will encounter it again in Section 2.6.

2.5 Fractional Brownian motion

The fractional Brownian motion (fBm) is a generalization of the Brownian motion (Bm) that has an extra parameter which affects the autocovariance of the process. Therefore, its increments need not to be independent, as opposed to the Bm. The fractional Brownian motion was first introduced by Kolmogorov [29] in 1940. It is defined as follows:

Definition 25. The *fractional Brownian motion* with the *Hurst parameter* $H \in (0,1)$ is a Gaussian process $B_t^H = \{B_t^H, t \geq 0\}$ adapted to the filtration $\mathcal{F}_t$ such that the following properties are satisfied:

- $B_0^H = 0$,
- $\mathbb{E}[B_t^H] = 0, \quad t \geq 0$,
- $\mathrm{Cov}(B_t^H, B_s^H) = \mathbb{E}\left[B_t^H B_s^H\right] = \frac{1}{2}(t^{2H} + s^{2H} - |t-s|^{2H}), \quad s,t \geq 0.$

Notice that when $H = 0.5$, we obtain the standard Brownian motion. The choice of the Hurst parameter H other than 0.5 affects the correlation of the process and therefore "roughness" of its trajectories. For $H > 0.5$, increments are positively correlated and it is said, that the process has long memory. In this case, its trajectories are smoother than those of the Bm. In contrast, for $H < 0.5$, the increments of the fBm are negatively correlated and thus the fBm has rougher trajectories. Figure 2.1 shows fBm trajectories for different values of H.
There are other properties of the fBm that can be derived from its definition. For example, we can see that the variance equals t^{2H} by computing $\mathrm{Var}[B_t^H] = \mathrm{Cov}[B_t^H, B_t^H] = t^{2H}$. Next, consider the increment between times s and t, such that $t \geq s$. Let us denote it $Y = B_t^H - B_s^H$. Then, we see that Y is stationary as $\mathbb{E}[Y] = \mathbb{E}[B_t^H] - \mathbb{E}[B_s^H] = 0$ and

$\mathrm{Var}[Y] = \mathrm{Var}[B_t^H] + \mathrm{Var}[B_s^H] - 2\mathrm{Cov}[B_t^H, B_s^H] = |t-s|^{2H}$. It can also be shown that fBm trajectories are continuous a.s. and the process is self-similar for an arbitrary constant $\alpha > 0$. It means that the scaled fBm $\{\alpha^{-H} B_{\alpha t}^H, t \geq 0\}$ has the same probability distribution as the standard fBm $\{B_t^H, t \geq 0\}$. For more details about properties of the fBm, see for example [30] or [36].
Additionally, the fBm for $H \neq 0.5$ is not a semi-martingale nor a Markov process which are both useful properties for financial modeling. Therefore, the fBm is usually used for modeling volatility and not asset prices.
Sometimes, it is useful to represent the fBm in terms of the standard Bm which is sometimes referred to as *integral representations*. One such representation that we later use for the simulation of the fBm is of the form

$$Y_t = \sqrt{2H} \int_0^t (t-s)^{H-\frac{1}{2}} \mathrm{d}W_s, \tag{2.13}$$

where W is the Brownian motion.
In fact, the process (2.13) is not exactly the fBm representation but it is a process that is a part of the broader class of processes – the Volterra processes, that behaves locally like the fBm. This representation is useful because it could be rewritten in terms of a TBSS process, for which an approximate method called Hybrid scheme is designed, and therefore, the process (2.13) can be efficiently simulated. We introduce the Hybrid scheme in Subsection **??**.
For the sake of future text, it is useful for us to state qth absolute moment of the fBm. We borrow the following Remark from [36, Remark 1.2.2.]:

Remark 26. We can express the qth absolute moment of the fBm for $q \in \mathbb{N}$ as

$$\mathbb{E}\left[|W_t|^q\right] = \frac{2^{\frac{q}{2}}}{\sqrt{\pi}} \Gamma\left(\frac{q+1}{2}\right) |t|^{qH}, \tag{2.14}$$

where $\Gamma(\cdot)$ is the gamma function.

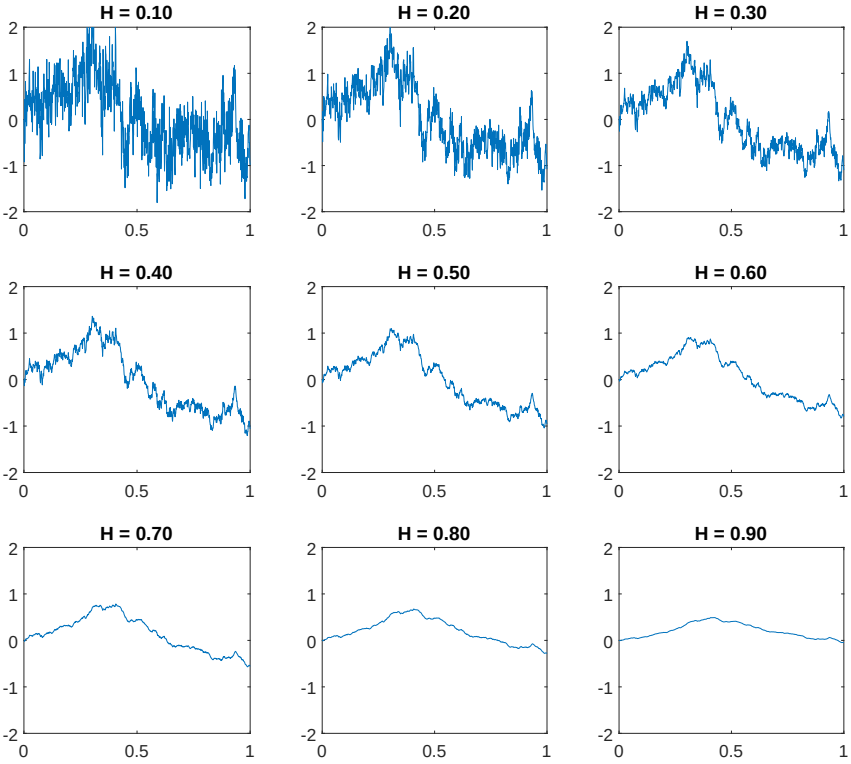

Figure 2.1: Trajectories of the fractional Brownian motion for different values of H.

2.6 Models

In order to determine the price of an option, different models were derived in the past. Probably the most well-known one was introduced by Fisher Black, Myron Scholes [10], and Robert Merton [34] in 1973. Later, in 1997, Scholes and Merton were awarded the Nobel Prize in Economics "for a new method to determine the value of derivatives". Unfortunately, Fisher Black died in 1995 and thus was not eligible for the prize.
The Black-Scholes-Merton (BSM) model laid the theoretical foundation for the whole framework for pricing options where it is assumed that the value of an option at time t is determined by the time to maturity $T - t$, strike price K, spot price of the underlying stock S_t, volatility of the underlying stock σ_t, and the risk-free interest rate r.
Additional assumptions underlying the theoretical framework are the following:

- The risk-free interest rate is constant and known.
- Markets are "frictionless". There are no taxes, no transaction costs, and no restrictions on short sales.
- The underlying asset has no cash flow, such as dividends when the asset is a stock.
- The option valued is an European option.
- Markets are efficient hence the future price of assets cannot be predicted and there are no arbitrage opportunities.

Then, the price evolution of the underlying stock is modeled by an SDE in the form

$$\mathrm{d}S_t = \mu_t S_t \mathrm{d}t + \sigma_t S_t \mathrm{d}W_t, \tag{2.15}$$

where S_0 it the initial value of the process S_t, coefficients μ_t and σ_t are called the drift and the diffusion (or the volatility term) respectively, and W_t is the Brownian motion.
One way to derive a pricing formula is to formulate the model in the form of a partial differential equation by eliminating the randomness using delta-hedging and solve it. That is possible for the Black-Scholes-Merton model and partially possible for example for the Heston model. However, if the original BSM assumptions are relaxed too much and the model becomes too complex, the PDE is not easy to find. Hence, we introduce a more general approach that does not require the knowledge of the PDE.
The more general approach is sometimes called the *risk-netural pricing* and involves sophisticated mathematical theory. While we do not aim to present the whole theory here, the reader can for example see [40].
The main idea of the risk-neutral pricing is that we can express the price of a derivative as the discounted expected value of its future payoff, however, not under the physical ("real") probability measure but rather under the *risk-neutral* probability measure, under which drifts of all stock price processes are equal to the risk-free rate r[2], i.e.,

$$\mathrm{d}S_t = rS_t \mathrm{d}t + \sigma_t S_t \mathrm{d}W_t. \tag{2.16}$$

[2]In other words, when all discounted stock price processes are martingales.

That means that the price of a derivative does not depend on investor's personal risk preferences. Moreover, from the *fundamental theorem of asset pricing* we know that when the market is arbitrage-free and complete, i.e., every asset can be replicated by a portfolio of other assets, there exists the unique risk-neutral measure.
To summarize it, having a derivative with payoff $V(T)$ at its maturity T, its price at time t can be expressed as

$$V(t) = \mathrm{e}^{-r(T-t)}\,\mathbb{E}_{\mathbb{Q}}[V(T)], \tag{2.17}$$

where $\mathbb{Q}$ is the risk-neutral probability measure and r is the risk-free interest rate.
For a European call option C with strike K and maturity T, the payoff at T is $C(T) = (S(T) - K)^+$, thus the pricing formula for C at time t can be expressed as

$$C(t) = \mathrm{e}^{-r(T-t)}\,\mathbb{E}_{\mathbb{Q}}\left[(S(T) - K)^+\right], \tag{2.18}$$

where $S(T) = S_T$ is the value of the stock price process (2.16) at time $t = T$.
Formula (2.18) provides a probabilistic price representation that can be exploited to find the price using Monte Carlo simulations, as we will describe in Subsection **??**, as long as we can simulate the stock price process.
From now, suppose that we operate under the risk-neutral probability measure $\mathbb{Q}$ if not stated otherwise.
While the drift is the risk-free rate under the risk-neutral measure, there are several different possibilities for the volatility term that lead to different models. In the following sections, we cover constant volatility and stochastic volatility models with focus on fractional stochastic volatility. Another option is to treat volatility as a deterministic function of time, i.e., $\sigma_t = \sigma(t)$, or alternatively, treat volatility as a function of time and the spot price $\sigma = \sigma(t, S_t)$. The latter leads to a local volatility model pioneered by Dupire [17].

2.6.1 Constant volatility – Black-Scholes-Merton model

When constant volatility $\sigma_t = \sigma$ of the underlying stock process (2.16) is assumed, we obtain the standard Black-Scholes-Merton (BSM) model, firstly introduced by Black and Scholes in [10] and Merton [34] in 1973. The popularity of the BSM model lies in the elegant theory behind it which nowadays provides the main general framework for derivative pricing. Another very important fact is that solving the model PDE yields an analytic closed-form solution.
The solution formula for the BSM model, sometimes known as the *Black-Scholes formula*, for the price C_t of a European call option with strike K, maturity T, on a stock of the price S_t at time t, can be written in the form

$$C_t = \mathrm{BS}(S_t, K, \tau, \sigma, r, t) = S_t\Phi(d_1) - K\,\mathrm{e}^{-r\tau}\,\Phi(d_2), \tag{2.19}$$

where $\tau = T - t$ is the time to maturity, $\Phi(\cdot)$ denotes the cumulative distribution function of the standard normal distribution, σ is the volatility of the stock, r is the risk-free

interest rate, and

$$d_1 = \frac{\log\left(\frac{S_t}{K}\right) + \left(r + \frac{\sigma^2}{2}\right)T}{\sigma\sqrt{T}}, \quad d_2 = \frac{\log\left(\frac{S_t}{K}\right) + \left(r - \frac{\sigma^2}{2}\right)T}{\sigma\sqrt{T}} = d_1 - \sigma\sqrt{T}.$$

The constant σ can be estimated by the sample standard deviation of log-returns of the stock.

There are different ways to derive the BS formula[3]. One of them is to solve the BSM model PDE with the boundary conditions corresponding to the given derivative, for example, by transforming it to the heat equation. For the derivation of the BSM PDE, see, for example, Chapter 1 in [9].

Because the BS formula is a closed-form solution formula, we can instantaneously compute the price of a given derivative and its sensitivities, so called Greeks. Therefore, BSM model is widely used in practice, despite all its shortcomings.

One of the main drawbacks of the BSM model is some of its assumptions that may be in many cases too far away from the reality. While the assumptions of the absence of a dividend paid by the stock and the absence of transaction costs can be generalized, the assumptions of arbitrage-free complete model and the possibility of borrowing and lending arbitrary amount of money at the risk-free rate are reasonable for developing such a model, there is a more serious departure from the reality in the assumption of constant volatility.

Having market data, i.e., prices of options of different combinations of strikes and maturities, we can use the BS formula also in a somewhat different manner. If we swap the role of the stock volatility and the price of an option, i.e., we treat the price as the input, we obtain volatility on the output that we call the implied volatility (implied by the option market price). Plotting the implied volatility over strikes and maturities (or sometimes over moneyness $M = S_t/K$ instead of strike to make clear whether the option is ATM, ITM or OTM), we obtain the so-called volatility surface. However, in real markets with sufficient liquidity, the volatility surface is not usually constant as it theoretically should be from the assumptions of the BSM model. In fact, curved structure, which is called the volatility smile, arises along the strike (moneyness) axis. This indicates that market data are not entirely consistent with the assumption of constant volatility. For illustration, in Figure 2.2, we can see the volatility surface for the market call option data of Apple Inc. from May 15, 2015 smoothed by the Gaussian kernel[4]. The smile is observable along the moneyness for $T \to 0$.

In general, option prices obtained from the BSM model are more accurate for options whose strike is near the spot price of underlying (near ATM) but options with strikes further from the spot price are usually under-priced, especially when the option is near its expiration. This phenomenon can be observed also in Figure 2.2. This is due to the assumption of constant volatility in (2.16) that implies the normality of underlying asset

[3] Rouah, F. D., *Four derivations of the Black-Scholes PDE*, available online at http://www.frouah.com/finance%20notes/Black%20Scholes%20PDE.pdf, cited April 18, 2019.

[4] We used MATLAB function `VolSurface()` available at https://www.mathworks.com/matlabcentral/fileexchange/23316-volatility-surface.

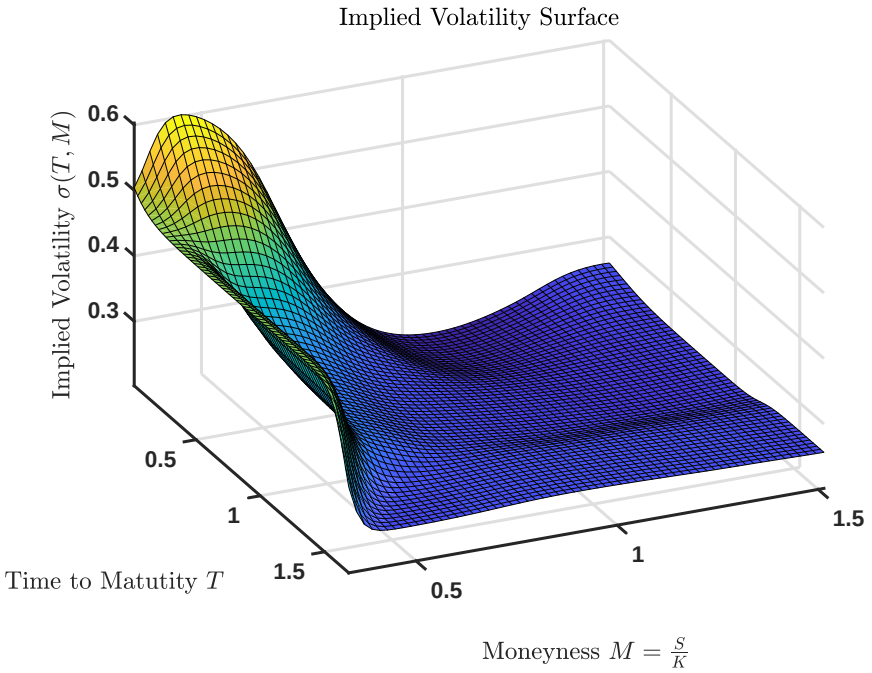

Figure 2.2: Volatility surface smoothed by the Gaussian kernel for the market call option data of Apple Inc. from May 15, 2015.

returns. However, stock returns usually follow a fat-tailed distribution. That means that rare events are more likely to occur in the reality then the BSM model assumes. Moreover, the fat tail is usually more prevalent on the left side of the distribution. In other words, big losses are more common than large gains. Therefore, the prices of OTM call options and ITM put options, whose combination are typically used to hedge a long position in a stock, are priced higher by markets than by the BSM model.
For the reasons mentioned above, new models assuming non-constant volatility term were proposed. Modeling volatility as a stochastic process shall, among others, model better the skewed or platykurtic stock returns. In the following section, we introduce the class of such models.

2.6.2 Stochastic volatility models

The assumption of stochastic volatility in the price evolution process (2.16) of the underlying stock that is modeled by a stochastic process as well, leads to the class of models called the stochastic volatility (SV) models. As we mentioned in earlier, modeling volatility by a stochastic process driven by the Brownian motion attempts to model the distribution of stock returns more accurately, so that such models generate implied volatility surfaces with smiles. Nonetheless, there are still a few other characteristics of the volatility (sometimes called the stylized facts) that are not captured by the SV mod-

els. One of them that has been researched recently is the autocorrelation of the realized volatility time series. Attempts have been made to model such a phenomenon in the volatility by a process with memory.
To incorporate the dependence of volatility on its past values into a model, processes driven by the fractional Brownian motion were suggested. At first, however, with the intention to obtain a long-memory process, as it was believed, align with the reality. For that reason, the fBm with $H > 1/2$ was employed. The class of processes that arose from this approach is referred to as fractional stochastic volatility models. Later, Gatheral et al. [21] in their 2014 paper *Volatility is Rough* argued that volatility should be modeled by the fBm with $H < 1/2$ based on an empirical analysis where they estimate H from realized volatility time series of common stock indexes. To underline that fact, they named their model rough fractional volatility (RFSV) model.
Another model that uses the the fBm with $H < 1/2$ is called the rough Bergomi (rBergomi) model introduced by Bayer, Friz, and Gatheral [5]. The model is similar to the RFSV model. In fact, the two model can be unified into a more general αRFSV model which we introduce in the next section.

αRFSV model

In this section we introduce the α Rough Fractional Stochastic Volatility (αRFSV) model. It was firstly suggested by Merino et al. [32] as a unifying formula for the RFSV and rBergomi models. The underlying stock is modeled by an SDE:

$$\mathrm{d}S_t = rS_t\mathrm{d}t + \sqrt{\sigma_t}S_t\mathrm{d}Z_t, \quad t \geq 0, \tag{2.20}$$

where $S_0 > 0$ is the initial spot price, $r \geq 0$ is the risk-free interest rate, and Z_t is the Brownian motion. The process that solves (2.20) can be obtained using the Itô's formula similarly as in Example 24. The resulting process can be written as

$$S_t = S_0 \exp\left\{\int_0^t \left(r - \frac{1}{2}\sigma_s\right) ds + \int_0^t \sqrt{\sigma_s}\mathrm{d}Z_s\right\}. \tag{2.21}$$

The volatility process σ_t, which is involved in the stock price process S_t, is of the form

$$\sigma_t = \sigma_0 \exp\left\{\xi B_t^H - \frac{1}{2}\alpha\xi^2 t^{2H}\right\}, \quad t \geq 0, \tag{2.22}$$

where $(B_t^H, t \geq 0)$ is the fBm with Hurst parameter $H < 1/2$ represented by one of its integral representations driven by the standard Bm $\widetilde{W}_t$, and $\sigma_0, \xi > 0, \alpha \in \{0, 1\}$ are coefficients.
The model also employs correlation between the stock price and the volatility process that is obtained by correlating the Bm $\widetilde{W}_t$ of the volatility process with another Bm driving the price process, i.e., the process Z_t in (2.20) is actually represented by

$$\mathrm{d}Z_t = \rho\mathrm{d}W_t + \sqrt{1-\rho^2}\mathrm{d}\widetilde{W}_t, \quad t \geq 0, \tag{2.23}$$

where $\rho \in [-1, 1]$ is the correlation between the volatility increments and the stock price increments. It is worth to note that Z_t is also the Brownian motion.
By choosing the coefficient $\alpha = 0$ in the volatility process (2.22), we obtain the RFSV model and on the contrary if $\alpha = 1$, we get the rBergomi model. Alternatively, values of α between 0 and 1 might give us a new degree of freedom that can be viewed as a weight between these two models.
While both cases of the αRFSV model are more likely to align with the stylized facts of volatility (see [22]) even using relatively small number of parameters (σ_0, ξ, ρ, H), the issue is the non-markovianity of the model. Because of this, we cannot derive any semi-closed form solution using the standard Itô calculus nor the Heston's framework. Therefore, to price a European call option, we have to rely on the Monte Carlo simulations.

Bibliography

[1] ANDERSEN, T. G. AND BOLLERSLEV, T. (1997). *Intraday periodicity and volatility persistence in financial markets*. Journal of Empirical Finance 4(2-3), 115–158.

[2] ASMUSSEN, S. AND GLYNN, P. (2007). Stochastic Simulation: Algorithms and Analysis. Stochastic Modelling and Applied Probability. Springer New York. ISBN 9780387690339.

[3] BACHELIER, L. (1900). Théorie de la Spéculation. Ph.D. thesis, Paris: Gauthier-Villars.

[4] BATES, D. S. (1996). *Jumps and stochastic volatility: Exchange rate processes implicit in Deutsche mark options*. Rev. Financ. Stud. 9(1), 69–107. DOI 10.1093/rfs/9.1.69.

[5] BAYER, C., FRIZ, P., AND GATHERAL, J. (2016). *Pricing under rough volatility*. Quant. Finance 16(6), 887–904. ISSN 1469-7688. DOI 10.1080/14697688.2015.1099717.

[6] BENNEDSEN, M., LUNDE, A., AND PAKKANEN, M. S. (2016). *Decoupling the short- and long-term behavior of stochastic volatility*. Available at arXiv: https://arxiv.org/abs/1610.00332.

[7] BENNEDSEN, M., LUNDE, A., AND PAKKANEN, M. S. (2017). *Hybrid scheme for Brownian semistationary processes*. Finance Stoch. 21(4), 931–965. ISSN 0949-2984. DOI 10.1007/s00780-017-0335-5.

[8] BERGOMI, L. (2005). *Smile dynamics II*. Risk Magazine 18(10), 67–73. Also available at SSRN: http://ssrn.com/abstract=1493302.

[9] BERGOMI, L. (2016). Stochastic Volatility Modeling. Chapman and Hall/CRC Financial Mathematics Series. Chapman and Hall/CRC, Boca Raton. ISBN 978-1-4822-4407-6.

[10] BLACK, F. S. AND SCHOLES, M. S. (1973). *The pricing of options and corporate liabilities*. J. Polit. Econ. 81(3), 637–654. ISSN 0022-3808. DOI 10.1086/260062.

[11] ÇINLAR, E. (2011). Probability and Stochastics. Graduate Texts in Mathematics. Springer New York. ISBN 9780387878591.

[12] COLEMAN, T. AND LI, Y. (1996). *An interior, trust region approach for nonlinear minimization subject to bounds*. SIAM Journal on Optimization 6, 418–445. DOI 10.1137/0806023.

[13] COMTE, F., COUTIN, L., AND RENAULT, E. (2012). *Affine fractional stochastic volatility models*. Ann. Finance 8(2–3), 337–378. ISSN 1614-2446. DOI 10.1007/s10436-010-0165-3.

[14] COMTE, F. AND RENAULT, E. M. (1998). *Long memory in continuous-time stochastic volatility models*. Math. Finance 8(4), 291–323. ISSN 0960-1627. DOI 10.1111/1467-9965.00057.

[15] DIEKER, A. B. (2002). *Simulation of fractional brownian motion*. Master's thesis (revised).

[16] DING, Z., GRANGER, C. W. J., AND ENGLE, R. F. (1993). *A long memory property of stock market returns and a new model*. J. Empir. Financ. 1(1), 83–106. ISSN 0927-5398. DOI 10.1016/0927-5398(93)90006-D.

[17] DUPIRE, B. (1994). *Pricing with a smile*. Risk Magazine pp. 18–20.

[18] EINSTEIN, A. (1905). *Über die von der molekularkinetischen theorie der wärme geforderte bewegung von in ruhenden flüssigkeiten suspendierten teilchen*. Annalen der Physik 322(8), 549–560. DOI 10.1002/andp.19053220806.

[19] ELICES, A. (2008). *Models with time-dependent parameters using transform methods: application to Heston's model*. Available at arXiv: https://arxiv.org/abs/0708.2020.

[20] GATHERAL, J. AND JACQUIER, A. (2014). *Arbitrage-free svi volatility surfaces*. Quant. Finance 14(1), 59–71. ISSN 1469-7688. DOI 10.1080/14697688.2013.819986.

[21] GATHERAL, J., JAISSON, T., AND ROSENBAUM, M. (2014). *Volatility is rough*. DOI 10.2139/ssrn.2509457. Available at arXiv: https://arxiv.org/abs/1410.3394.

[22] GATHERAL, J., JAISSON, T., AND ROSENBAUM, M. (2018). *Volatility is rough*. Quant. Finance 18(6), 933–949. ISSN 1469-7688. DOI 10.1080/14697688.2017.1393551.

[23] GLASSERMAN, P. (2003). Monte Carlo methods in financial engineering. Applications of Mathematics. Springer.

[24] HESTON, S. L. (1993). *A closed-form solution for options with stochastic volatility with applications to bond and currency options*. Rev. Financ. Stud. 6(2), 327–343. ISSN 0893-9454. DOI 10.1093/rfs/6.2.327.

[25] HORVATH, B., JACQUIER, A., AND MUGURUZA, A. (2017). *Functional central limit theorems for rough volatility*. SSRN Electronic Journal DOI 10.2139/ssrn.3078743.

[26] HORVATH, B., MUGURUZA, A., AND TOMAS, M. (2019). *Deep learning volatility*. SSRN Electronic Journal DOI 10.2139/ssrn.3322085.

[27] HULL, J. C. AND WHITE, A. D. (1987). *The pricing of options on assets with stochastic volatilities*. J. Finance 42(2), 281–300. ISSN 1540-6261. DOI 10.1111/j.1540-6261.1987.tb02568.x.

[28] KARATZAS, I. AND SHREVE, S. (1991). Brownian motion and stochastic calculus. Graduate Texts in Mathematics Series. Springer London, Limited. ISBN 9780387976556.

[29] KOLMOGOROV, A. N. (1940). *Wienersche Spiralen und einige andere interessante Kurven im Hilbertschen Raum*. Dokl. Akad. Nauk SSSR 26, 115–118.

[30] MANDELBROT, B. AND VAN NESS, J. (1968). *Fractional Brownian motions, fractional noises and applications.* SIAM Rev. 10(4), 422–437. DOI 10.1137/1010093.

[31] MCCRICKERD, R. AND PAKKANEN, M. S. (2018). *Turbocharging Monte Carlo pricing for the rough Bergomi model*. Quant. Finance ISSN 1469-7688. DOI 10.1080/14697688.2018.1459812.

[32] MERINO, R., POSPÍŠIL, J., SOBOTKA, T., SOTTINEN, T., AND VIVES, J. (2017). *Decomposition formula for rough fractional stochastic volatility models*. Manuscript to be submitted.

[33] MERINO, R., POSPÍŠIL, J., SOBOTKA, T., AND VIVES, J. (2018). *Decomposition formula for jump diffusion models*. Int. J. Theor. Appl. Finance ISSN 0219-0249. DOI 10.1142/S0219024918500528. In press (published online first 2018-11-02).

[34] MERTON, R. C. (1973). *Theory of rational option pricing*. Bell J. Econ. 4(1), 141–183. ISSN 0005-8556. DOI 10.2307/3003143.

[35] MIKHAILOV, S. AND NÖGEL, U. (2003). *Heston's stochastic volatility model - implementation, calibration and some extensions.* Wilmott magazine 2003(July), 74–79.

[36] MISHURA, Y. (2008). Stochastic calculus for fractional Brownian motion and related processes, vol. 1929 of *Lecture Notes in Mathematics*. Springer-Verlag, Berlin. ISBN 978-3-540-75872-3. DOI 10.1007/978-3-540-75873-0.

[37] POSPÍŠIL, J., SOBOTKA, T., AND ZIEGLER, P. (2018). *Robustness and sensitivity analyses for stochastic volatility models under uncertain data structure*. Empir. Econ. ISSN 0377-7332. DOI 10.1007/s00181-018-1535-3. In press (published online first 2018-07-31).

[38] RIEDEROVÁ, S. AND RŮŽIČKOVÁ, K. (2011). *Historical development of derivatives' underlying assets*. Acta Universitatis Agriculturae et Silviculturae Mendelianae Brunensis 59, 521–526. DOI 10.11118/actaun201159070521.

[39] SAMUELSON, P. A. (1965). *Rational theory of warrant pricing*. Industrial Management Review 6, no. 2 (Spring):, 13–31. DOI 10.1007/978-3-319-22237-0_11.

[40] SHREVE, S. E. (2004). Stochastic calculus for finance. II. Springer Finance. Springer-Verlag, New York.

[41] WIENER, N. (1920). *The mean of a functional of arbitrary elements*. Ann. of Math. 22 pp. 66–72.

[42] YIN, Z.-M. (1996). *New methods for simulation of fractional brownian motion*. J. Comput. Phys. 127(1), 66–72. ISSN 0021-9991. DOI 10.1006/jcph.1996.0158.

Chapter 3

Attached papers

This part consists of two papers that resulted from the work on this thesis.
The first paper gives recommendations on the simulation of rough Voleterra stochastic volatility models (a generalization of rough fractional volatility models) focusing on the use of simulations for derivative pricing. We compare the Cholesky, rDonsker methods, and the Hybrid scheme and give a recommendation on selection of the most suitable method for a given task taking accuracy and time complexity into consideration. Then, we show obstacles of the variance reduction method called turbocharging and propose a simple modification and conditions when the turbocharging is sage to use.
The second paper shows, based on an empirical study, that the rough Volterra stochastic volatility models do not outperform other stochastic volatility models (Heston, Bates, AFSVJD) but are remarkably robust, i.e., the models are not sensitive to the changes in the option data structure when calibrated. The most robust model seems to be the αRFSV model which unifies the RFSV model ($\alpha = 0$) and the rBergomi model. The significance tests for the roughness parameter H and the weight parameter α showed that both of the parameters significantly improves the fit of a model when being calibrated.

On simulation of rough Volterra stochastic volatility models

Jan Matas[1] and Jan Pospíšil*[1]

[1]NTIS - New Technologies for the Information Society, Faculty of Applied Sciences, University of West Bohemia, Univerzitní 2732/8, 301 00 Plzeň, Czech Republic,

Received 26 July 2021

Abstract

Rough Volterra volatility models are a progressive and promising field of research in derivative pricing. Although rough fractional stochastic volatility models already proved to be superior in real market data fitting, techniques used in simulation of these models are still inefficient in terms of speed and accuracy. This paper aims to present the accurate tools and techniques that could be used also in nowadays largely emerging pricing methods based on machine learning. In particular, we compare three widely used simulation methods: the Cholesky method, the Hybrid scheme, and the rDonsker scheme. We also comment on implementation of variance reduction techniques. In particular, we show the obstacles of the so-called turbocharging technique whose performance is sometimes contra productive. To overcome these obstacles, we suggest several modifications.

Keywords: Volterra stochastic volatility; rough volatility; rough Bergomi model; fractional Brownian motion

MSC classification: 60G22; 91G60

JEL classification: C63; G12

Contents

*Corresponding author, honik@kma.zcu.cz

1 Introduction

In mathematical finance, it is well known that one of the main issues of the Black-Scholes model lies in its assumptions about volatility of the modeled instrument's underlying asset. Opposed to the model assumptions, the realized volatility time series tends to cluster depending on the spot asset level and it certainly does not take on a constant value within a reasonable time-frame Cont (2001). To deal with such aforementioned inconsistencies, stochastic volatility (SV) models were proposed originally by Hull and White (1987) and later e.g. by Heston (1993). These models do not only assume that the asset price follows a specific stochastic process, but also that the instantaneous volatility of asset returns is of random nature as well. Specifically, the latter approach by Heston became popular in the eyes of both practitioners and academics. Several modifications of this model have been proposed over the last 20 years, see for example the literature review in Merino, Pospíšil, Sobotka, Sottinen, and Vives (2021).

Although many SV models have been proposed since the original Hull and White (1987) model, it seems that none of them can be considered as the universal best market practice approach. Several models might perform well when calibrated to describe complex volatility surfaces, but can suffer from over-fitting or they might not be robust in the sense described in Pospíšil, Sobotka, and Ziegler (2019). Also, a model with a good fit to an implied volatility surface might not be in-line with the observed time-series properties. Independent increments of the Brownian motion turned out to be such a one severe limitation. This helped to boost the popularity of the fractional Brownian motion (fBm), a generalization of the Brownian motion, which allows correlation of increments depending on the so-called Hurst index $H \in (0, 1)$.

The pioneers of the fractional SV models – Comte and Renault (1998), Comte, Coutin, and Renault (2012) – assumed the Hurst parameter ranged within $H \in (1/2, 1)$ which implies that the spot variance evolution is represented by a persistent process, i.e. it would have the long-memory property. In Alòs, León, and Vives (2007), a mean-reverting fractional stochastic volatility model with $H \in (0, 1)$ was presented. Gatheral, Jaisson, and Rosenbaum (2018); Bayer, Friz, and Gatheral (2016) came up with a more detailed analysis of rough fractional volatility models that should be consistent with market option prices, with realized volatility time series, and also provide superior volatility prediction results to several other models (Bennedsen, Lunde, and Pakkanen 2017). An approach considering a two factor fractional volatility model, combining a rough term ($H < 1/2$) and a persistent term ($H > 1/2$), was presented in Funahashi and Kijima (2017).

Since the well-known monographs on numerical methods for stochastic differential equations (SDEs) by Kloeden and Platen (1992); Milstein (1995); Milstein and Tretyakov (2004), numerical SDEs with colored or fractional noise have gained popularity, and there have been several papers available. For numerical methods for SDEs with color noise, books by Le Maître and Knio (2010) or Xiu (2010) might be considered as a good starting point. In order to simulate SDEs with fractional noise, one can consider for example a natural fractional modification of the classical Euler-Maruyama and Milstein methods (Deya, Neuenkirch, and Tindel 2012) including multi-level Monte Carlo methods (Kloeden, Neuenkirch, and Pavani 2011). Similar approach has been applied to stochastic Volterra equations only very recently, see e.g. preprints by Li, Huang, and Hu (2020) and Richard, Tan, and Yang (2020). However, it is worth to mention that not all techniques for simulating fBm (Dieker 2002) are suitable for simulation of the fractional SV models.

In this paper, we consider the αRFSV model recently introduced by Merino, Pospíšil, Sobotka, Sottinen, and Vives (2021). This model unifies and generalizes the RFSV model ($\alpha = 1$) and the rBergomi model ($\alpha = 0$). For the pricing of European-type options, we employ Monte-Carlo (MC) simulations. We compare three simulation methods: the Cholesky method (exact method), the Hybrid scheme, and the rDonsker scheme (both are approximate methods). We show that all methods are appropriate for the simulation of the model and we compare them all in terms of accuracy and speed. We also implement a variance reduction method referred to as turbocharging (McCrickerd and Pakkanen 2018) and analyze its effect on the variance in price estimations. We believe that its importance is somewhat overestimated in the literature and we show on specific examples that it does not always work well. As a solution, we propose a simple modification to overcome theses obstacles.

The structure of the paper is the following. In Section 2, we introduce the studied rough Volterra stochastic volatility models. In Section 3, we describe the methodology, in particular the details about Monte-Carlo simulations techniques used (Sections 3.1 and 3.2), as well as the suitability of the so called turbocharging variance reduction technique (Section 3.3). In Section 4, we present numerical results and compare all the three considered methods. Then, we provide results for our modified variance reduction techniques. We conclude all obtained results in Section 5.

2 Preliminaries and notation

2.1 Rough Volterra volatility models

Let $S = (S_t, t \in [0,T])$ be a strictly positive asset price process under a market-chosen risk-neutral probability measure Q that can be represented as

$$\mathrm{d}S_t = rS_t\,\mathrm{d}t + \sigma_t S_t\left(\rho\,\mathrm{d}W_t + \sqrt{1-\rho^2}\,\mathrm{d}\widetilde{W}_t\right), \tag{1}$$

where S_0 is the current spot price, $r \geq 0$ is the interest rate, W_t and $\widetilde{W}_t$ are independent standard Wiener processes defined on a probability space $(\Omega, \mathcal{F}, Q)$ and $\rho \in [-1,1]$ represents the correlation between the W_t and $\widetilde{W}_t$. Also, recall that for any $\rho \in [-1,1]$, a process $\rho W_t + \sqrt{1-\rho^2}\,\widetilde{W}_t$ is also a standard Wiener process. Let $\mathcal{F}_t^W$ and $\mathcal{F}_t^{\widetilde{W}}$ be the two filtrations generated by W_t and $\widetilde{W}_t$ respectively and let $\mathcal{F}_t := \mathcal{F}_t^W \cup \mathcal{F}_t^{\widetilde{W}}$ (for each $t \geq 0$, $\mathcal{F}_t$ is the minimal sigma algebra that includes both sigma algebras $\mathcal{F}_t^W$ and $\mathcal{F}_t^{\widetilde{W}}$).

The *stochastic volatility process* σ_t is a square-integrable process, adapted to the filtration generated by W_t whose trajectories are assumed to be a.s. càdlàg and stricly positive a.e. For convenience, we let $X_t = \ln S_t$, $t \in [0,T]$ which lead to the differential representation

$$\mathrm{d}X_t = \left(r - \frac{1}{2}\sigma_t^2\right)\mathrm{d}t + \sigma_t\left(\rho\,\mathrm{d}W_t + \sqrt{1-\rho^2}\,\mathrm{d}\widetilde{W}_t\right). \tag{2}$$

From now on, we consider the model represented by Equation (2) with *general Volterra volatility process* defined as

$$\sigma_t := f(t, Y_t), \quad t \geq 0, \tag{3}$$

where $f : [0,+\infty)\times\mathbb{R} \mapsto [0,+\infty)$ is a deterministic function such that σ_t belongs to $L^1(\Omega\times[0,+\infty))$ and $Y = (Y_t, t \geq 0)$ is the Gaussian Volterra process

$$Y_t = \int_0^t K(t,s)\;\mathrm{d}W_s, \tag{4}$$

where $K(t,s)$ is a kernel such that for all $t > 0$

$$\int_0^t K^2(t,s)\,\mathrm{d}s < \infty \tag{A1}$$

and

$$\mathcal{F}_t^Y = \mathcal{F}_t^W. \tag{A2}$$

Next, denote the autocovariance function of Y_t by $r(t,s)$ and the variance of Y_t by $r(t)$, i.e.:

$$\begin{aligned} r(t,s) &:= \mathbb{E}[Y_t Y_s], \quad t,s \geq 0, \\ r(t) &:= r(t,t) = \mathbb{E}[Y_t^2], \quad t \geq 0. \end{aligned} \tag{5}$$

In particular we assume that X_t is the log-price process (2) with σ_t being the *exponential Volterra volatility process*

$$\sigma_t = f(t, Y_t) = \sigma_0 \exp\left\{\xi Y_t - \frac{1}{2}\alpha\xi^2 r(t)\right\}, \quad t \geq 0, \tag{6}$$

where $(Y_t, t \geq 0)$ is the Gaussian Volterra process (4) satisfying assumptions (A1) and (A2), $r(t)$ is its autocovariance function (5), and $\sigma_0 > 0$, $\xi > 0$, and $\alpha \in [0, 1]$ are model parameters.

Let us now focus on a very important example of a Gaussian Volterra process, namely the *standard fractional Brownian motion* (fBm) B_t^H which can be represented by

$$B_t^H = \int_0^t K(t, s)\, \mathrm{d}W_s, \tag{7}$$

where $K(t, s)$ is a kernel that depends also on the Hurst parameter $H \in (0, 1)$. Recall that the autocovariance function of B_t^H is given by

$$r(t, s) := \mathbb{E}[B_t^H B_s^H] = \frac{1}{2}\left(t^{2H} + s^{2H} - |t - s|^{2H}\right), \quad t, s \geq 0,$$

and in particular $r(t) := r(t, t) = t^{2H}$, $t \geq 0$.

Nowadays, the most precise Volterra representation of fBm is the one by Molchan and Golosov (1969)

$$K(t, s) = C_H \left[\left(\frac{t}{s}\right)^{H-\frac{1}{2}} (t - s)^{H-\frac{1}{2}} - \left(H - \frac{1}{2}\right) s^{H-\frac{1}{2}} \int_s^t z^{H-\frac{3}{2}} (z - s)^{H-\frac{1}{2}}\, \mathrm{d}z \right] \tag{8}$$

$$C_H = \sqrt{\frac{2H\Gamma\left(\frac{3}{2} - H\right)}{\Gamma\left(H + \frac{1}{2}\right)\Gamma(2 - 2H)}}.$$

However, especially due to its tractability, only the simplified represenation

$$B_t^H = \sqrt{2H} \int_0^t (t - s)^{H-1/2}\, \mathrm{d}W_s. \tag{9}$$

is sufficient to consider (Alòs, Mazet, and Nualart 2000). To understand the connection between Molchan-Golosov and other representations of fBm such as the original Mandelbrot and Van Ness (1968) representation, we refer readers to the paper by Jost (2008).

Finally, in this paper, we consider the αRFSV model, firstly introduced by Merino, Pospíšil, Sobotka, Sottinen, and Vives (2021), in which the volatility process follows

$$\sigma_t = \sigma_0 \exp\left\{\xi B_t^H - \frac{1}{2}\alpha\xi^2 r(t)\right\}, \quad t \geq 0, \tag{10}$$

where $(B_t^H, t \geq 0)$ is one of the above mentioned representations of fBm and $\sigma_0 > 0$, $\xi > 0$ and $\alpha \in [0, 1]$ are model parameters together with empirical $H < 1/2$. For $\alpha = 0$ we get the RFSV model (Gatheral, Jaisson, and Rosenbaum 2018), for $\alpha = 1$ the rBergomi model (Bayer, Friz, and Gatheral 2016). Values of α between 0 and 1 give us a new degree of freedom that can be viewed as a weight between these two models.

Remark 2.1. *Since fBm is not a semimartingale, it is often useful to consider the so called* approximative fractional Brownian motion *(afBm), i.e. a process with the Volterra kernel*

$$\widetilde{K}(t, s) = \sqrt{2H}(t - s + \varepsilon)^{H-1/2}\mathbf{1}_{\{s \leq t\}}, \quad \varepsilon \geq 0, H \in (0, 1).$$

Then for every $\varepsilon > 0$, such a process is a semimartingale and as ε tends to zero, afBm converges to fBm. In such a case:

$$r(t, s) = \int_0^{t \wedge s} \widetilde{K}(t, v)\widetilde{K}(s, v)\, \mathrm{d}v,$$

$$r(t) = \int_0^t \widetilde{K}^2(t, v)\, \mathrm{d}v = 2H \int_0^t (t - v + \varepsilon)^{2H-1}\, \mathrm{d}v = (t + \varepsilon)^{2H} - \varepsilon^{2H},$$

Notice that if $\varepsilon = 0$, we obtain $r(t) = t^{2H}$, i.e., exactly the variance of the standard fractional Brownian motion.

While the both cases $\alpha \in \{0, 1\}$ of the αRFSV model are more likely to replicate the stylized facts of volatility (Gatheral, Jaisson, and Rosenbaum 2018) even by using relatively small number of parameters (σ_0, ξ, ρ, H), the issue is the non-markovianity of the model. Because of this, we cannot derive any semi-closed-form solution using the standard Itô calculus nor the Heston's framework. Therefore, to price mere vanilla options, we have to rely on Monte-Carlo (MC) simulations.

3 Methodology

In this section, we introduce the Monte-Carlo simulations methods to simulate the rough Volterra models, in particuar the αRFSV model. Furthermore, we investigate the suitability of the so-called turbocharging variance reduction technique (McCrickerd and Pakkanen 2018).

3.1 Monte-Carlo simulations

The price C_t at time t of a European call option with the strike K and maturity T can be expressed as

$$C_t = \mathrm{e}^{-r(T-t)}\mathbb{E}_Q\left[(S_T - K)^+\right], \tag{11}$$

where Q is the risk-neutral probability measure, S_T is the value of the process (1) at time $t = T$, and $(S_T - K)^+ = \max(S_T - K, 0)$. Thus, having M sample paths of the stock price process S under the risk-neutral measure, the price of a call option (11) can be estimated by

$$\hat{C}(t) = \mathrm{e}^{-r(T-t)}\frac{1}{M}\sum_{i=1}^{M}((S_T)_i - K)^+, \tag{12}$$

where $(S_T)_i$ denotes the i-th realization. The more sample paths we employ, the more accurate the result is. In fact, the rate of convergence of MC is $O(M^{-1/2})$.

There are various methods to simulate Volterra processes but we focus on simulation of the fractional Brownian motion. We often divide these methods into two classes: exact methods and approximate methods (Dieker 2002). Exact methods usually exploit the covariance function of the fBm to simulate exactly the fBm (the output of the method is a sampled realization of the fBm). The advantage is obviously the exactness, however the simulation using exact methods get much slower, the more steps we simulate. For example, the Hosking method or the Cholesky method use a covariance matrix to generate the fBm from two independent normal samples. The matrix grows with every step and the calculation becomes very time and memory demanding for large samples. The second class consists of approximate methods that often use some of the integral representations of the fBm (Stochastic representation method) or they are based on the Fourier transform and its implementation fast Fourier transform (FFT), such as the spectral method Yin (1996). For an extensive list of simulation methods of the fBm, see Dieker (2002).

Recently, an approximate method called the Hybrid scheme introduced by Bennedsen, Lunde, and Pakkanen (2017) has been recognized. The main idea is to discretize the stochastic integral representation of the process in the time domain and approximate the kernel function by a power function near zero and by a step function elsewhere. Later, an extension of the Hybrid scheme consisting of several variance reduction techniques was introduced by McCrickerd and Pakkanen (2018). Yet another approximation method has been proposed recently by Horvath, Jacquier, and Muguruza (2017). It is based on the idea of extending the Donsker's approximation of the Bm to the fBm.

When we simulate the fBm using either exact or approximate methods, we should investigate whether the numerical samples satisfy the theoretical properties of the simulated process. In

Section 4, we compare moments estimates to the corresponding exact values. For a deeper analysis of the quality of approximate samples, see Dieker (2002), Chapters 3 and 4.

We should also mention that there are several sources of potential error (Higham 2001, Sec. 5):

- *Sampling error*: the error of estimation of an expected value by a sample mean. This error is sometimes referred to as the *standard MC error* and it decays with $1/\sqrt{M}$, where M is the number of sample paths used.
- *Random number generator error*: the bias arising from the method of generating pseudo-random numbers, the lack of independence in the samples, etc.
- *Rounding error*: the error arising from the limitations of the finite precision arithmetic.
- *Discretization error*: the error resulting from the fact that a continuous-time process is represented by a finite number of discrete-time evaluations in the computer.

3.2 Simulation methods

We examine three methods for simulation of the fractional Brownian motion that can be further used for simulating the αRFSV model. We mention this because not all methods suitable for simulation of fBm paths can be used for simulation of paths of the αRFSV model. The potential problem lies in the fact that the Bm driving the stock price process is correlated with the Bm that is used to simulate the fBm that drives the volatility process. If a method does not use the Bm to simulate the fBm, i.e., it does not operate with an integral representation of the fBm, it cannot be properly correlated with the stock price process. The example is Spectral method Yin (1996) that generates the fBm from a sample of uniformly distributed variables using the Fast Fourier Transform.

The three methods, we focus on, are the Cholesky method, which is an exact (no approximation is involved) method, the Hybrid scheme, and the rDonsker scheme which are both approximate methods. We briefly describe the idea behind the algorithms in the following text.

Since we can simulate only discrete-time processes, we adapt a discrete-time notation $Y_{t_0}, Y_{t_1}, \ldots$ for the values of the fBm at the time moments $t_0, t_1, \ldots$. Once the path of the fBm is simulated for equidistant time steps, realization on another eqidistantly spaced interval is obtained by using the self-similarity property.

3.2.1 Cholesky method

The Cholesky method is an exact method that exploits the Cholesky decomposition of the covariance matrix of the simulated process. It means that the covariance matrix can be expressed as LL^T , where L is a lower triangular matrix and L^T is its transposition. A matrix L is said to be a lower triangular matrix if its elements $l_{ij} = 0$ for every $i < j$. It can be shown that such a decomposition exists for every symmetric positive definite matrix.

If we consider a discrete realization of the fBm $Y_0, Y_1, \ldots, Y_n$, we can denote the corresponding covariance matrix Γ_n, which is a $(n+1) \times (n+1)$ matrix that can be expressed as

$$\Gamma_n = \begin{bmatrix} \gamma(0) & \gamma(1) & \gamma(2) & \ldots & \gamma(n) \\ \gamma(1) & \gamma(0) & \gamma(3) & \ldots & \gamma(n-1) \\ \gamma(2) & \gamma(3) & \gamma(0) & \ldots & \gamma(n-2) \\ \vdots & \vdots & \vdots & \ddots & \vdots \\ \gamma(n) & \gamma(n-1) & \gamma(n-2) & \ldots & \gamma(0) \end{bmatrix},$$

where $\gamma(k) = \mathrm{Cov}[B_n^H, B_{n+k}^H] = \mathbb{E}[B_n^H B_{n+k}^H] = \frac{1}{2}[(k+1)^{2H} + (k-1)^{2H} - 2k^{2H}]$ is the autocovariance function of the fBm that is derived from the definition of the fBm (7).

Since Γ_n is a symmetric positive definite matrix, we can find its Cholesky decomposition. Then, we have $\Gamma_n = L_n L_n^T$, where $L_n = (l_{i,j})_{i,j=0}^n$. By generating a sample $v_0, \ldots, v_n$ from i.i.d. standard normal variables $(V_i)_{i=0}^n$, we can compute

$$B_i^H = \sum_{k=0}^{n} l_{ik} v_k$$

for every $i = 1, \ldots, n$. Then $(0, B_1^H, \ldots, B_n^H)$ is a path of the fBm.

For simulating P paths of the fBm, the matrix notation is useful. First, generate P samples from $(V_i)_{i=0}^n$ and organize the realizations into a matrix $X_n = (v_{ij})_{i=0,j=1}^{n,P}$, where v_{ij} is the jth realization of V_i. Then compute

$$B = L_n X_n$$

and replace the first row of B by zeros. Finally, notice that B^T is a $P \times (n+1)$ matrix that consists of P paths of the fBm B^H organized in the rows of the matrix B^T.

To practically simulate P paths of n steps, we firstly compute the covariance matrix Γ_n for the required Hurst parameter H in the form given above. Then, we find the Cholesky decomposition of Γ_n by computing the lower triangular matrix L_n. Next generate matrix V of numbers from the standard normal distribution. By computing $(L_n V_n)^T$ we obtain $P \times (n+1)$ matrix of fBm paths organized by rows.

The price for exact simulation is, however, the time complexity of $O(n^3)$, see Asmussen and Glynn (2007), Chapter XI, Sect. 2.

3.2.2 Hybrid scheme

The Hybrid scheme introduced by Bennedsen, Lunde, and Pakkanen (2017) is an approximate method that can be used for simulation of a broader class of stochastic processes called truncated Brownian semi-stationary (TBSS) processes. If X_t is such a process, it can be represented as

$$X_t = \int_0^t g(t-s)\nu_s \, \mathrm{d}W_s, \tag{13}$$

where W is the Brownian motion, $g : (0, \infty) \to [0, \infty)$ is a Borel-measurable function (a deterministic kernel function), and $\nu = \{\nu_t, t \geq 0\}$ is a stochastic process with locally bounded trajectories that drive the volatility (intermittency) of the process. The authors list more specific assumptions on g and ν in their paper to ensure that the integral (13) is well defined for the whole class of TBSS processes.

In order to use the Hybrid scheme to simulate the fBm, we recall the Volterra process (4) and let

$$Y_t = \sqrt{2H} \int_0^t (t-s)^{H-\frac{1}{2}} \, \mathrm{d}W_s,$$

where $H \in (0, 1)$ is the roughness parameter. The process Y_t is, in fact, a TBSS process that can be obtained from (13) by substituting

$$g(x) = \sqrt{2H} x^{H-\frac{1}{2}}, \tag{14}$$

and $\nu \equiv 1$. Since this Volterra process behaves locally like the fBm (Alòs, Mazet, and Nualart 2000), the Hybrid scheme use it as an approximation of the fBm.

The main idea behind the Hybrid scheme, as described in the abstract of the paper by Bennedsen, Lunde, and Pakkanen (2017), is to *approximate the kernel function g by a power function near zero and by a step function elsewhere. Then, the resulting approximation of the process is a combination of Wiener integrals of the power fucntion and a Riemann sum, which is why we call the method the Hybrid scheme.*

We summarize the technical part briefly and specifically only for the Volterra process (3.2.2). Let $\mathcal{G}_t^n := \{t, t-\frac{1}{n}, t-\frac{2}{n}, \ldots\}$ be the grid for the discretization of the Volterra process and let κ be an integer greater than 1. Then, the discretization of the process (3.2.2) can be represented by

$$Y_t = \sum_{k=1}^{\infty} \sqrt{2H} \int_{t-\frac{k}{n}}^{t-\frac{k}{n}+\frac{1}{n}} (t-s)^{H-\frac{1}{2}} \, \mathrm{d}W_s.$$

For "large" $k > \kappa \geq 2$, we approximate

$$(t-s)^{H-\frac{1}{2}} \approx \left(\frac{b_k}{n}\right)^{H-\frac{1}{2}}, \quad t-s \in \left[\frac{k-1}{n}, \frac{k}{n}\right], \tag{15}$$

where $b_k \in [k-1, k]$. For "small" $k \leq \kappa$, we retain the term $(t-s)^{H-\frac{1}{2}}$ as is. Proceeding in such a way, we obtain

$$Y_t \approx \sqrt{2H} \left(\sum_{k=1}^{\kappa} \int_{t-\frac{k}{n}}^{t-\frac{k}{n}+\frac{1}{n}} (t-s)^{H-\frac{1}{2}} \, \mathrm{d}W_s + \sum_{k=\kappa+1}^{\infty} \left(\frac{b_k}{n}\right)^{H-\frac{1}{2}} \int_{t-\frac{k}{n}}^{t-\frac{k}{n}+\frac{1}{n}} \mathrm{d}W_s \right). \tag{16}$$

To make a numerical simulation feasible, we truncate the second sum in (16). Furthermore, the values of b_k that minimizes the mean square error induced by the discretization are in the form

$$b_k^* = \left(\frac{k^{H+\frac{1}{2}} - (k-1)^{H+\frac{1}{2}}}{H+\frac{1}{2}} \right), k \geq \kappa + 1.$$

For derivation of the optimal b_k^*, see (Bennedsen, Lunde, and Pakkanen 2017, Prop. 2.8). Considering the truncation and the optimal b_k^* for (16), we obtain the so-called Hybrid scheme.

We implement the Hybrid scheme similarly as in the (Bennedsen, Lunde, and Pakkanen 2017, Sec. 3.1). Suppose we simulate the process Y on an equidistant grid $t_i = iT/n$, $i = 0, 1, 2, \ldots, n$, where n is the number of steps in the interval $[0, T]$, for some $T > 0$, i.e., we generate the discrete samples $Y_i := Y_{t_i}$, $i = 0, 1, 2, \ldots, n\rfloor$. We consider only the first order of approximation ($\kappa = 1$), so the numeric scheme for the Volterra process is in the form

$$Y_i = \sqrt{2H} \left(W_{\max\{i-1,0\},1} + \sum_{k=2}^{i} \left(\frac{b_k^*}{n}\right)^{H-\frac{1}{2}} W_{i-k,2} \right), \tag{17}$$

where $W_{i,1}$ and $W_{i,2}, i = 0, 1, \ldots, n-1$ denote two random i.i.d. vectors from a bivariate normal distribution with zero mean and covariance matrix Σ given by

$$\Sigma = \begin{bmatrix} \frac{1}{n} & \frac{1}{(H+\frac{1}{2})n^{(H+\frac{1}{2})}} \\ \frac{1}{(H+\frac{1}{2})n^{(H+\frac{1}{2})}} & \frac{1}{2Hn^{2H}} \end{bmatrix}.$$

For the sake of the efficiency, we denote the second term on the right-hand side of (17) by

$$\sum_{k=2}^{i} \left(\frac{b_k^*}{n}\right) W_{i-k,2}^n = \sum_{k=1}^{i} \Gamma_k \Xi_{i-k} = (\Gamma \star \Xi)_i,$$

where $\Gamma \star \Xi$ stands for discrete convolution and

$$\Gamma_k := \begin{cases} 0, & k = 1, \\ \left(\frac{b_k^*}{n}\right)^{H-\frac{1}{2}}, & k = 2, \ldots, i, \end{cases}$$
$$\Xi_k := W_{k,2}, \quad k = 0, 1, \ldots, n-1.$$

The final form of the numeric scheme is

$$Y_i = \sqrt{2H}\left(W_{\max\{i-1,0\},1} + (\Gamma \star \Xi)_i\right).$$

We implemented the Hybrid scheme in MATLAB and we used the Fast Fourier Transform to compute the discrete convolution. This way the complexity of the method is $O(n \log n)$, see (Bennedsen, Lunde, and Pakkanen 2017, Remark 3.2).

3.2.3 rDonsker scheme

We now describe the rDonsker scheme as it was introduced by Horvath, Jacquier, and Muguruza (2017). Following the Section 3.3 therein, we update their Algorithm 3.3 for the purposes of our studied model.

For a fixed $n \in \mathbb{N}$, we consider again the equidistant time partition $t_i = iT/n$, $i = 0, 1, 2, \ldots, n$, of $[0, T]$ with $T > 0$. Let Y_i^j, σ_i^j and X_i^j denote the j-th discrete numerical approximation (path), $j = 1, \ldots, M$, of the Volterra process Y, the volatility process σ and the log-stock price process X respectively, evaluated at the time point t_i, $i = 0, 1, 2, \ldots, n$.

Algorithm 3.1 (Simulation of the process (4) using the rDonsker scheme)**.**

1. *Simulate two* $\mathcal{N}(0,1)$ *matrices* $\{\xi_{j,i}\}_{\substack{j=1,\ldots,M \\ i=1,\ldots,n}}$ *and* $\{\zeta_{j,i}\}_{\substack{j=1,\ldots,M \\ i=1,\ldots,n}}$ *with* $corr(\xi_{j,i}, \zeta_{j,i}) = \rho$*. Denote*
$$\Delta W_i^j = \sqrt{T/n}\zeta_{i,j}, \quad i = 1, \ldots, n \text{ and } j = 1, \ldots, M.$$
2. *Simulate* M *paths of the Volterra process* Y *by*
$$Y_i^j = \sum_{k=1}^{i} g(t_{i-k+1})\Delta W_k^j = \sum_{k=1}^{i} g(t_k)\Delta W_{i-k+1}^j, \quad i = 1, \ldots, n \text{ and } j = 1, \ldots, M,$$
where $g(x)$ *is given by* (14)*. This step is easily implemented using discrete convolution with complexity* $\mathcal{O}(n \log n)$ *(Horvath, Jacquier, and Muguruza 2017, App. B).*

3.2.4 Simulation of the αRFSV model

Once we have simulated numerically the Volterra process Y using once of the above described method, we still need to simulate the volatility process (3) and the log-price process (2) and consequently the price process (1).

Algorithm 3.2 (Simulation of the αRFSV model)**.**

1. *Simulate* M *sample paths of the Volterra process* Y_i^j, $i = 1, \ldots, n$, $j = 1, \ldots, M$, *by one of the methods described in Sections 3.2.1, 3.2.2 or 3.2.3 respectively.*
2. *Simulate* M *sample paths of the volatility process* σ *by*
$$\sigma_i^j = f(t_i, Y_i^j), \quad i = 1, \ldots, n \text{ and } j = 1, \ldots, M,$$
where f *is given in* (3)*.*
3. *Use the forward Euler scheme to simulate the* M *sample paths of the log-price process* X *by*
$$X_i^j = X_{i-1}^j - \left(r - \frac{1}{2}\sum_{k=1}^{i}\sigma_{k-1}^j\right)\frac{T}{n} + \sqrt{\frac{T}{n}}\sum_{k=1}^{i}\sqrt{\sigma_{k-1}^j}\xi_{j,k}, \quad i = 1, \ldots, n \text{ and } j = 1, \ldots, M.$$
4. *Finally, we obtain the* M *sample paths of the asset price process* S *as*
$$S_i^j = \exp\{X_i^j\}, \quad i = 1, \ldots, n \text{ and } j = 1, \ldots, M.$$

3.3 Variance reduction techniques – turbocharging

Monte-Carlo simulations can be time demanding when we want to achieve higher precision. To further improve its efficiency, one or a combination of more variance reduction techniques can be implemented. The idea is to reduce the variance of the final estimation, and thus be able to achieve the same level of precision with smaller samples.

There are several approaches that can be used such as antithetic variates, control variates, or importance sampling. However, there is not a universal way to implement them. Instead, according to Glasserman (2003), *the greatest gains in efficiency from variance reduction techniques result from exploiting specific features of a problem, rather than form generic application of generic methods.* To reduce the variance of the price estimator for the αRFSV model, we use the approach developed by McCrickerd and Pakkanen (2018), called *turbocharging*.

Pricing a call option with strike K and maturity T under the αRFSV model, the idea of turbocharging is to use a *mixed estimator* for the estimation of the call option price $C(t) = \mathrm{e}^{-r(T-t)}\mathbb{E}[(S_T - K)^+]$, instead of the standard MC estimator (12). The mixed estimator is defined as

$$\begin{aligned} \tilde{C(t)} &= \frac{1}{M}\sum_{i=1}^{M}(X_i + \hat{\omega}Y_i) - \hat{\omega}\mathbb{E}[Y], \\ X &= \mathrm{BS}\left(S_t^1, K, T, (1-\rho^2)\int_0^t \sigma_u \,\mathrm{d}u, r, t\right), \\ Y &= \mathrm{BS}\left(S_t^1, K, T, \rho^2\left(\hat{Q} - \int_0^t \sigma_u \,\mathrm{d}u\right), r, t\right), \end{aligned} \tag{18}$$

where $\mathrm{BS}(\cdot)$ is the standard Black-Scholes formula for a call option and instead of using the αRFSV stock price process S_t (1) with volatility process (6), it operates with its orthogonal separation into S_t^1 and S_t^2, where the process S_t^1 solves an SDE of the form

$$\frac{\mathrm{d}S_t^1}{S_t^1} = \left(r - \frac{1}{2}\rho^2\sigma_t\right)\mathrm{d}t + \rho\sqrt{\sigma_t}\,\mathrm{d}W_t. \tag{19}$$

Parameters $\hat{\omega}$ and $\hat{Q}$ are computed after simulation of X and Y as

$$\begin{aligned} \hat{\omega} &= -\frac{\sum_{i=1}^{P}(X_i - \hat{X})(Y_i - \hat{Y})}{\sum_{i=1}^{P}(Y_i - \hat{Y})^2}, \\ \hat{Q} &= \max\left\{\left(\int_0^t \sigma_u \,\mathrm{d}u\right)_i : i = 1, \ldots, P\right\}. \end{aligned} \tag{20}$$

The mixed estimator (18) is always biased because of non-linearity of $\mathrm{BS}(\cdot)$. However, in McCrickerd and Pakkanen (2018), it is stated that for $n = 1000$ the bias is *never practically meaningful*. We verify that in subsection 4.3. Moreover, we empirically compare variances of the standard Hybrid scheme and turbocharged Hybrid scheme and test its stability and reliability also in subsection 4.3.1.

Ultimately, the turbocharging method is not restricted only for the Hybrid scheme. It can be successfully implemented for the Cholesky method and for the rDonsekr scheme and used for high-precision pricing (Matas and Pospíšil 2021).

4 Numerical results

In this section, we compare the exact Cholesky method (CM) and the approximate methods of Hybrid scheme (HS) and rDonsker scheme (rDS). We examine the quality of samples obtained from the Hybrid scheme, examine how much variance is reduced by the turbocharging technique, and we analyze the price estimation by the Hybrid scheme.

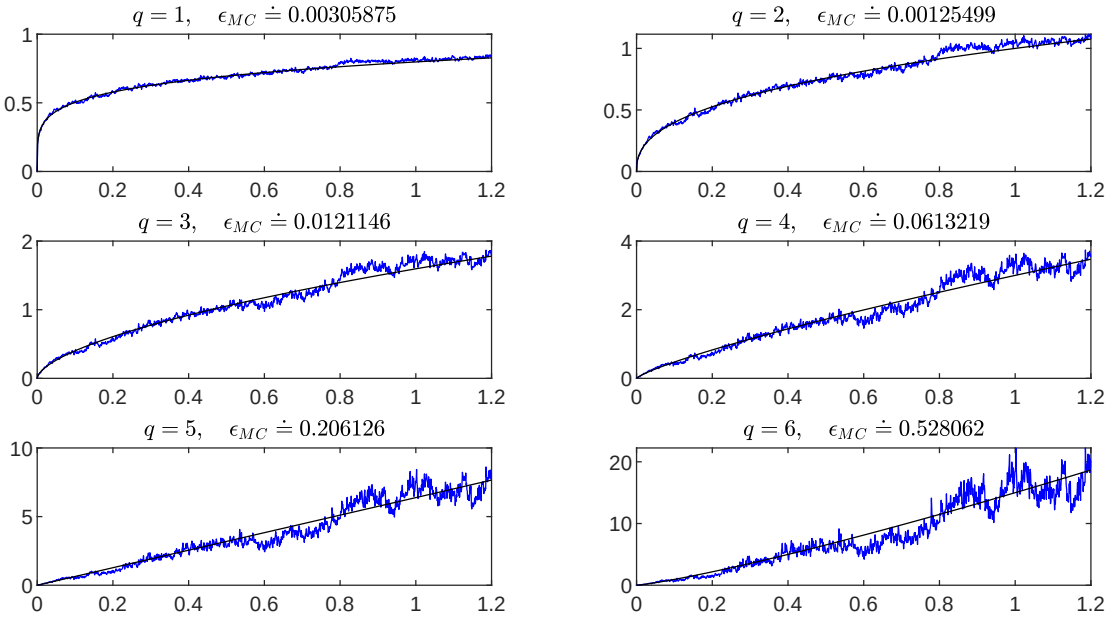

Figure 1: The sample absolute moments (blue) matching the corresponding theoretical values $\mathbb{E}\left[\left|B_t^H\right|^q\right]$ (black), see (21), of the fBm $\{B_t^H, 0 \leq t \leq 1.2\}$ for $H = 0.20$. We simulated $P = 1000$ paths, with granularity $n = 4 \times 252$ steps, using the Hybrid scheme. We denote ϵ_{MC} the absolute error of the end value.

We usually choose the number of steps n discretizing a path we simulate to be multiples of 252, which is the average number of trading days in a year. For example, choosing $n = 4 \times 252$ for the stock price process means that the numerous daily price movements are approximated by 4 steps of the process.

4.1 Quality of fBm samples

As we mentioned earlier in Subsection 3.1, when an approximate method is used to simulate paths of a random process, we should verify whether the generated samples possess corresponding theoretical properties. In the case of the fBm, we check whether the absolute[1] sample moments fit the theoretical values.

According to Mishura (2008, Remark 1.2.2.), the qth absolute moment of the fBm for $q \in \mathbb{N}$ can be expressed as

$$\mathbb{E}\left[|W_t|^q\right] = \frac{2^{\frac{q}{2}}}{\sqrt{\pi}} \Gamma\left(\frac{q+1}{2}\right) |t|^{qH}, \tag{21}$$

where $\Gamma(\cdot)$ denotes the gamma function. Then, we estimate the q-th absolute moment (21) from a sample of P paths by

$$\widehat{\mathbb{E}\left[\left|B_t^H\right|^q\right]} = \frac{1}{P} \sum_{t=1}^{P} (B_t^H)^q.$$

In Figure 1, we see an illustrative example of the sample moments fitting the corresponding theoretical values for $q = 1, \ldots, 6$. Naturally, as the number of paths in the a sample increases, the sample moments fit the theoretical values better, see Appendix in Matas (2021).

[1] We consider absolute moments instead of standard moments because it is more illustrative when visualized.

	Cholesky Method		Hybrid Scheme		rDonsker Scheme	
q	Mean	Variance	Mean	Variance	Mean	Variance
1	0.004806	0.000016	0.005338	0.000014	0.004569	0.000011
2	0.011143	0.000088	0.011928	0.000078	0.011294	0.000063
3	0.028106	0.000464	0.028511	0.000514	0.028618	0.000429
4	0.078726	0.003109	0.077577	0.004037	0.078654	0.003733
5	0.240790	0.028809	0.238690	0.036784	0.241030	0.038056
6	0.786010	0.419270	0.797030	0.348610	0.823770	0.436250

Table 1: The average absolute errors (and its variances) of end values of the qth absolute moment of the fBm for $H = 0.15$ and for different values of q calculated from 100 batches, each consisted of a sample of 10,000 fBm paths on $[0, 1]$ with granularity $n = 4 \times 252$, generated by the Cholesky method, Hybrid scheme, and the rDonsker scheme. We can see that the samples generated by HS and rDS are very similar to the samples generated by CM. For other H, results were similar.

We also compared samples generated by CM, HS, and rDS methods. Thus, we compared approximate methods with an exact method that we considered as a benchmark. We focused only on the end values as we are interested in pricing European options whose payoff depends only on the price of the stock at its maturity.

We measured the average absolute error of the end values of the sample mean and sample absolute moments of the fBm from 30 batches, each consisted of $P = 1000$ fBm paths on $[0, 1]$ with granularity $n = 4 \times 252$ steps. The results were very similar for different values[2] of H hence in Table 1, we summarize the results only for $H = 0.15$. The conclusion is that based on the mentioned empirical results, both HS and rDS produce samples very similar to those obtained by an exact method.

Runtime experiment

Next, we compared runtimes of the CM, HS, and rDS. The asymptotic time complexity of simulation of one path is known for all of the methods we compare. Using the big O notation, the time complexity of HS and rDS is $O(n \log n)$ and the time complexity of CM is $O(n^3)$. It is apparent that the approximate methods are superior to the CM considering the asymptotic complexity. However, the asymptotic behavior does not convey which method is more efficient for generating P paths when P is big.

In fact, the Cholesky method is vectorized implicitly by implementing it using matrix notation. We only compute the Cholesky decomposition of the covariance matrix of the fractional Brownian motion and apply it to an $n \times P$ matrix of normally distributed random numbers. The result after transposition is P paths of the fBm organized in $P \times n$ matrix. Increasing the number of paths thus leads to the increase in the time complexity of the matrix multiplication.

Contrarily, neither the HS nor rDS can be easily vectorized. The problem is the discrete convolution of a Bm path with the convolution kernel. Therefore, the very fast computation of a fBm path has to be repeated P times in a cycle. Hence, the runtime increases linearly with the increasing number of paths.

To empirically compare the time efficiency of the three methods, we measured runtimes of simulations of P fBm paths of n steps using both methods for different values of P and n on a grid. The results are visualized in Figure 2 where we see that while the rDS is clearly superior for small samples followed by the HS, from a certain number of paths P, the CM is the most efficient. The break even value of P is no more than 1000 for the values of n we examined. Since usually much bigger samples are necessary, the CM appears to be the best choice.

[2] We examined $H = 0.05, 0.10, \ldots, 0.45$.

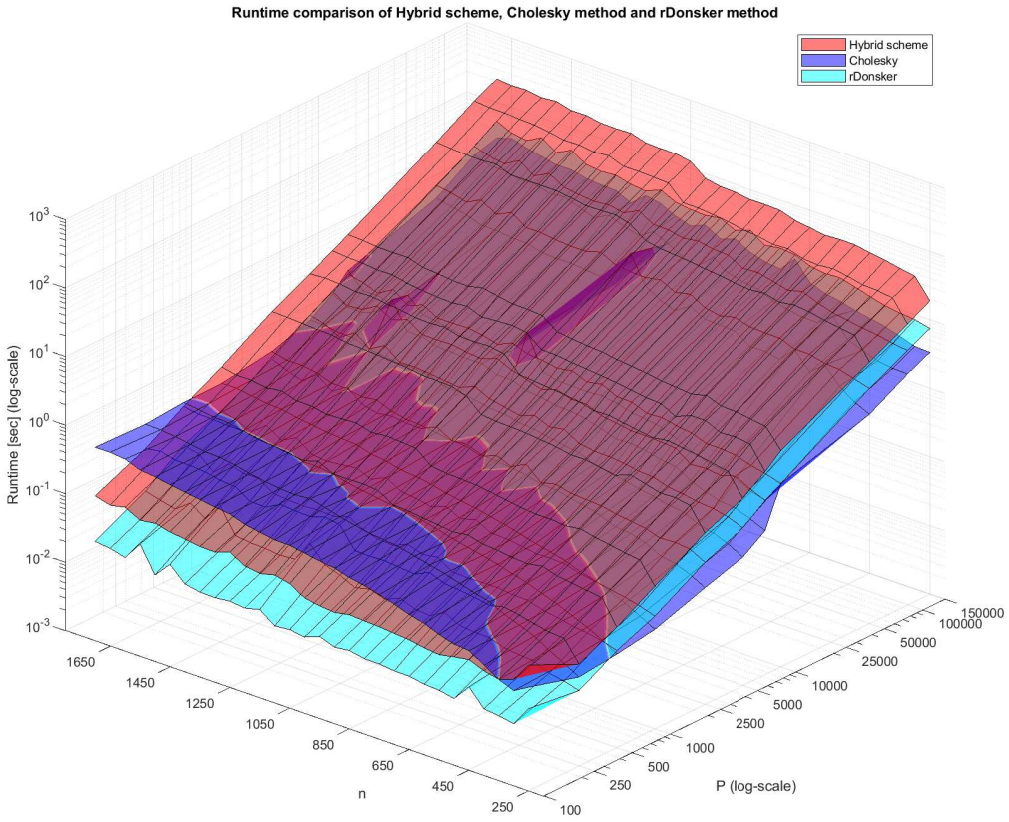

Figure 2: Runtimes of the Hybrid scheme, the Cholesky method, and the rDonsker scheme of simulations for different values of P and n on a grid.

Conclusion

Both the Hybrid scheme and the rDonsker scheme, despite being an approximate methods, generate reliable samples of fBm that are very similar to the samples obtained from an exact method - the Cholesky method. Needless to say, the rDS generates a path much faster. The asymptotic time complexity of the rDS and the HS scheme is $O(n \log n)$ while the asymptotic time complexity of the Cholesky method is $O(n^3)$. However, when we take the number of paths into consideration, the HS and rDS are not ultimately superior to the CM in runtime. From the experiment, whose results are visualized in Figure 2, we conclude that it is more time-efficient to simulate less paths of higher granularity by the rDS or HS while the CM is better for simulation of large number of paths.

4.2 Simulation of the αRFSV model

In the previous section, we verified that the Cholesky method, the Hybrid scheme, and the rDonsker scheme produce samples of the fBm of similar preciseness and we also compared the time efficiency of the three methods. In this section, we simulate the αRFSV model, i.e., the volatility process and the stock price process. We then analyze the effect of sample size on the pricing ability of the model and we introduce and examine the variance reduction technique turbocharging. Finally, we give recommendation on the sample size to guarantee given preciseness of the model prices.

First, we derive formulas for the mean and the variance of the αRFSV volatility process (10). To compute the mean, consider first the exponential fBm process $\mathrm{e}^{\xi B_t^H}$. Since B_t^H is a Gaussian process with zero mean and variance t^{2H}, the random variable $\mathrm{e}^{\xi B_t^H}$ has the log-normal distribution with mean $\mathrm{e}^{\frac{1}{2}\xi^2 t^{2H}}$ for every $t > 0$ and hence its q-th moment is

$$\mathbb{E}\left[\left(\mathrm{e}^{\xi B_t^H}\right)^q\right] = \mathrm{e}^{\frac{1}{2}\xi^2 q^2 t^{2H}}.$$

The q-th moment of the volatility process (10) is therefore

$$\begin{aligned}
\mathbb{E}\left[\sigma_t^q\right] &= \mathbb{E}\left[\sigma_0^q \exp\left(\xi q B_t^H - \frac{1}{2}\alpha\xi^2 q t^{2H}\right)\right] \\
&= \sigma_0^q \mathrm{e}^{-\frac{1}{2}\alpha\xi^2 q t^{2H}} \mathbb{E}\left[\mathrm{e}^{q\xi B_t^H}\right] \\
&= \sigma_0^q \mathrm{e}^{-\frac{1}{2}\alpha\xi^2 q t^{2H}} \mathrm{e}^{\frac{1}{2}\xi^2 q^2 t^{2H}} \\
&= \sigma_0^q \mathrm{e}^{\frac{1}{2}\xi^2 q(q-\alpha) t^{2H}}.
\end{aligned} \tag{22}$$

For illustration, we simulated $P = 10,000$ paths of the αRFSV model on $[0, 0.6]$ for $n = 2 \times 252$ discretization steps per unit interval and for model parameters $\alpha = 1, H = 0.07, \xi = 1.9, \rho = -0.9$, and $\sigma_0 = 0.235^2$ that had been shown by Bayer, Friz, and Gatheral (2016) that are consistent with the market data set used in the paper. We set $S_0 = 2.5$ and $r = 0.05$ for the stock price process. The results are visualized in Figure 3. In each plot, five illustrative trajectories are visualized together with theoretical mean and variance (green dashed) and sample mean and variance (red). We can see that for each process, the estimated values are aligned with the corresponding theoretical values.

4.3 Comparison of the Hybrid scheme and its turbocharged version

To quantify the effect of the turbocharging technique explained in Subsection 3.3 on the variance of the option price estimation, we use the variance reduction factor that is simply a ratio of the variance of the prices obtained using the method with the variance reduction implemented and the variance obtained by the standard method. Its reciprocal value thus convey how many times the variance in estimated prices using the turbocharged method is smaller than the variance in estimated prices using a standard method. In this simulation study, we use the Hybrid scheme since

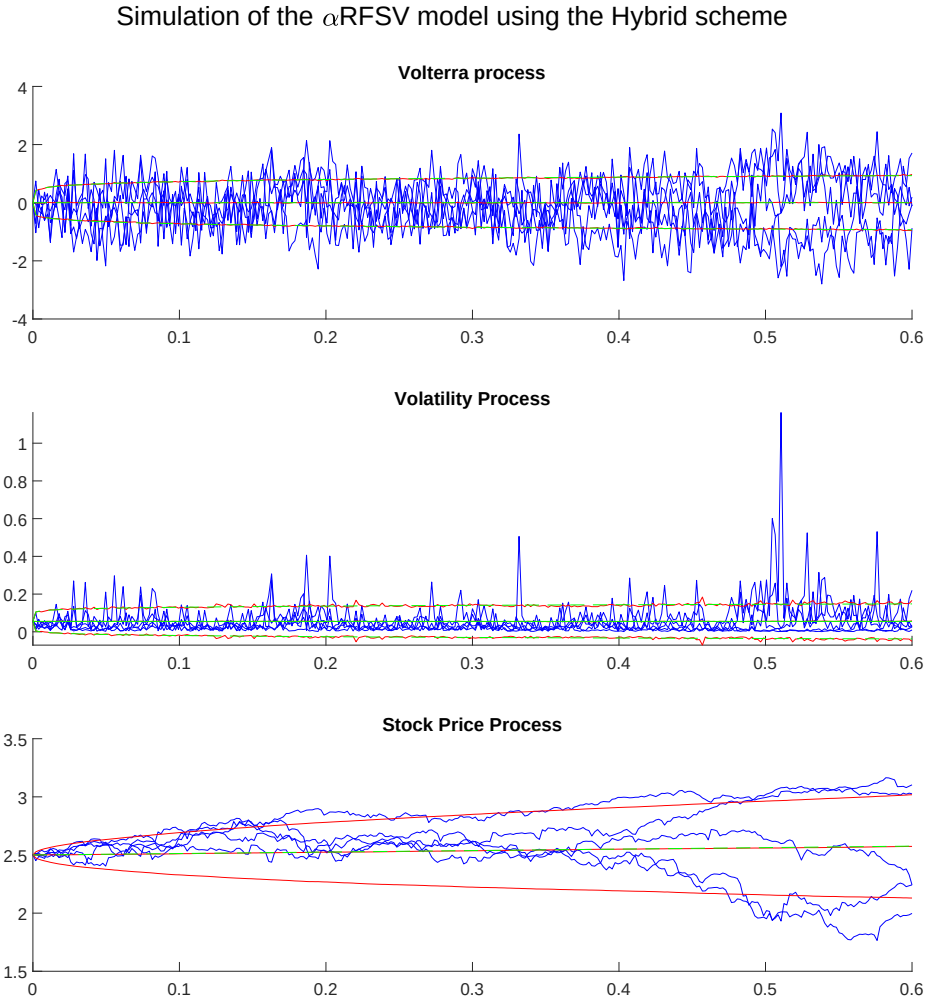

Figure 3: The results of simulation of the αRFSV model on $[0, 0.6]$ for $n = 2 \times 252$ discretization steps and for model parameters $\alpha = 1, H = 0.07, \xi = 1.9, \rho = -0.9$, and $\sigma_0 = 0.235^2$. Five illustrative trajectories of each of the Volterra process, the volatility process, and the stock price process with $S_0 = 2.5$ and risk-free rate $r = 0.05$ are visualized. Also, the expectation and the variance for each process estimated from $P = 10,000$ paths are plotted. The red curves are estimations and the green dashed curves are exact values. For the stock price process its sample standard deviation is plotted only, because we do not know the formula of its variance.

the turbocharging was introduced in a paper where the HS was utilized, although the turbocharging can be implemented to other methods as well including the Cholesky method.

We performed analyses of variance reduction by calculating the sample variances of the price obtained from the standard HS and from the turbocharged HS for different parameters. We ran simulations of P paths, discretized by n steps per year, in 30 batches and for each batch we calculated the prices of options for different strikes K.

For example, In Figure 4, we can see how the variance is reduced while the mean does not change significantly. We chose $P = 300$ paths with $n = 4 \times 252$ steps per year and model parameters that are consistent with the SPX index Bayer, Friz, and Gatheral (2016). The variance was reduced approximately $65, 27, 10, 5, 3, 3, 11, 9$ times for the strikes $80, 90, \ldots, 150$ respectively. The spot price S_0 was set to 100.

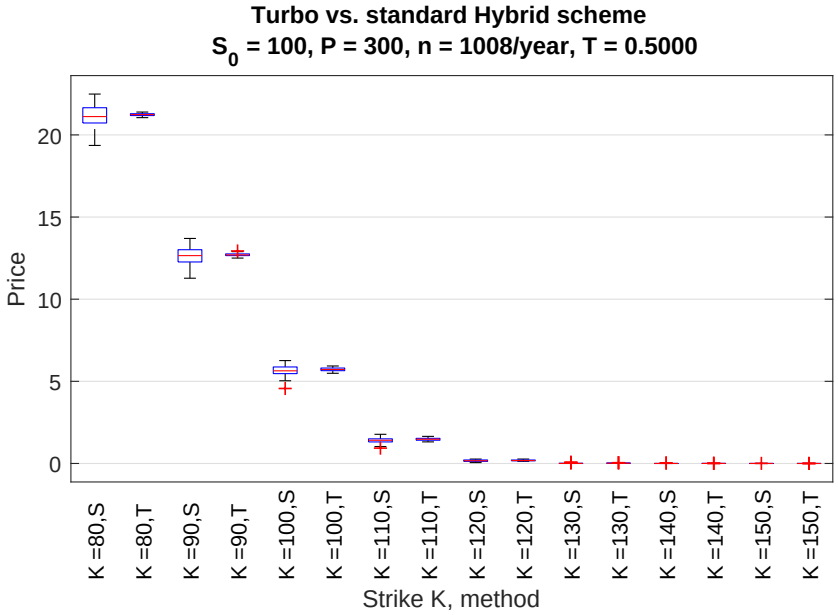

Figure 4: The visualization of variance reduction from utilizing the turbocharged Hybrid scheme (T) compared to the standard Hybrid scheme (S). We simulated the αRFSV model for $\alpha = 1, \sigma_0 = 0.235^2, H = 0.07, \rho = -0.9$, and $\xi = 1.9$. We generated 30 batches of $P = 300$ paths, discretized by 4×252 steps, for each strike price K for both methods. The boxplots depict the resulting 30 price estimates.

However, the turbocharging method does not always perform well. For example, choosing $\alpha = 1, \sigma_0 = 0.62, H = 0.22, \rho = -0.05, \xi = 0.18$, and setting the other parameters as before, the resulting proce estimates are not concentrated around its mean. In fact, the variance is not reduced but extended and moreover, a bias in the estimation becomes more evident. In Figure 5, we cab see that the more an option is OTM, the more the prices are scattered or completely wrong. Nonetheless, even more extreme results can be obtained for different choice of parameters.

Based on the findings that the turbocharged HS is not always stable, we further analyzed variance reduction factors for different combinations of coefficients and parameters in order to determine, what is the source of the malfunction of the turbocharging and what is the effect of different parameters on variance reduction.

For that reason, we fixed the spot price $S_0 = 1$ and vary model coefficients σ_0, ξ, ρ, H, the risk-free rate r and the maturity T. For each combination, we generated 30 batches, each comprised of a sample of $P = 1,000$ paths, discretized by $n = 4 \times 252$ steps per year. From each batch, we calculated prices using the turbo HS and the standard HS for strikes $K = 0.5, 0.6, \ldots, 1.6$. Then,

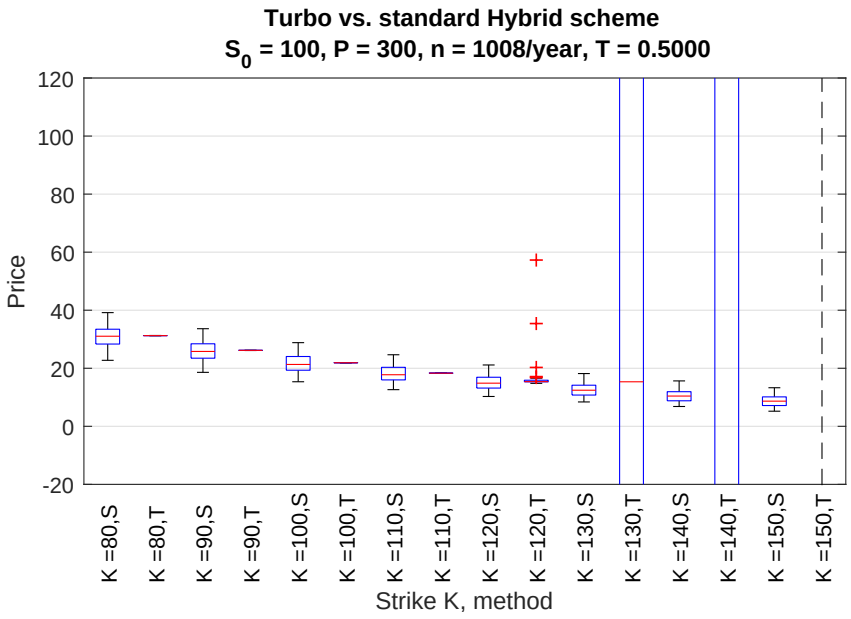

Figure 5: The visualization of variance reduction from utilizing the turbocharged Hybrid scheme (T) compared to the standard Hybrid scheme (S). Coefficients of the αRFSV model were set to $\alpha = 1, \sigma_0 = 0.62, H = 0.22, \rho = -0.05, \xi = 0.18$. We generated 30 batches of $P = 300$ paths discretized by 4×252 steps for each strike price K for both methods. The boxplots depict the resulting 30 price estimates. It is apparent that in this case, the turbocharging does perform worse than the standard technique for options that are deep OTM.

we calculated the means and variances of prices obtained from the turbo HS and the standard HS.

The resulting variance reduction factors which are ratios of the variances in prices obtained from the turbocharged HS and the variances in prices obtained by the standard HS are depicted in Figure 6 where we can observe that the amount of variance reduced clearly depends the most on ρ. Turbocharging appears to be the most effective for $-1 < \rho 0$. For $\rho \approx 0$ and $\rho \approx -1$, the variance is still reduced except for a few outliers. Nonetheless, for $\rho > 0$, the variance is not reduced, i.e., the variance reduction factor is greater than 1, in more than 10% of the cases. We can also see some dependence on ξ. For $\xi > 1$, the turbocharging becomes less stable. Last but not least, the coefficient α also seems to affect the variance reduction. For $\alpha = 1$, the turbocharging is more stable than for $\alpha = 0$.

That leads us to conclude that for pricing a European option, we recommend using the turbocharging method only for $\rho \leq 0$. Otherwise, for $\rho > 0$, there is a significant chance, that the obtained price estimates will be very far from the true prices. In the following section we analyze the variation and bias of the estimates in a similar way.

4.3.1 Analysis of quality of price estimation using the turbocharged Hybrid scheme

Now, we analyze the effect of turbocharging on variability and bias of model prices. To measure the variability, we use the coefficient of variation

$$\frac{\sqrt{\frac{1}{N-1}\sum_{i=1}^{N}\left(C_i^{\mathcal{T}} - C^{\mathcal{T}}\right)^2}}{C^{\mathcal{T}}}, \tag{23}$$

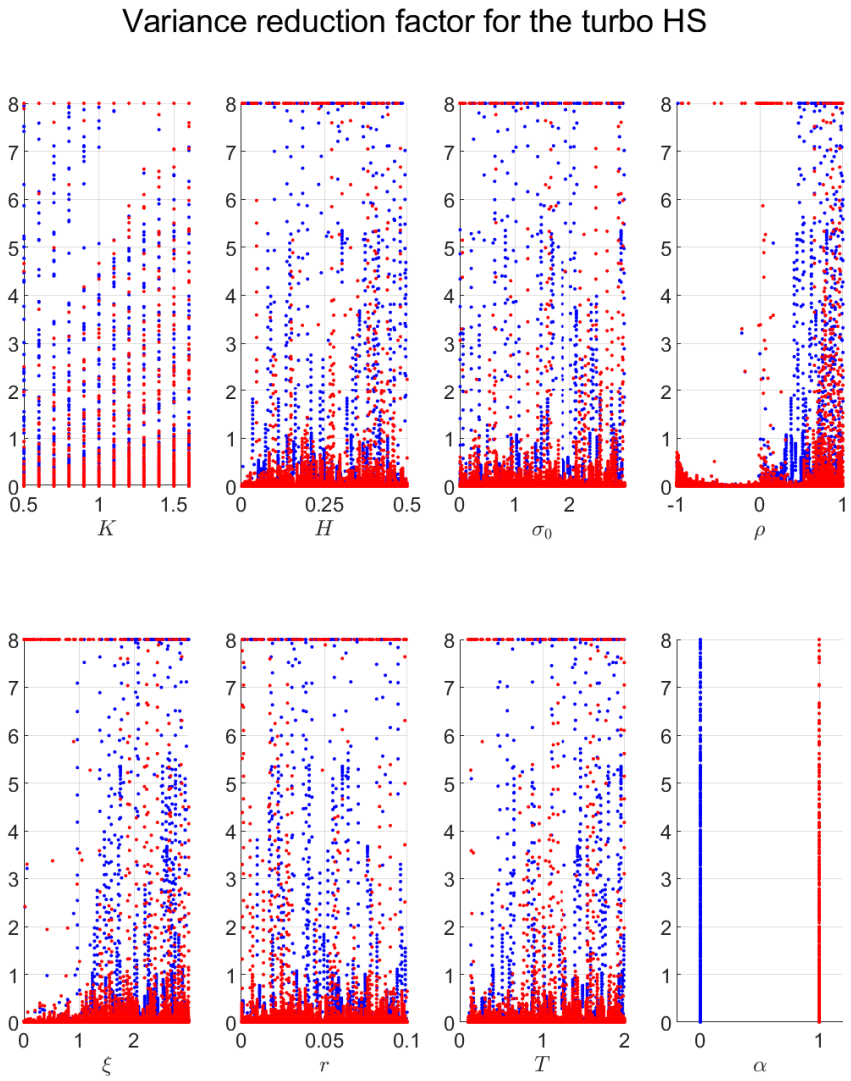

Figure 6: Results of the variance reduction analysis described in Subsection 4.3 for rBergomi model $\alpha = 1$ (red) and RFSV model $\alpha = 0$ (blue). Each point depicts the variance reduction factor computed from 30 batches for the given combination of the model parameters. In each batch, we simulated $P = 1,000$ paths, discretized by 4×252 steps per $[0, 1]$.

where $C_i^{\mathcal{T}}$ is the estimated price from the ith batch and

$$C^{\mathcal{T}} = \frac{1}{N} \sum_{i=1}^{N} C_i^{\mathcal{T}}$$

is the sample mean of the price estimates.

We analyzed the bias for the prices obtained using the turbo HS by comparing it to the the prices obtained by the standard HS. To measure bias, we use the absolute relative error

$$\frac{|C^{\mathcal{T}} - C^{\mathcal{S}}|}{C^{\mathcal{S}}}, \tag{24}$$

where $C^{\mathcal{S}}$ is the average of price estimates obtained by the standard HS and $C^{\mathcal{T}}$ is the average of price estimates obtained by the turbocharged HS

The results are visualized in Figures 7 and 8. Comparing the two figures, we see that the variance were significantly reduced in most cases. However, in the second figure, many outliers occurred and some negative values were obtained due to the malfunction of the turbocharging that produced negative prices. The most problematic cases arose for $\rho \approx 0$ and $\xi < 1$. Moreover, it seems that the malfunctions appear for OTM options ($K > 1$).

The relative errors are plotted in Figure 9. Again, we can see that problems occur when $\rho > 0$, for which the estimation using turbocharging is apparently strongly biased compared to the estimation using the standard HS. We also see better results for $\alpha = 1$ than for $\alpha = 0$.

4.3.2 Modified turbocharging and the Hybrid scheme

As a solution to the issues described earlier, we propose a modification of the turbocharging method. It is rather a naive approach that tries to identify the cases when the turbocharging does not work properly and replace the incorrect estimates by the original estimates (not turbocharged). To identify that the price of a call option is estimated incorrectly, we propose three natural criteria:

1) the price estimate is non-negative,

2) the price estimate is greater than the spot price of the underlying,

3) the price estimates of options with the same maturity are in descending order for increasing strike prices.

If at least one of those criteria is violated, suspicious price estimations are replaced by estimations using only the standard pricing method without the turbocharging. Suspicious prices are considered all prices that violates the first or the second criteria. When the third criterion is violated, having options with a given maturity T, the first price of an option with the strike K_0 that violates the descending order is considered suspicious and all prices of options with maturity T and strike $K > K_0$ are considered suspicious. This way, we reduce the number and intensity of outliers among price estimates and it is guaranteed that the price estimates are non-negative and lesser than the spot price. The advantage of this approach is that it can be easily implemented and it is time-efficient – the pricing is not slowed down.

For illustration, we consider the same coefficients and parameters as for the example of the turbo HS malfunction in Figure 5 but we use the modified turbocharging instead. We visualized the results in Figure 10. In that case, modification was activated for the prices of option with $K = 120$ and all following options with strike $K > 120$. All those suspicious prices were replaced by the price estimates using the standard HS.

To test the modification, we ran identical simulation as before. The results are visualized in Figure 11. We see that the modification eliminated all the negative price estimates and also majority of outlying positive estimates, especially for $\alpha = 1$. Moreover, we can observe that almost all the outlying values are now concentrated around $\sigma_0 \approx 0$. For $\alpha = 0$. In general it appears that the turbocharging works better for $\alpha = 1$.

However, even though we managed to reduce variance and eliminate majority of cases where excessive variance can be an issue, we have to remember that for $\rho > 0$ the estimation can be strongly biased. We tested the bias of modified turbo HS but we ended up with similar results as for the turbo HS that are visualized in Figure 9.

To sum this part up, we found out that the turbocharging method is not stable for every combination of parameters and model coefficients, especially for $\rho > 0$. We proposed a simple modification but we still recommend to avoid using turbocharging when $\rho > 0$ due to strong bias in the estimation. In fact, we suggest using the turbocharging technique only for $\rho < -0.05$. Also, we recommend avoiding turbocharging for $\sigma_0 \approx 0$ and $\xi > 2$ when $\alpha = 0$ due to higher variance compared to the standard HS.

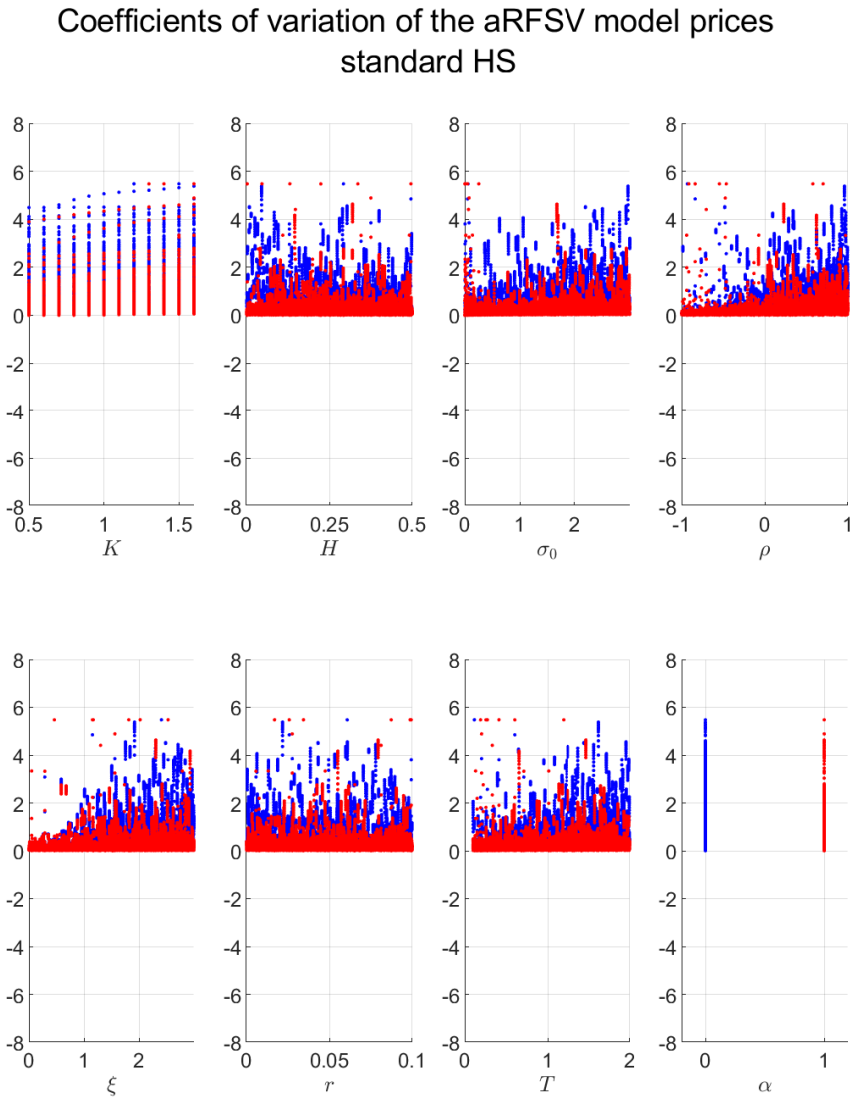

Figure 7: Results of the variance analysis for the rBergomi model $\alpha = 1$ (red) and the RFSV model $\alpha = 0$ (blue). Each point depicts the coefficient of variation (23) computed from 30 batches for the given combination of the model parameters. In each batch, we simulated $P = 1000$ paths, discretized by 4×252 points per $[0, 1]$, using the standard HS.

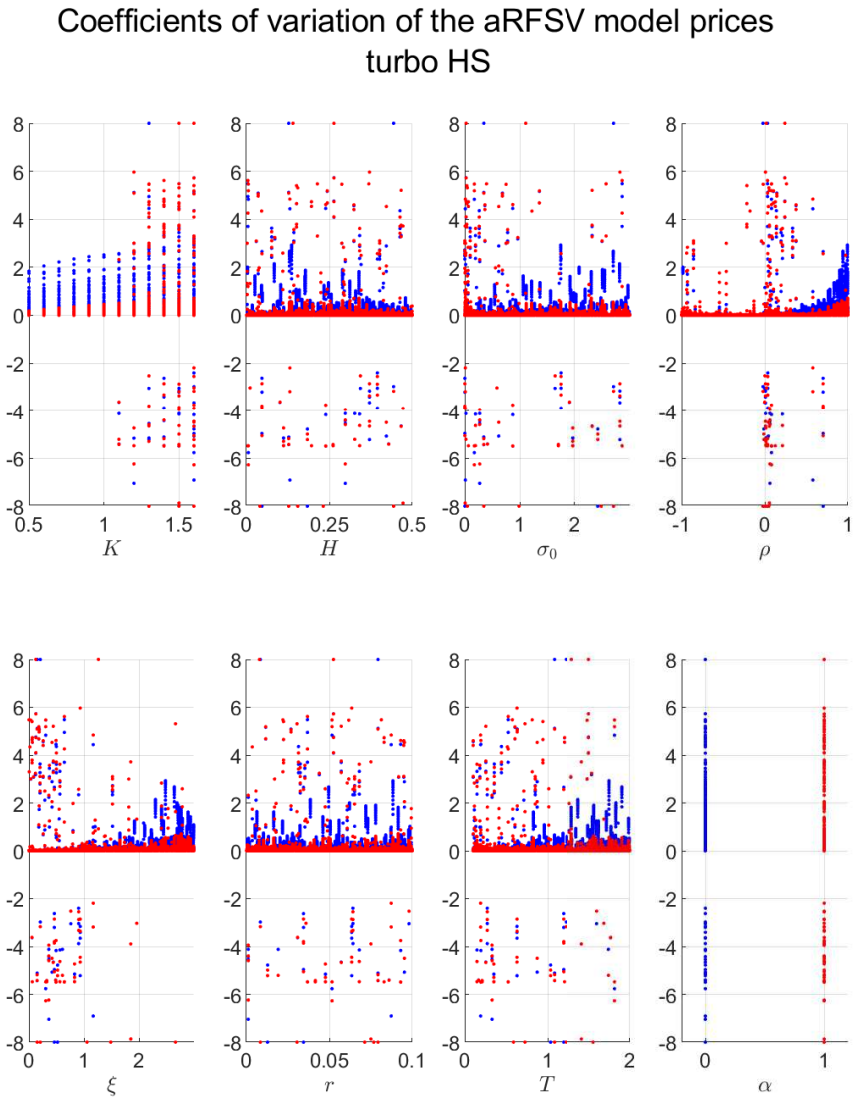

Figure 8: Results of the variance analysis for the rBergomi model $\alpha = 1$ (red) and the RFSV model $\alpha = 0$ (blue). Each point depicts the coefficient of variation (23) computed from 30 batches for the given combination of the model parameters. In each batch, we simulated $P = 1000$ paths, discretized by 4×252 points per $[0, 1]$, using the turbo HS.

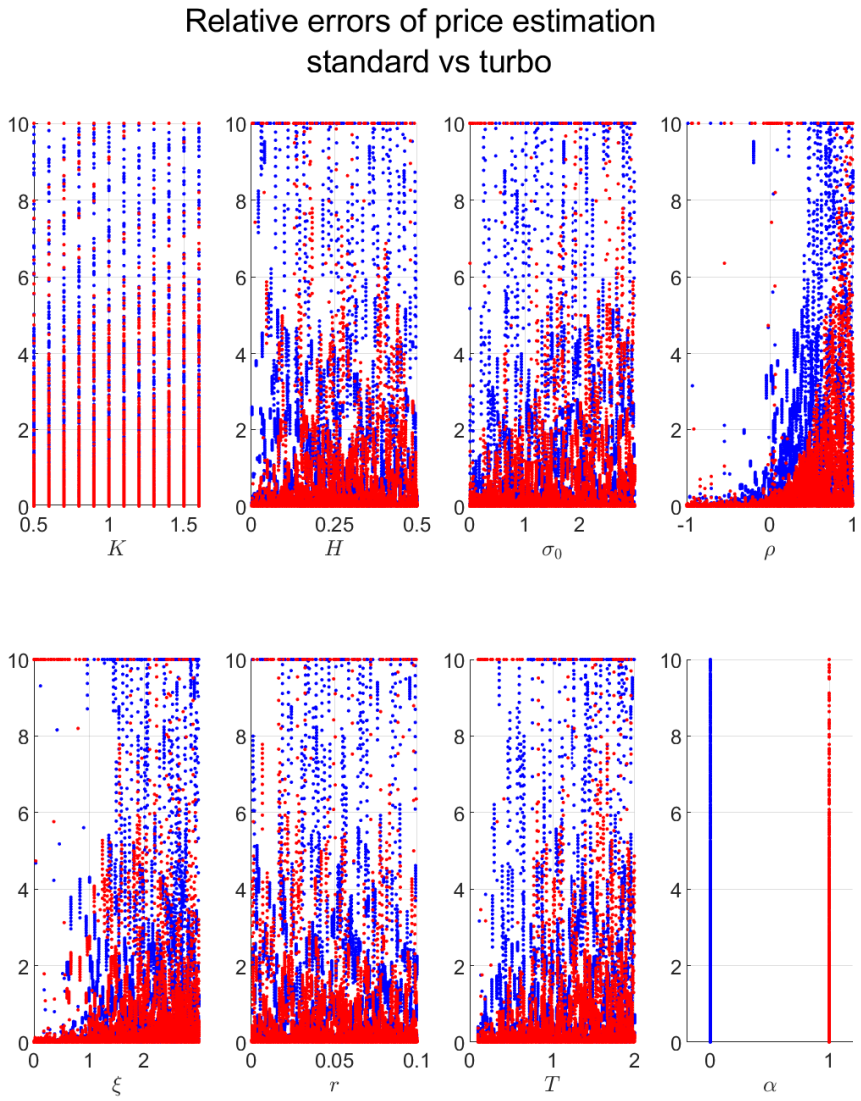

Figure 9: Results of the bias analysis for the rBergomi model $\alpha = 1$ (red) and the RFSV model $\alpha = 0$ (blue). Each point depicts the absolute relative error (24) computed from 30 batches for the given combination of the model parameters. In each batch, we simulated $P = 1000$ paths, discretized by 4×252 points per $[0, 1]$, using the turbo HS and the standard HS.

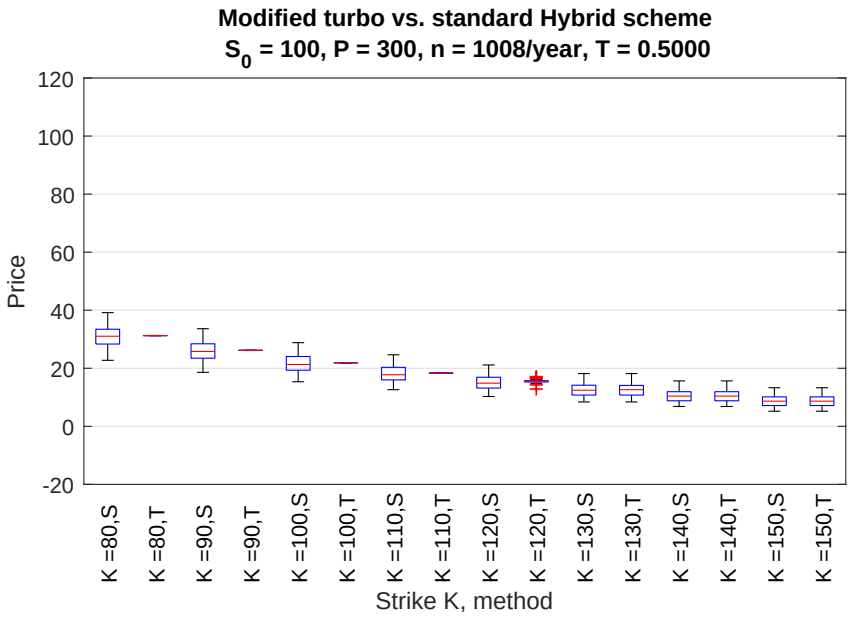

Figure 10: Variance reduction visualization for the modified turbocharged Hybrid scheme w.r.t the standard Hybrid scheme (S). Coefficients of the αRFSV model are set to $\alpha = 1, \sigma_0 = 0.62, H = 0.22, \rho = -0.05, \xi = 0.18$. We generated 30 batches of $P = 300$ paths discretized by 4×252 steps for each strike price K for both methods. The boxplots depict the resulting price estimations. Compare with Figure 5.

4.3.3 Sample Size

When pricing options, we are usually concerned with the accuracy of obtained model prices. Monte Carlo simulations converge with $O(1/\sqrt(P))$, where, in our case, P is the number of trajectories generated thus a question of how many trajectories we need to have a certain accuracy guaranteed arises. By employing a simple confidence interval for the future value of the mean of the stock price process at time T that corresponds to an estimate of the price of an ATM call option with maturity T, we can come to a result that when $P = 100,000$ the length of the 99% confidence interval is smaller than 0.005. The more OTM an option is, the wider the confidence interval is but for reasonable strikes compared to the spot price, the length of the confidence interval should not exceed 0.01. When variance reduction techniques are employed, the number of trajectories required may be smaller but that depends on the combination of model parameters thus we recommend using at least $P = 100,000$ as a safe option even when reduction techniques are used. Also, we recommend using the Cholesky method since it is more time efficient compared to the HS or rDonsker scheme.

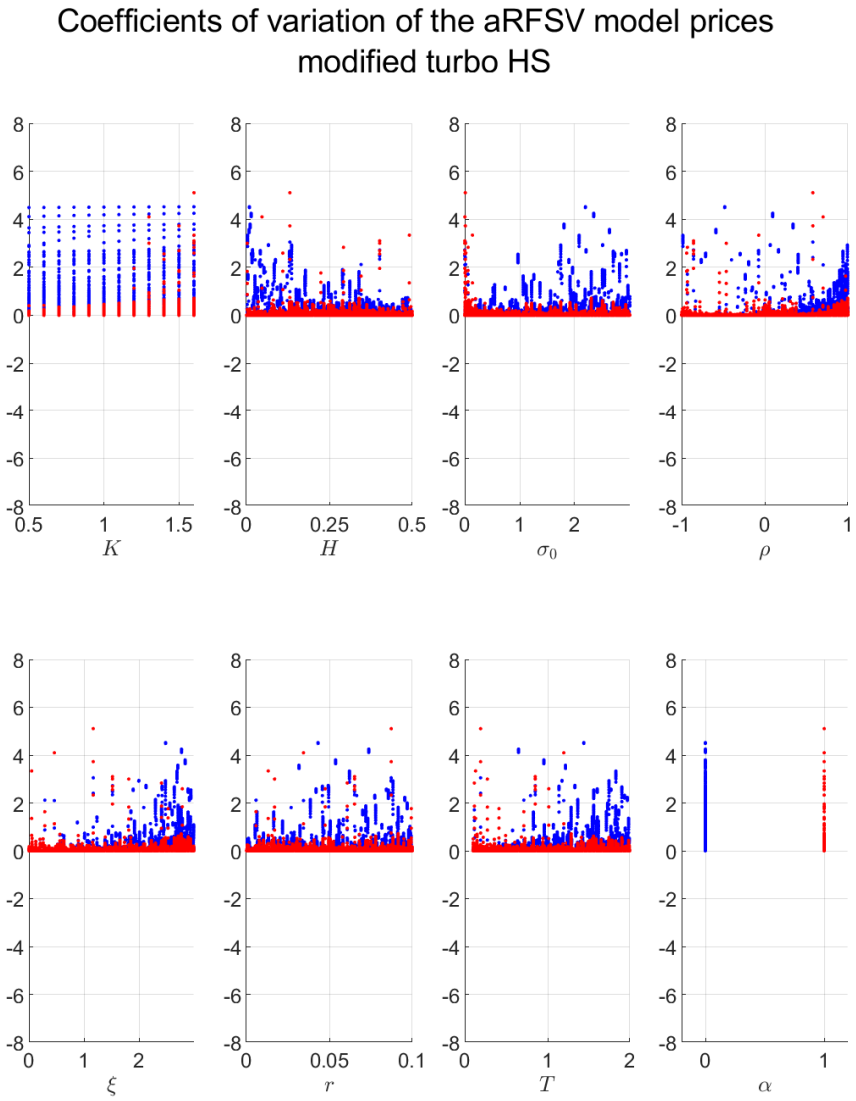

Figure 11: Results of the variance analysis for the rBergomi model $\alpha = 1$ (red) and the RFSV model $\alpha = 0$ (blue). Each point depicts the coefficient of variation (23) computed from 30 batches for the given combination of the model parameters. In each batch, we simulated $P = 1,000$ paths, discretized by 4×252 points per $[0, 1]$, using the modified turbo HS.

5 Conclusion

The main objectives of the paper were rough Volterra stochastic volatility models, in particular the αRFSV model that covers both the RFSV and rBerhomi models, and their MC simulations. We showed that all considered methods (Cholesky method, Hybrid scheme, and rDonskere scheme) are appropriate for the simulation of the αRFSV model and that the rDonsker and HS is faster for small samples of densely discretized paths, while the CM is more efficient for larger samples of path. Although the CM is of cubic complexity, it can get very efficient due to its vector implementation than the FFT implementation of rDS.

Further, we examined the variance reduction techniques for price estimation fulfilled by the turbocharging method applied specifically to the HS. We observed that for $\rho < 0$, the variance is reduced significantly; however, for $\rho > 0$, the turbocharging is not stable, and the variance is, in fact, higher in many cases.

We also analyzed variability of the price estimations for different combinations of the model coefficients. We showed that for certain combinations, the turbocharged HS produces outlying price estimates and that, in some instances, the estimates are heavily biased. In order to prevent excessive and incorrect prices from occurring, we proposed a simple modification of the method that identifies suspicious prices and replaces them with the estimates from the standard HS. Moreover, we recommended using stricter boundary condition $\rho < -0.05$ in order to prevent malfunctions. Using the modified turbo HS for the αRFSV model under the given condition, the variance is being reduced around 60 times on average. Moreover, the average coefficient of variation of price estimation is around 1.5%, while the median around 0.005%.

Writing the paper, several additional questions and issues arose. First of all we showed that none of the studied simulation methods is "perfect", however, we may conclude that the combination of CM and modified turbocharging variance reduction techniques is the most suitable for derivative pricing purposes that use MC simulations of rough Volterra processes. However, it is worth to mention, that other control variate variance reduction techniques might improve the simulations even further, but their investigation is still an open issue.

Only recently an approximation of the price for the αRFSV model was proposed by Merino, Pospíšil, Sobotka, Sottinen, and Vives (2021). Promising numerical properties of the approximation allows to propose a hybrid calibration scheme which combines the approximation formula alongside MC simulations that were analyzed in this paper.

Funding

The work was partially supported by the Czech Science Foundation (GAČR) grant no. GA18-16680S "Rough models of fractional stochastic volatility".

Acknowledgements

This work is a part of the Master's thesis Matas (2021) titled *Rough fractional stochastic volatility models* that was written by Jan Matas and supervised by Jan Pospíšil.

Computational resources were supplied by the project "e-Infrastruktura CZ" (e-INFRA LM2018140) provided within the program Projects of Large Research, Development and Innovations Infrastructures.

References

Alòs, E., León, J. A., and Vives, J. (2007), *On the short-time behavior of the implied volatility for jump-diffusion models with stochastic volatility*. Finance Stoch. 11(4), 571–589, ISSN 0949-2984, DOI 10.1007/s00780-007-0049-1, Zbl 1145.91020, MR2335834.

Alòs, E., Mazet, O., and Nualart, D. (2000), *Stochastic calculus with respect to fractional Brownian motion with Hurst parameter lesser than* $\frac{1}{2}$. Stochastic Process. Appl. 86(1), 121–139, ISSN 0304-4149, DOI 10.1016/S0304-4149(99)00089-7, Zbl 1028.60047, MR1741199.

Asmussen, S. and Glynn, P. (2007), Stochastic Simulation: Algorithms and Analysis. Stoch. Model. Appl. Probab., New York: Springer, ISBN 9780387690339, MR2541632.

Bayer, C., Friz, P., and Gatheral, J. (2016), *Pricing under rough volatility*. Quant. Finance 16(6), 887–904, ISSN 1469-7688, DOI 10.1080/14697688.2015.1099717, MR3494612.

Bennedsen, M., Lunde, A., and Pakkanen, M. S. (2017), *Hybrid scheme for Brownian semistationary processes*. Finance Stoch. 21(4), 931–965, ISSN 0949-2984, DOI 10.1007/s00780-017-0335-5, Zbl 1385.65010, MR3723378.

Comte, F., Coutin, L., and Renault, E. (2012), *Affine fractional stochastic volatility models*. Ann. Finance 8(2–3), 337–378, ISSN 1614-2446, DOI 10.1007/s10436-010-0165-3, Zbl 1298.60067, MR2922801.

Comte, F. and Renault, E. (1998), *Long memory in continuous-time stochastic volatility models*. Math. Finance 8(4), 291–323, ISSN 0960-1627, DOI 10.1111/1467-9965.00057, Zbl 1020.91021, MR1645101.

Cont, R. (2001), *Empirical properties of asset returns: stylized facts and statistical issues*. Quant. Finance 1(2), 223–236, ISSN 1469-7688, DOI 10.1080/713665670, Zbl 1408.62174.

Deya, A., Neuenkirch, A., and Tindel, S. (2012), *A Milstein-type scheme without Lévy area terms for SDEs driven by fractional Brownian motion*. Ann. Inst. Henri Poincaré Probab. Stat. 48(2), 518–550, ISSN 0246-0203, DOI 10.1214/10-AIHP392, Zbl 1260.60135, MR2954265.

Dieker, A. B. (2002), Simulation of fractional Brownian motion. Master's thesis, Vrije Universiteit Amsterdam, revised 2004, URL `http://www.columbia.edu/~ad3217/fbm/thesis.pdf`.

Funahashi, H. and Kijima, M. (2017), *Does the Hurst index matter for option prices under fractional volatility?* Ann. Finance 13(1), 55–74, ISSN 1614-2446, DOI 10.1007/s10436-016-0289-1, Zbl 1398.91588, MR3623799.

Gatheral, J., Jaisson, T., and Rosenbaum, M. (2018), *Volatility is rough*. Quant. Finance 18(6), 933–949, ISSN 1469-7688, DOI 10.1080/14697688.2017.1393551, Zbl 1400.91590, MR3805308.

Glasserman, P. (2003), Monte Carlo methods in financial engineering, vol. 53 of *Appl. Math.* New York: Springer, ISBN 978-0-387-00451-8/hbk; 978-1-4419-1822-2/pbk; 978-0-387-21617-1/e-book, DOI 10.1007/978-0-387-21617-1, Zbl 1038.91045, MR1999614.

Heston, S. L. (1993), *A closed-form solution for options with stochastic volatility with applications to bond and currency options*. Rev. Financ. Stud. 6(2), 327–343, ISSN 0893-9454, DOI 10.1093/rfs/6.2.327, Zbl 1384.35131, MR3929676.

Higham, D. J. (2001), *An algorithmic introduction to numerical simulation of stochastic differential equations*. SIAM Rev. 43(3), 525–546, ISSN 0036-1445, DOI 10.1137/S0036144500378302, Zbl 0979.65007, MR1872387.

Horvath, B., Jacquier, A., and Muguruza, A. (2017), *Functional central limit theorems for rough volatility*, DOI 10.2139/ssrn.3078743, available at arXiv: `https://arxiv.org/abs/1711.03078`.

Hull, J. C. and White, A. D. (1987), *The pricing of options on assets with stochastic volatilities*. J. Finance 42(2), 281–300, ISSN 1540-6261, DOI 10.1111/j.1540-6261.1987.tb02568.x.

Jost, C. (2008), *On the connection between Molchan-Golosov and Mandelbrot- van Ness representations of fractional Brownian motion*. J. Integral Equations Appl. 20(1), 93–119, ISSN 0897-3962, DOI 10.1216/JIE-2008-20-1-93, Zbl 1147.60024, MR2396956.

Kloeden, P. E., Neuenkirch, A., and Pavani, R. (2011), *Multilevel Monte Carlo for stochastic differential equations with additive fractional noise*. Ann. Oper. Res. 189, 255–276, ISSN 0254-5330; 1572-9338/e, DOI 10.1007/s10479-009-0663-8, Zbl 1235.60064, MR2833620.

Kloeden, P. E. and Platen, E. (1992), Numerical solution of stochastic differential equations, vol. 23 of *Probab. Appl.* Berlin: Springer-Verlag, ISBN 978-3-540-54062-5/hbk; 978-3-642-08107-1/pbk; 978-3-662-12616-5/ebook, DOI 10.1007/978-3-662-12616-5, Zbl 0752.60043, MR1214374.

Le Maître, O. P. and Knio, O. M. (2010), Spectral methods for uncertainty quantification. Scientific Computation, Dordrecht: Springer, ISBN 978-90-481-3519-6/hbk; 978-94-007-3192-9/pbk; 978-90-481-3520-2/ebook, DOI 10.1007/978-90-481-3520-2, with applications to computational fluid dynamics, Zbl 1193.76003, MR2605529.

Li, M., Huang, C., and Hu, Y. (2020), *Numerical methods for stochastic Volterra integral equations with weakly singular kernels*, available at arXiv: `https://arxiv.org/abs/2004.04916`.

Mandelbrot, B. B. and Van Ness, J. W. (1968), *Fractional Brownian motions, fractional noises and applications*. SIAM Rev. 10(4), 422–437, ISSN 0036-1445, DOI 10.1137/1010093, Zbl 0179.47801, MR0242239.

Matas, J. (2021), Rough fractional stochastic volatility models. Master's thesis, University of West Bohemia.

Matas, J. and Pospíšil, J. (2021), *Robustness and sensitivity analyses for rough Volterra stochastic volatility models*, available at arXiv: `http://arxiv.org/a/0000-0002-4288-1614`.

McCrickerd, R. and Pakkanen, M. S. (2018), *Turbocharging Monte Carlo pricing for the rough Bergomi model*. Quant. Finance 18(11), 1877–1886, ISSN 1469-7688, DOI 10.1080/14697688.2018.1459812, Zbl 1406.91486, MR3867719.

Merino, R., Pospíšil, J., Sobotka, T., Sottinen, T., and Vives, J. (2021), *Decomposition formula for rough Volterra stochastic volatility models*. Int. J. Theor. Appl. Finance 24(2), 2150008, ISSN 0219-0249, DOI 10.1142/S0219024921500084.

Milstein, G. N. (1995), Numerical integration of stochastic differential equations, vol. 313 of *Mathematics and its Applications*. Dordrecht: Kluwer Academic Publishers, ISBN 0-7923-3213-X, DOI 10.1007/978-94-015-8455-5, translated and revised from the 1988 Russian original, Zbl 0810.65144, MR1335454.

Milstein, G. N. and Tretyakov, M. V. (2004), Stochastic numerics for mathematical physics. Scientific Computation, Berlin: Springer-Verlag, ISBN 3-540-21110-1/hbk; 978-3-642-05930-8/pbk, DOI 10.1007/978-3-662-10063-9, Zbl 1085.60004, MR2069903.

Mishura, Y. (2008), Stochastic calculus for fractional Brownian motion and related processes, vol. 1929 of *Lecture Notes in Mathematics*. Springer-Verlag, Berlin, ISBN 978-3-540-75872-3, DOI 10.1007/978-3-540-75873-0, MR2378138.

Molchan, G. M. and Golosov, J. I. (1969), *Gaussian stationary processes with asymptotic power spectrum*. Sov. Math. Dokl. 10, 134–137, ISSN 0197-6788, translation from Dokl. Akad. Nauk SSSR 184, 546–549 (1969), Zbl 0181.20704, MR0242247.

Pospíšil, J., Sobotka, T., and Ziegler, P. (2019), *Robustness and sensitivity analyses for stochastic volatility models under uncertain data structure*. Empir. Econ. 57(6), 1935–1958, ISSN 0377-7332, DOI 10.1007/s00181-018-1535-3.

Richard, A., Tan, X., and Yang, F. (2020), *Discrete-time simulation of stochastic Volterra equations*, available at arXiv: https://arxiv.org/abs/2004.00340.

Xiu, D. (2010), Numerical methods for stochastic computations. Princeton, NJ: Princeton University Press, ISBN 978-0-691-14212-8/hbk, a spectral method approach, Zbl 1210.65002, MR2723020.

Yin, Z.-M. (1996), *New methods for simulation of fractional brownian motion*. J. Comput. Phys. 127(1), 66–72, ISSN 0021-9991, DOI 10.1006/jcph.1996.0158, Zbl 0859.65145.

Robustness and sensitivity analyses of rough Volterra stochastic volatility models

Jan Matas[1] and Jan Pospíšil*[1]

[1]NTIS - New Technologies for the Information Society, Faculty of Applied Sciences, University of West Bohemia, Univerzitní 2732/8, 301 00 Plzeň, Czech Republic,

Received 26 July 2021

Abstract

In this paper we perform robustness and sensitivity analysis of several continuous-time rough Volterra stochastic volatility models with respect to the process of market calibration. Robustness is understood in the sense of sensitivity to changes in the option data structure. The the latter analysis consists of statistical tests to determine whether a given studied model is sensitive to the changes in the option data structure. Empirical study is performed on a data set of Apple Inc. equity options traded in four different days in April and May 2015. In particular, the results for RFSV, rBergomi and aRFSV models are provided.

Keywords: Volterra stochastic volatility; rough volatility; rough Bergomi model; robustness analysis; sensitivity analysis

MSC classification: 62F35; 62F40; 60G22; 91G20; 91G70; 91G60

JEL classification: C52; C58; G12; C63; C12

Contents

*Corresponding author, honik@kma.zcu.cz

1 Introduction

In the field of mathematical finance, the stochastic volatility (SV) models are widely used to evaluate derivative securities such as options. The SV models do not only assume that the asset price follows a specific stochastic process but also that the instantaneous volatility of asset returns is of random nature.

The origin of these models goes back to the paper by Hull and White (1987) however the SV models became particularly popular thanks to the model by Heston (1993), in which the volatility is modeled by the mean-reverting square root process. This model became popular among both practitioners and academics.

Although many other SV models have been proposed since then, it seems that none of them can be considered to be the universal best market practice approach. Some models may perform well when calibrated to real market data with complex volatility surfaces but at the same time, they can suffer from over-fitting or they might not be robust to the changes in the option data structure as it is described by Pospíšil, Sobotka, and Ziegler (2019). Moreover, a model with a good fit to an implied volatility surface might not be in-line with the observed properties of the corresponding realized volatility time series.

One sever limitation of the classical SV models might be for example the independence of increments of the driving Brownian motion. This motivated Comte and Renault (1998), Comte, Coutin, and Renault (2012), and independently for example Alòs, León, and Vives (2007) to consider the fractional Brownian motion (fBm) as the driving process since the fBm is a generalization of the Brownian motion which allows correlation of increments depending on the so-called Hurst index $H \in (0, 1)$. For $H > 1/2$, the increments are positively correlated and the process has the so-called long memory property. For $H < 1/2$, the increments are negatively correlated and we speak about the short memory or more recently about the so-called rough regime. Gatheral, Jaisson, and Rosenbaum (2018) showed empirically that $H < 1/2$ by estimating it from the realized volatility time series of major stock indexes and argues that the RFSV model is more consistent with the reality.

In this paper, we consider the αRFSV model recently introduced by Merino, Pospíšil, Sobotka, Sottinen, and Vives (2021). This model unifies and generalizes the RFSV model ($\alpha = 1$) and the rBergomi model ($\alpha = 0$). For the pricing of a European call, we employ Monte-Carlo (MC) simulations using the Cholesky method equipped with the control variate variance reduction technique as it is suggested by Matas and Pospíšil (2021).

We then calibrate the model to a real market dataset and analyze its robustness to the changes in option data structure (options of different combinations of strikes and expiration dates may be available for trading in different days) using the methodology proposed by Pospíšil, Sobotka, and Ziegler (2019) which is based on data bootstrapping. In this paper authors showed that pricing using the classical SV models such as Heston (1993) and Bates (1996) models is highly sensitive to changes in option data structure. More robust results were obtained for the long-memory approximative fractional SV model, but not for all considered datasets. Then, a natural question arises: can the RFSV models perform better? Apparently, the answer is yes as we show in this paper. Since the RFSV models belong to a wider class of the rough Volterra processes, the presented methodology is applicable to this wider class as well.

The structure of the paper is the following. In Section 2, we introduce the studied rough Volterra stochastic volatility models. In Section 3, we describe the methodology, in particular the calibration of considered models to real market data. We describe the bootstrapping of option data, as well as the details of the robustness and sensitivity analyses. In Section 4, we summarize the obtained calibration results by comparing all the models in terms of variation in model parameters and in bootstrapped option model prices. We also test the roughness parameter and the parameter α for significance. Then, we provide the results of the sensitivity analysis fulfilled by a Monte Carlo filtering technique, testing whether a given studied model is sensitive to the changes in the option data structure when being calibrated. We conclude all obtained results in Section 5.

2 Preliminaries and notation

2.1 Volterra volatility process

Let $W = (W_t, t \geq 0)$ be a standard Wiener process defined on a probability space $(\Omega, \mathcal{F}, Q)$ and let $\mathcal{F}^W = (\mathcal{F}_t^W, t \geq 0)$ be the filtration generated by W. We consider a *general Volterra volatility process* defined as

$$\sigma_t := g(t, Y_t), \quad t \geq 0, \tag{1}$$

where $g : [0, +\infty) \times \mathbb{R} \mapsto [0, +\infty)$ is a deterministic function such that σ_t belongs to $L^1(\Omega \times [0, +\infty))$ and $Y = (Y_t, t \geq 0)$ is the *Gaussian Volterra process*

$$Y_t = \int_0^t K(t, s)\, \mathrm{d}W_s, \tag{2}$$

where $K(t, s)$ is a kernel such that for all $t > 0$

$$\int_0^t K^2(t, s)\, \mathrm{d}s < \infty, \tag{A1}$$

and

$$\mathcal{F}_t^Y = \mathcal{F}_t^W. \tag{A2}$$

By $r(t, s)$ we denote the autocovariance function of Y_t and by $r(t)$ the variance

$$\begin{aligned} r(t, s) &:= \mathbb{E}[Y_t Y_s], \quad t, s \geq 0, \\ r(t) &:= r(t, t) = \mathbb{E}[Y_t^2], \quad t \geq 0. \end{aligned} \tag{3}$$

In particular we will model volatility as the *exponential Volterra volatility process*

$$\sigma_t = g(t, Y_t) = \sigma_0 \exp\left\{\xi Y_t - \frac{1}{2}\alpha \xi^2 r(t)\right\}, \quad t \geq 0, \tag{4}$$

where $(Y_t, t \geq 0)$ is the Gaussian Volterra process (2) satisfying assumptions (A1) and (A2), $r(t)$ is its autocovariance function (3), and $\sigma_0 > 0$, $\xi > 0$ and $\alpha \in [0, 1]$ are model parameters.

A very important example of Gaussian Volterra processes is the *standard fractional Brownian motion* (fBm) B_t^H (the exponent H has the meaning of index, not power)

$$B_t^H = \int_0^t K(t, s)\, \mathrm{d}W_s, \tag{5}$$

where $K(t, s)$ is a kernel that depends also on the Hurst parameter $H \in (0, 1)$. Recall that the autocovariance function of B_t^H is given by

$$r(t, s) := \mathbb{E}[B_t^H B_s^H] = \frac{1}{2}\left(t^{2H} + s^{2H} - |t - s|^{2H}\right), \quad t, s \geq 0, \tag{6}$$

and in particular $r(t) := r(t, t) = t^{2H}$, $t \geq 0$.

Nowadays, the most precise Volterra representation of fBm is the one by Molchan and Golosov (1969)

$$B_t^H := \int_0^t K_H(t, s)\, \mathrm{d}W_s, \tag{7}$$

where

$$K_H(t,s) := C_H\left[\left(\frac{t}{s}\right)^{H-\frac{1}{2}}(t-s)^{H-\frac{1}{2}} - \left(H-\frac{1}{2}\right)s^{H-\frac{1}{2}}\int_s^t z^{H-\frac{3}{2}}(z-s)^{H-\frac{1}{2}}\,\mathrm{d}z\right] \tag{8}$$

$$C_H := \sqrt{\frac{2H\Gamma\left(\frac{3}{2}-H\right)}{\Gamma\left(H+\frac{1}{2}\right)\Gamma\left(2-2H\right)}}.$$

To understand the connection between Molchan-Golosov and other representations of fBm such as the original Mandelbrot and Van Ness (1968) representation, we refer readers to the paper by Jost (2008).

There exists various methods how to simulate the fractional Brownian motion numerically. We often divide these methods into two classes: exact methods and approximate methods (Dieker 2002). We focus on more accurate exact methods that usually exploit the covariance function (6) of the fBm to simulate exactly the fBm (the output of the method is a sampled realization of the fBm) without the necessity to treat the complicated Volterra kernel. In particular, the Cholesky method use a covariance matrix to generate the fBm from two independent normal samples. Despite its higher computational complexity, this method has already proved to be the most suitable for simulation of the volatility models, see below.

2.2 Rough Volterra volatility models

Let $S = (S_t, t \in [0,T])$ be a strictly positive asset price process under a market chosen risk neutral probability measure Q that follows the stochastic dynamics:

$$\mathrm{d}S_t = rS_t\,\mathrm{d}t + \sigma_t S_t\left(\rho\,\mathrm{d}W_t + \sqrt{1-\rho^2}\,\mathrm{d}\widetilde{W}_t\right), \tag{9}$$

where S_0 is the current *spot* price, $r \geq 0$ is the all-in interest rate, W_t and $\widetilde{W}_t$ are independent standard Wiener processes defined on a probability space $(\Omega, \mathcal{F}, Q)$ and $\rho \in [-1,1]$ represents the correlation between W_t and $\widetilde{W}_t$.

Let $\mathcal{F}^W$ and $\mathcal{F}^{\widetilde{W}}$ be the filtrations generated by W and $\widetilde{W}$ respectively and let $\mathcal{F} := \mathcal{F}^W \cup \mathcal{F}^{\widetilde{W}}$. The *stochastic volatility process* σ_t is a square-integrable Volterra process assumed to be adapted to the filtration generated by W and its trajectories are assumed to be a.s. càdlàg and stricly positive a.e. exponential Volterra volatility process satisfies these properties).

For convenience we let $X_t = \ln S_t$, $t \in [0,T]$, and consider the model

$$\mathrm{d}X_t = \left(r - \frac{1}{2}\sigma_t^2\right)\mathrm{d}t + \sigma_t\left(\rho\,\mathrm{d}W_t + \sqrt{1-\rho^2}\,\mathrm{d}\widetilde{W}_t\right). \tag{10}$$

Recall that $Z := \rho W + \sqrt{1-\rho^2}\widetilde{W}$ is a standard Wiener process.

In this paper we will study the αRFSV model firstly introduced by Merino, Pospíšil, Sobotka, Sottinen, and Vives (2021). In this model, the volatility is modelled as the exponential Volterra process with fBm, i.e.

$$\sigma_t = \sigma_0 \exp\left\{\xi B_t^H - \frac{1}{2}\alpha\xi^2 r(t)\right\}, \quad t \geq 0, \tag{11}$$

where $\sigma_0 > 0$, $\xi > 0$ and $\alpha \in [0,1]$ are model parameters together with empirical $H < 1/2$ that guarantees the *rough* regime. For $\alpha = 0$ we get the RFSV model (Gatheral, Jaisson, and Rosenbaum 2018), for $\alpha = 1$ the rBergomi model (Bayer, Friz, and Gatheral 2016).

While both cases of the αRFSV model are more likely to replicate the stylized facts of volatility (Gatheral, Jaisson, and Rosenbaum 2018) even by using relatively small number of parameters (σ_0, ξ, ρ, H), the issue is the non-markovianity of the model. Because of this, we cannot derive any semi-closed form solution using the standard Itô calculus nor the Heston's framework. Therefore, to

price even vanilla options, we have to rely on Monte-Carlo (MC) simulations. For these purposes, a modified Cholesky method will be used together with the control variate variance reduction technique as it was described by Matas and Pospíšil (2021).

We close this section by mentioning, that there exists yet another pricing approach that takes advantages of the so called approximation formula derived by Merino, Pospíšil, Sobotka, Sottinen, and Vives (2021). This formula can be used either as a standalone fast approximation or together with the MC simulations to speed up the calibration tasks. However, in this paper we will focus on rbustness and sensitivity analyses based on pricing approaches that are as accurate as possible and this can be achieved currently only by the MC simulations that use exact simulation technique for fBm.

3 Methodology

In this section, we describe the methodology for calibrations of the rough Volterra models to real market data and we focus on the robustness and sensitivity analysis.

3.1 Calibration to market data

Model calibration constitutes a way to estimate model parameters from available market data. The alternative approach suggests estimating the parameters directly from time series data such as for example Gatheral, Jaisson, and Rosenbaum (2018) did for the Hurst parameter. We understand model calibration as the problem of estimating the model parameters by fitting the model to market data with pre-agreed accuracy.

Mathematically, we express the calibration problem as an optimization problem

$$\inf_{\Theta} G(\Theta), \quad G(\Theta) = \sum_{i=1}^{N} w_i [C_i^{\Theta}(T_i, K_i) - C_i^{\text{mkt}}(T_i, K_i)]^2, \tag{12}$$

where $C_i^{\text{mkt}}(T_i, K_i)$ is the observed market price of the ith option, $i = 1, \ldots, N$, with time to maturity T_i and of strike price K_i, while w_i is a weight and $C^{\Theta}(T_i, K_i)$ denotes the option price computed under the model with a vector of parameters Θ. For αRFSV, we have $\Theta = [\sigma_0, \rho, H, \xi, \alpha]$.

In fact, the representation of the calibration problem in (12) is a non-linear weighted least squares problem. To obtain a reasonable output, we have to assume that the market prices are correct, i.e., there is no inefficiency in the prices, which is usually not the case, especially for options being further ITM or OTM. To fix this, let us assume that the more an option is traded, the more accurate the price is. We can then weight the importance of a given option in the least squares problem by the traded volume of the given option. However, there is also another, and in fact a more convenient and popular way to implement weights. We can get the information of uncertainty about the price of an option from its bid-ask spread. The greater the bid-ask spread, the more uncertainty (and usually less trading volume) there is about the price. Therefore, we will use functions of bid and ask prices as the weights thus $w_i = g(C_i^{\text{bid}} - C_i^{\text{ask}})$, where $g(x)$ can be, for example, $1/x^2, 1/|x|, 1/\sqrt{x}$, etc. Based on the empirical results (Mrázek, Pospíšil, and Sobotka 2016), we will consider only the case $g(x) = 1/x^2$.

Because the objective function is non-linear, we cannot solve the problem analytically as in the case of standard linear regression. Hence, we revert to iterative numerical optimizers.

For the minimization of (12), we use the MATLAB function `lsqnonlin()` that implements an interior trust region algorithm, described by Coleman and Li (1996). The algorithm assumes, among other things, that the target function is convex. However, we cannot even show the convexity of the target function since we have no analytical expression to describe it. Therefore, if the algorithm ends up in a local minimum, it is not guaranteed that it is the global minimum.

In fact, the target function can have more than one local minimum (the source is the non-linearity of the model price function). To determine the initial point for gradient-based `lsqnonlin()`,

we use another MATLAB function `ga()` that implements a genetic algorithm minimization approach. It deploys a predefined number[1] of initial points across the domain of the function and then, each point serves as an initial condition for minimization that is performed for a pre-defined number of steps. Based on genetic rules of random mutation, crossbreeding, and preservation of the fittest, the most successful points are preserved, perturbated by a random mutation, and crossbred among themselves. This approach (Mrázek, Pospíšil, and Sobotka 2016) has been shown to produce sound results.

To measure the quality of the fit of a calibrated model, we use the following metrics. Having N options in the data set, we denote C_i^{mkt} the market price of the ith option and $\tilde{C}_i$ the estimated price of the ith option based on the calibrated model. Denoting S_0 the spot price, the first metric is the *average relative fair value* (ARFV) and the second one is the *maximum relative fair value* (MRFV). They can be expressed as

$$ARFV = \frac{1}{N}\sum_{i=1}^{N}\frac{\left|\tilde{C}_i - C_i^{\text{mkt}}\right|}{S_0}, \qquad MRFV = \max_{i=1,\dots,N}\frac{\left|\tilde{C}_i - C_i^{\text{mkt}}\right|}{S_0}.$$

It is worth to mention that these measures offer a better error understanding than the originally used *average absolute relative error* (AARE) and *maximum absolute relative error* (MARE)

$$AARE = \frac{1}{N}\sum_{i=1}^{N}\frac{\left|\tilde{C}_i - C_i^{\text{mkt}}\right|}{C_i^{\text{mkt}}}, \qquad MARE = \max_{i=1,\dots,N}\frac{\left|\tilde{C}_i - C_i^{\text{mkt}}\right|}{C_i^{\text{mkt}}}.$$

3.2 Robustness analysis

We calibrate the αRFSV model the way described in the previous section to a real market dataset. In the ideal hypothetical case, all combinations of strikes and times to maturity for a given option would be available, i.e., we would have a continuous price surface to which we would calibrate a selected model. However, in the reality, we have only a finite number of different options available to trade and moreover, the combinations of strikes and times to maturities (we call that the option data structure) changes and even the number of combinations itself changes over time. Therefore the obtained coefficient estimates can differ, should the model calibration be sensitive to the option data structure.

In this paper, we understand *robustness* as the property of a model that conveys the sensitivity of the model being calibrated to changes in the option structure. To study the robustness of the αRFSV model, we use the methodology suggested by Pospíšil, Sobotka, and Ziegler (2019). Therefore, our results of the robustness analysis of the αRFSV model are comparable with those of the Heston, Bates, and the AFSVJD model, presented in the referenced paper.

To analyze robustness, we have to simulate the changes in the option structure. To do this, we employ bootstrapping of given option structures. Bootstrapping is a technique when random samples are selected with replacement from the initial dataset. For example, to bootstrap the data set $(X_1, X_2, \dots, X_6)$, we need to generate uniformly distributed random integers from $\{1, 2, \dots, 6\}$. Suppose the realization is $\{2, 3, 5, 4, 4, 3\}$. Then, the obtained bootstrapped sample is $(X_2, X_1, X_5, X_4, X_4, X_3)$.

Mathematically, an option structure is the set of all the combinations of strikes K and times to maturity T available for trading in a given day. Having market data consisting of N options, the set $\mathcal{X} = \{(K_i, T_i), i = 1, \dots, N\}$ is the option structure for the given day where each option has the market price $C_i^{\text{mkt}} = C^{\text{mkt}}(K_i, T_i)$.

By bootstrapping $\mathcal{X}$ in total of M times, we obtain M new option structures $\mathcal{X}_1, \dots, \mathcal{X}_M$. Then each $\mathcal{X}_j$, together with the option prices from the initial dataset assigned to the corresponding combinations of strikes and times to maturities, produces bootstrapped sample B_j. Next, we calibrate the model separately to each B_j and obtain estimates of the model parameters and

[1] We use 150 points.

model prices for each. Let us denote $\tilde{\Theta}_j$ the parameter estimates obtained from the bootstrapped sample B_j, and $\tilde{C}^j = [\tilde{C}_1^j, \ldots, \tilde{C}_N^j]$, where $\tilde{C}_i^j = \tilde{C}_i^j(K_i, T_i)$, is the vector of corresponding model prices.

Having the results of the calibrations from $B_1, \ldots, B_M$, we can compute the bootstrap estimates of the parameters and models prices. The bootstrap estimate of a parameter is the mean across all the estimated parameters:

$$\hat{\Theta} = \frac{1}{M} \sum_{i=1}^{M} \tilde{\Theta}_i \tag{13}$$

and the bootstrap estimate of a model price of the ith option is

$$\hat{C}_i = \frac{1}{M} \sum_{j=1}^{M} \tilde{C}_i^j.$$

Next, we look at the variance of the errors of the price estimates of the ith option $\left|\tilde{C}_i^j - C_i^{\text{mkt}}\right|$. However, to be able to better compare the variances among different options, we normalize the error. Then, let us denote

$$V_i = \text{Var}\left[\frac{\left|\tilde{C}_i^j - C_i^{\text{mkt}}\right|}{C_i^{\text{mkt}}}\right] \tag{14}$$

the variance of the normalized errors of the ith option. It is also useful to examine the *bootstrap relative error* (BRE) for the ith option:

$$BRE_i = \frac{\left|\hat{C}_i - C_i^{\text{mkt}}\right|}{C_i^{\text{mkt}}} = \frac{\left|\frac{1}{M}\sum_{j=1}^{M}(\tilde{C}_i^j - C_i^{\text{mkt}})\right|}{C_i^{\text{mkt}}}. \tag{15}$$

We analyze variation in coefficients visually by plotting a scatter plot matrices. Denoting d the number of model coefficients being calibrated, the scatter plot matrix is a $d \times d$ matrix, where histograms for each coefficient are on the diagonal, and 2D scatter plots of corresponding values of coefficients elsewhere. Hence, from a scatter plot matrix, we get a grasp of the distributions of coefficients and also whether there is any dependence between pairs of coefficients and variation in the estimates.

3.3 Sensitivity analysis

In this paper, we use a similar method to carry out a sensitivity analysis introduced by Pospíšil, Sobotka, and Ziegler (2019) based on the ideas of Saltelli, Ratto, Andres, Campolongo, Cariboni, Gatelli et al. (2008). In short, we aim to test whether the αRFSV model is sensitive to changes in option structure through a given parameter.

In our context, we chose the following Monte-Carlo filtering technique[2]: To each vector of calibrated model parameters obtained from the bootstrapped data, we calculate the average relative fair value (ARFV) as a quality measure for the calibrated model fit. Then, we separate the calibrated models into three groups: (I) the calibrated models with the corresponding values of the ARFV up to the third octile, (II) the models with the ARFV between the third and the fifth octile, and (III) the models with the ARFV above the fifth octile. Next, for each calibrated parameter, we compare the distribution of the parameter estimates corresponding to models from group (I) with the distribution from group (III). We use the Kolmogorov-Smirnov test for the comparison. The null hypothesis is that the parameter estimates from group (I) comes from the same distribution as those from group (III).

[2]For more details on Monte-Carlo filtering approaches see, for instance Saltelli, Ratto, Andres, Campolongo, Cariboni, Gatelli et al. (2008).

4 Numerical results

In this section we present the results of the calibration and the robustness analysis of the αRFSV model. For that purpose, we used the same real market dataset as in the paper by Pospíšil, Sobotka, and Ziegler (2019).

4.1 Data description

We operate with a real market dataset that consists of market prices of call options on Apple Inc. stock (NASDAQ: AAPL) quoted on four days of 2015: 04/01, 04/15, 05/01, 05/15. Naturally, the combinations of strikes and times to maturity of the options (the option data structure) change over time. There are 113 options in the option chain on the first day. The second day, the total number of different options rises to 158, the next day to 201, and the last day decreases to 194.

For convenience we visualize the data from May, 15, in Figure 1, in order to give some perspective. For each listed call option with the strike K and time to maturity T, a disk is plotted with center in (K, T). The diameter of the disk relates to the price of the option.

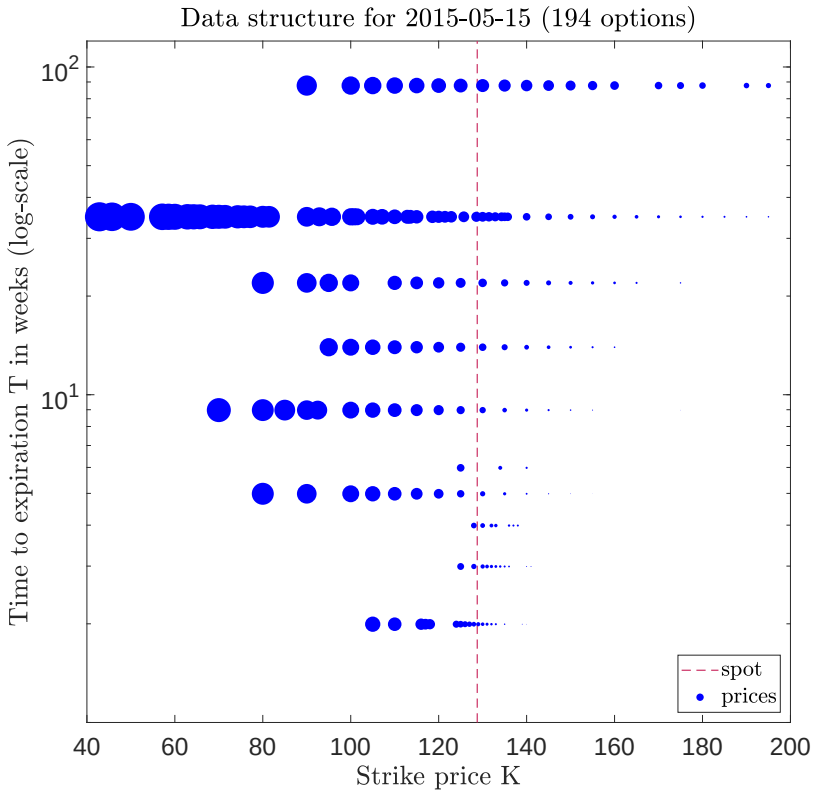

Figure 1: Call option data structure for AAPL dataset from May, 15, 2015. The positions of disks are given by the combinations of the strikes K on the x-axis and the maturities T on the y-axis of the options listed at the time. The diameter of each disk relates to the corresponding close price.

4.2 Calibration routine

In order to calibrate the αRFSV model, we use the Cholesky method with the modified turbocharging method introduced by Matas and Pospíšil (2021) and we follow the recommendation given there to employ at least $P = 150,000$ paths discretized by $n = 4 \times 252$ per interval $[0, 1]$,

so the pricing method assures sufficient accuracy. Then, we are able to price any option with $T < T_{\max}$ from the paths, which were already simulated, by truncating them to corresponding interval $[0, T]$.

We tried to use different weights[3] for the target function (12), but the best results were obtained for the weight type

$$w_i = \frac{1}{\left(C_i^{\text{bid}} - C_i^{\text{ask}}\right)^2}, \tag{16}$$

which aligns with the results in Mrázek, Pospíšil, and Sobotka (2016) for other SV models. For that reason, we present only the results for this type of weights. To compare weighted prices with the market prices, see Figure 2 and 1.

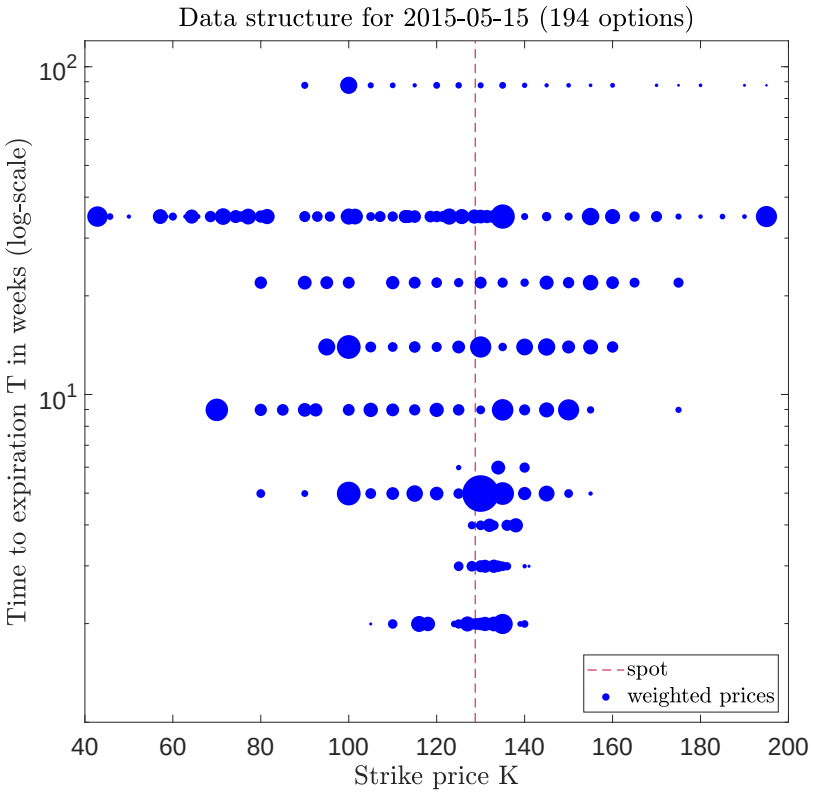

Figure 2: Example of the options call data structure for AAPL call option prices from May, 15, 2015, weighted by (16). The positions of disks are given by the combinations of the strikes K on the x-axis and the maturities T on the y-axis of the options listed at the time. The diameter of each disk relates to the corresponding weighted close price. Compare with Figure 1.

4.3 Overall calibration

First, we summarize the results of the calibrations to the market data. Then, we compare the results to those obtained for other SV models in Pospíšil, Sobotka, and Ziegler (2019) where different SV models were analyzed using similar methods and the identical dataset. For the comparison, we adopt Table 1 from the mentioned paper as Table 1. It contains AAREs of of the calibrated Heston, Bates, and AFSVJD models. Lastly, we test the significance of the H and α parameters.

[3]Having $w_i = g(C_i^{\text{bid}} - C_i^{\text{ask}})$, we tried $g(x) = \frac{1}{x^2}$, $g(x) = \frac{1}{|x|}$, and $g(x) = \frac{1}{\sqrt{x}}$.

Table 1: Average ($AARE$) of overall calibrations of the Heston, Bates, and AFSVJD models for the same dataset as we use, reprint of (Pospíšil, Sobotka, and Ziegler 2019, Table 1).

Trading day	1/4/2015	15/4/2015	1/5/2015	15/5/2015
Heston	5.15%	3.79%	6.58%	3.39%
Bates	3.73%	3.57%	5.77%	3.41%
AFSVJD	2.21%	2.16%	5.89%	3.20%

Table 2: Lower and upper bounds for the model coefficients we considered for the overall calibration.

Coefficient	σ_0	ρ	H	ξ	α
Lower bound	0.01	-1	0.05	0.01	0
Upper bound	0.20	-0.05	0.25	3	1

For the MATLAB function `ga()`, we set the number of initial points on 150 and the number of iterations on 5, as more than 5 did not make much significant improvement. For `lsqnonlin()`, which is ran after `ga()` and which further minimizes its output, we set the tolerance on the value of the target function on 10^{-6} and the tolerance on the norm of the difference between two subsequent points on 10^{-7}. Although the global optimization part is heavily time consuming, it is crucial in the situations when any initial guess is available to be used for the local optimization part that is significantly faster for obvious reasons. The whole procedure takes just a couple of minutes on a personal computer and no supercomputing power is necessary.

The bounds of the coefficients considered for the calibration are summarized in Table 2. While the bounds $\sigma_0 > 0$ and $\rho > -1$ are naturally arising from the definition of the αRFSV model, the upper bound for σ_0 and the bounds for ξ were determined based on several test calibrations such that they provided a suitable area for the genetic algorithm while not limiting the calibration procedure in finding the global maximum. The upper bound $\rho \geq -0.05$ is based on the recommendation given in Matas and Pospíšil (2021) and the range for the Hurst parameter was set as $0.05 \leq H \leq 0.25$ which is, according to Bennedsen, Lunde, and Pakkanen (2016), a common range for H based on estimates for 2000 different equities.

Table 3: Average ($AARE$) of overall calibrations of the RFSV, rBergomi, and αRFSV models.

Trading day	1/4/2015	15/4/2015	1/5/2015	15/5/2015
RFSV	27.03%	7.00%	7.38%	7.48%
rBergomi	6.46%	6.99%	9.74%	15.63%
αRFSV	5.74%	6.70%	9.71%	11.20%

Table 3 presents the results of the overall calibration procedure for the studied models. We can see that for the first two days, rBergomi provides better fits than RFSV. For the next two days, the situation reverses and the fits obtained by RVSF are superior to those obtained by rBergomi. An interesting result is that the αRFSV model that unifies the two models by introducing a new parameter α that fulfills the role of the weight between the models fits the data in the most consistent way. We discovered that for the first two days, the parameter α is closer to 1 which corresponds to the rBergomi model and the next two days, α leans towards 0 thus the RFSV model. However, the αRFSV model does not always provide the best fit.

Comparing the values of AARE in Table 3 to those obtained for other SV models tabulated in Table 1, we can observe that the rough models do not provide better fits than the SV models. Nevertheless, rough models, as we will see in the next sections, are much more robust compare to the SV models.

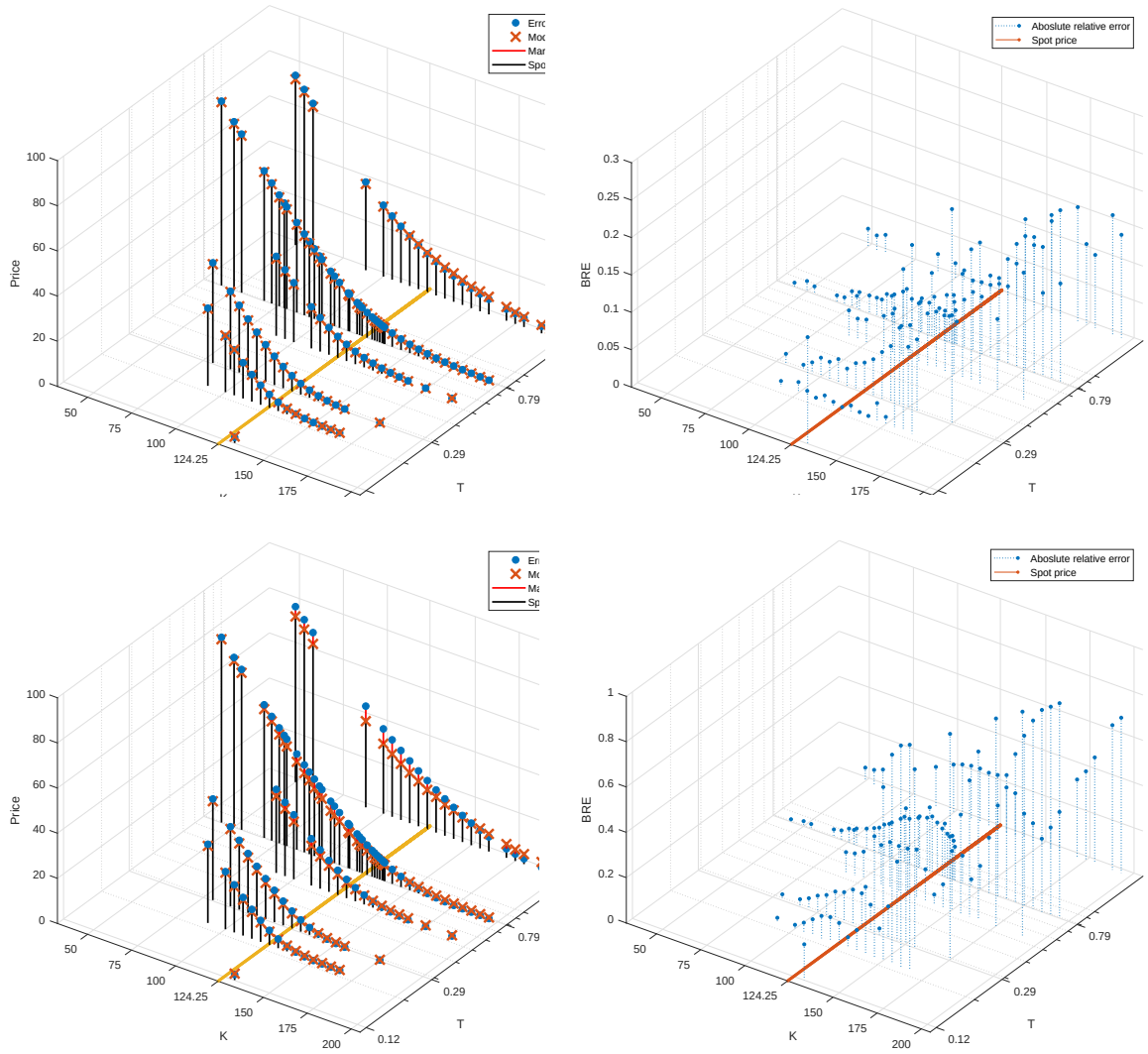

Figure 3: The market and model prices (left) and s (right) for the rBergomi model (first row) and the RFSV model (second row) on April 01.

To illustrate the difference in the fit of two different models on one day, we visualized the model prices, the market prices, and the s in Figure 3. We chose April 01 because there is the biggest difference in the AARE of rBergomi and RFSV (second row). Above the $K-T$ plane we plotted the market and model prices together (left side) and the corresponding s (in the right). On this day, the rBergomi model provides much better fit than the RFSV model.

4.3.1 Parameter significance testing

We also test for parameter significance. We are particularly interested whether the parameters H and α have any affect on the model fit, i.e., whether the fit of the αRFSV model is better/worse when H (resp. α) is being calibrated compared to the model with fixed H (resp. α). We consider the fixed value of H being $1/2$, thus it constituted a model with the volatility process being driven just by the Bm instead of the fBm. To test the significance of α, we compare the fit of the αRFSV model with the rBergomi model which corresponds to $\alpha = 1$.

If we had a deterministic pricing formula, we could simply calibrate the models and compare the fit directly. But since the pricing involves randomness (Monte Carlo simulations), we need

Table 4: The overall calibration results.

Overall calibration of the RFSV model									
day	σ_0	ρ	H	ξ	α	$AARE$	$MARE$	$WRSS$	$ARFV$
Overall calibration of the rBergomi model									
4-01	0.0782	-0.1792	0.2324	0.9875	1	6.46%	28.60%	0.0226	0.3983%
4-15	0.0700	-0.1771	0.0518	0.8858	1	6.99%	48.92%	0.0282	0.2825%
5-01	0.0615	-0.0755	0.1047	0.3520	1	9.74%	94.17%	0.0516	0.4439%
5-15	0.0470	-0.1243	0.0634	0.3126	1	15.63%	107.46%	0.0443	0.4111%
Overall calibration of the αRFSV model									
4-01	0.0714	-0.1830	0.2336	0.8229	0.8213	5.74%	49.76%	0.0286	0.3357%
4-15	0.0714	-0.1830	0.1434	0.3910	0.9721	6.70%	64.83%	0.0384	0.2683%
5-01	0.0553	-0.0578	0.1038	0.9510	0.3796	9.71%	55.56%	0.0522	0.4451%
5-15	0.0433	-0.3302	0.1607	1.1077	0.2585	11.20%	80.82%	0.0247	0.2800%

to conduct a statistical test to decide whether the difference in the fit measured by the ARFV is significant. We thus conducted 100 simulations to that resulted in different prices and thus a sample of different values of the ARFV for a given calibrated model. We then used the two-sample t-test to compare the mentioned pairs of models.

We first used this method to compare the rBergomi model with H being calibrate and with H fixed to $1/2$. For all the four days, rBergomi provided significantly better fit. Then we compared the αRFSV model with the rBergomi model which corresponds to $\alpha = 1$. Again, the null hypothesis was rejected for all the days. It is worth to mention that all the p-values were smaller than 0.001.

4.4 Robustness analysis

To analyze the robustness of the studied models, we ran calibrations on 200 bootstrapped samples as described in Subsection 3.2 and examined errors and the variation in the prices and coefficients.

For the initial points for the bootcalibrations, we chose the parameters estimated by the overall calibration (Table 4) while keeping the other calibration procedure parameters the same as before.

First, we examine the errors of prices and its variation with respect to the changing option structure and then we analyze the variation in the model parameter estimates. Lastly, we present the result of the sensitivity analysis.

4.4.1 Prices – errors and variation

We examined how the model prices, which we obtained from bootcalibrations, differ from the market prices and the variances of the distances (absolute errors). For that reason we plotted the bootstrap relative errors BRE (15) and the variances of the s V (14).

Figure 4 depicts the values of BRE and V for the option structure on April 1 produced by the αRFSV model (first row) and the rBergomi model (second row). For both models, the largest errors and concentrates on the right side relative to the spot price which is natural since deep OTM options have zero intrinsic value hence all the value comes from the time component, i.e. the probability that a given option will be exercised with a profit at the expiration time. The time component is difficult to model since it often depends on unique market circumstances thus it involves the biggest portion of uncertainty. Comparing the two models for this particular day, rBergomi provides much better fit than αRFSV and also rBergomi is less sensitive to the changes in the option structure since the variances are smaller.

Complete results for all the three models for each day are available in similar format in Appendix of the thesis Matas (2021). From comparing all the figures, we can see the same pattern of the bigger errors for the OTM option. However, an interesting result is that the αRFSV model

has the smallest variation (sometimes by even more than two orders of magnitude) of the errors for all the days which suggests that the αRFSV model may the most robust of the three models.

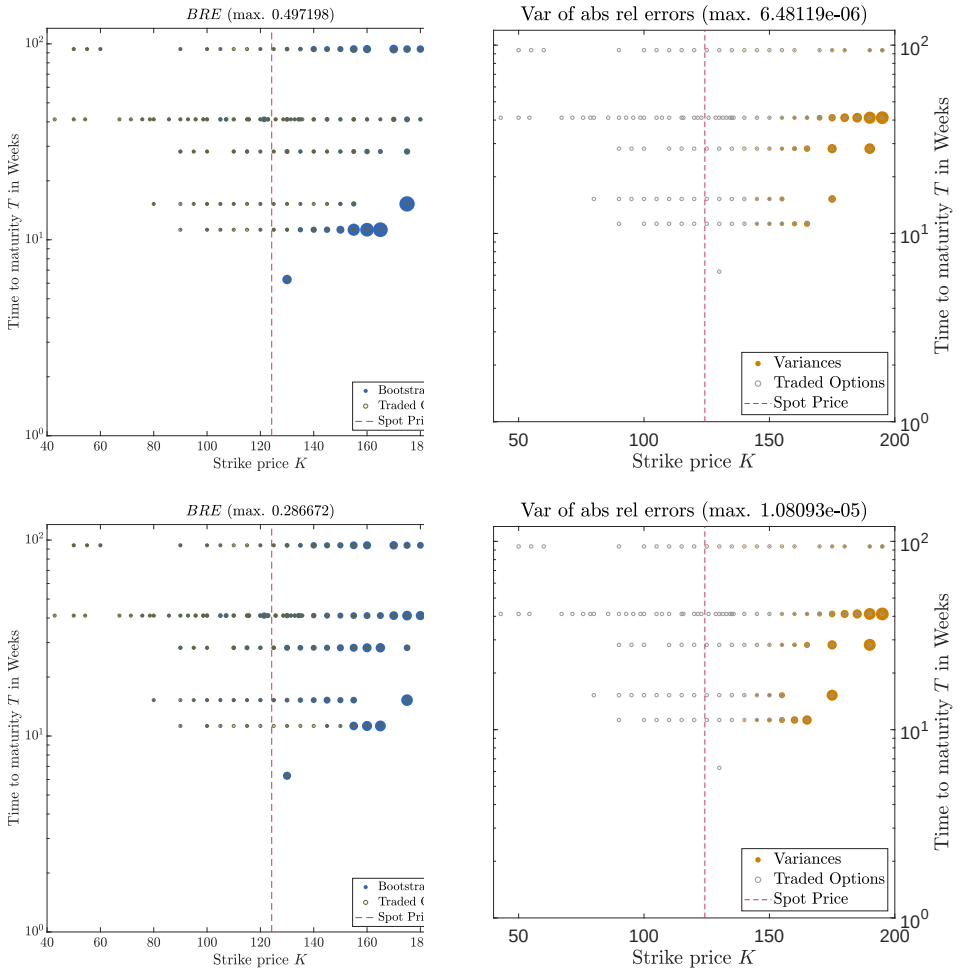

Figure 4: Option data structure from April 1, where the diameter of the size of a disk depicts the bootstrap relative error (BRE) (15) (left column) and the variance of the (14) (right column) corresponding to an option of a given combination of K (x-axis) and T (y-axis). The top row belongs to the RFSV model and the bottom one to rBergomi.

4.4.2 Variability of estimations of model coefficients

In order to analyze the variability of the estimated model coefficients obtained from the bootcalibrations, we plot and examine scatterplot matrices.

Figure 5 illustrates the model parameter estimates of the αRFSV model obtained from the bootcalibrations. Since the 5-dimensional parameter space is visualized as a matrix of 2D scatter plots, we can visually examine any patterns between the parameter estimates, while the histograms on the diagonal can provide some insight about the distributions of the parameter estimates. We can observe that there are no visible patterns and the distributions are symmetric with positive kurtosis which are both good properties for estimates. Also, notice that the variation around the bootstrap estimate is of a very small order of magnitude.

In fact, the scatter plot matrix in Figure 5 is very similar to the scatter plot matrices for other models and days. There are no visible patterns suggesting dependency between any two

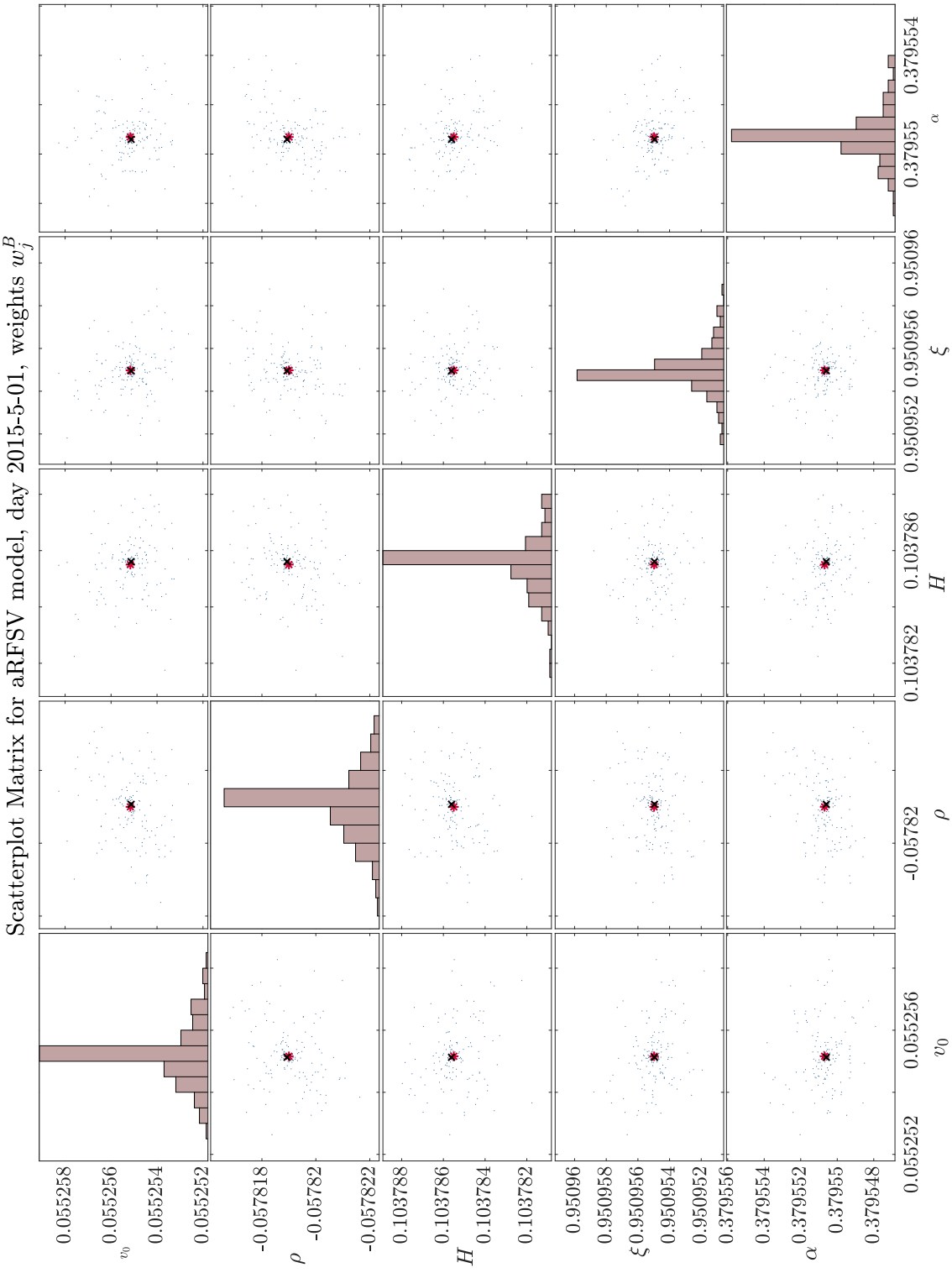

Figure 5: A scatter plot matrix of the parameter estimates from bootcalibrations of the αRFSV model for May 1. The red stars represent the bootstrap estimates (13), while the black crosses represent the estimates from the overall calibration.

parameter estimates, all the distribution are symmetric with positive kurtosis, and the variation around bootstrap estimates is remarkably low, especially compared to similar scatter plot matrices for the Heston, Bates, and AFSVJD models presented in Pospíšil, Sobotka, and Ziegler (2019). Therefore, we can conclude that the fractional SV models are more robust than the mentioned SV models.

4.5 Sensitivity analysis

We conducted the sensitivity analysis as described in Subsection 3.3, i.e., for each parameter in a given day and for a given model, we tested the null hypothesis that the distribution of the parameter estimates corresponding to the 3/8 "worst" bootcalibrations is the same as the distribution of the parameter estimates belonging to the 3/8 "best" bootcalibrations, using the KS test.

The KS test did not reject the null hypothesis for any of the parameter-model-day combination. That shows that the studied models are not sensitive to changes in the option structure when being calibrated. Although considerable variation in the values of the ARFV is still prevalent, the results of the sensitivity analysis suggest that the variation comes mainly from the changes in the option structure, independently of the parameter estimates.

5 Conclusion

First, we compared the fits of the studied rough SV models between each other and also with the Heston, Bates, and AFSVJD models in terms of the average absolute relative error. We concluded that for the used data sets, none of the fractional SV models is superior but αRFSV appears to be the most consistent. When RFSV performs better for a given data set, the parameter α is closer to 0 and when rBergomi provides better fit, the parameter α is closer to 1. Based on our comparison of the AARE, the studied rough models do not appear to be superior to the Heston, Bates, and AFSVJD models.

Then we presented the parameter estimates of the overall calibrations and tested the parameters H and α for significance. The two-sample t-test confirmed that both the parameters very significantly improve the model fit when calibrated for all the four data sets used.

Next, we analyzed the robustness of the rough SV models based on plots of BRE, variances of absolute relative errors across the bootstrapped data sets, and the scatter plot matrices of the parameter estimates. While the BREs were higher for the OTM option in all cases, an interesting results was that the αRFSV had the smallest variation (sometimes by more than two orders of magnitude) of the errors for all days compared to the two other studied models. The scatterplot matrices revealed that there are no patterns suggesting that any pair of parameter estimates would be dependent and the variance of the estimates turned out to be remarkably small, especially compared to the standard SV models. We concluded that the rough SV models are very robust and the αRFSV the most of them.

Lastly, we tested the sensitivity of the models to the changes in the option structure when being calibrated, We used a Monte Carlo filtering technique and the KS test. The statistical procedure did not show that the fit of a given model is significantly sensitive to the changes in the option structure. Thus, we concluded that the still prevalent variation in the errors comes from the changes in the option structure, independently of the parameter estimates.

Writing the paper, several additional questions and issues arose. Regarding calibration, we could estimate some of the model coefficients from time series, e.g., the Hurst parameter H can be estimated by the method proposed in Gatheral, Jaisson, and Rosenbaum (2018), or the coefficient ρ can be estimated as the correlation between stock price returns and realized volatility changes. We could then analyze the robustness of the models for such cases in a similar fashion. Another possibility is to try a different approach for the calibration itself. Instead of the deterministic gradient-based trust region approach of `lsqnonlin()`, we could employ a stochastic approximation approach or even a deep-learning method developed by Horvath, Muguruza, and Tomas (2019).

In the paper by Merino, Pospíšil, Sobotka, Sottinen, and Vives (2021), an approximation of the option price in the αRFSV model was derived and numerical experiments therein propose a promising hybrid calibration scheme which combines the approximation formula alongside MC simulations. Since the aim of this paper was to study the model as accurately as possible, we avoided the usage of approximation formula in our robustness and sensitivity analyses tests, however, repeating the same experiments with the usage of approximation formula should be straightforward.

Funding

The work was partially supported by the Czech Science Foundation (GAČR) grant no. GA18-16680S "Rough models of fractional stochastic volatility".

Acknowledgements

This work is a part of the Master's thesis Matas (2021) titled *Rough fractional stochastic volatility models* that was written by Jan Matas and supervised by Jan Pospíšil.

Computational resources were supplied by the project "e-Infrastruktura CZ" (e-INFRA LM2018140) provided within the program Projects of Large Research, Development and Innovations Infrastructures.

Disclaimer and disclosure statement

The authors declare that they have no conflict of interest.

References

Alòs, E., León, J. A., and Vives, J. (2007), *On the short-time behavior of the implied volatility for jump-diffusion models with stochastic volatility*. Finance Stoch. 11(4), 571–589, ISSN 0949-2984, DOI 10.1007/s00780-007-0049-1, Zbl 1145.91020, MR2335834.

Bates, D. S. (1996), *Jumps and stochastic volatility: Exchange rate processes implicit in Deutsche mark options*. Rev. Financ. Stud. 9(1), 69–107, DOI 10.1093/rfs/9.1.69.

Bayer, C., Friz, P., and Gatheral, J. (2016), *Pricing under rough volatility*. Quant. Finance 16(6), 887–904, ISSN 1469-7688, DOI 10.1080/14697688.2015.1099717, MR3494612.

Bennedsen, M., Lunde, A., and Pakkanen, M. S. (2016), *Decoupling the short-and long-term behavior of stochastic volatility*, available at arXiv: https://arxiv.org/abs/1610.00332.

Coleman, T. and Li, Y. (1996), *An interior, trust region approach for nonlinear minimization subject to bounds*. SIAM J. Optim. 6(2), 418–445, DOI 10.1137/0806023, Zbl 0855.65063, MR1387333.

Comte, F., Coutin, L., and Renault, E. (2012), *Affine fractional stochastic volatility models*. Ann. Finance 8(2–3), 337–378, ISSN 1614-2446, DOI 10.1007/s10436-010-0165-3, Zbl 1298.60067, MR2922801.

Comte, F. and Renault, E. (1998), *Long memory in continuous-time stochastic volatility models*. Math. Finance 8(4), 291–323, ISSN 0960-1627, DOI 10.1111/1467-9965.00057, Zbl 1020.91021, MR1645101.

Dieker, A. B. (2002), Simulation of fractional Brownian motion. Master's thesis, Vrije Universiteit Amsterdam, revised 2004, URL http://www.columbia.edu/~ad3217/fbm/thesis.pdf.

Gatheral, J., Jaisson, T., and Rosenbaum, M. (2018), *Volatility is rough*. Quant. Finance 18(6), 933–949, ISSN 1469-7688, DOI 10.1080/14697688.2017.1393551, Zbl 1400.91590, MR3805308.

Heston, S. L. (1993), *A closed-form solution for options with stochastic volatility with applications to bond and currency options*. Rev. Financ. Stud. 6(2), 327–343, ISSN 0893-9454, DOI 10.1093/rfs/6.2.327, Zbl 1384.35131, MR3929676.

Horvath, B., Muguruza, A., and Tomas, M. (2019), *Deep learning volatility*, DOI 10.2139/ssrn.3322085, available at arXiv: https://arxiv.org/abs/1901.09647.

Hull, J. C. and White, A. D. (1987), *The pricing of options on assets with stochastic volatilities*. J. Finance 42(2), 281–300, ISSN 1540-6261, DOI 10.1111/j.1540-6261.1987.tb02568.x.

Jost, C. (2008), *On the connection between Molchan-Golosov and Mandelbrot- van Ness representations of fractional Brownian motion*. J. Integral Equations Appl. 20(1), 93–119, ISSN 0897-3962, DOI 10.1216/JIE-2008-20-1-93, Zbl 1147.60024, MR2396956.

Mandelbrot, B. B. and Van Ness, J. W. (1968), *Fractional Brownian motions, fractional noises and applications*. SIAM Rev. 10(4), 422–437, ISSN 0036-1445, DOI 10.1137/1010093, Zbl 0179.47801, MR0242239.

Matas, J. (2021), Rough fractional stochastic volatility models. Master's thesis, University of West Bohemia.

Matas, J. and Pospíšil, J. (2021), *On simulation of rough Volterra stochastic volatility models*, available at arXiv: http://arxiv.org/a/0000-0002-4288-1614.

Merino, R., Pospíšil, J., Sobotka, T., Sottinen, T., and Vives, J. (2019), *Decomposition formula for rough Volterra stochastic volatility models*, available at arXiv: https://www.arxiv.org/abs/1906.07101.

Merino, R., Pospíšil, J., Sobotka, T., Sottinen, T., and Vives, J. (2021), *Decomposition formula for rough Volterra stochastic volatility models*. Int. J. Theor. Appl. Finance 24(2), 2150008, ISSN 0219-0249, DOI 10.1142/S0219024921500084.

Molchan, G. M. and Golosov, J. I. (1969), *Gaussian stationary processes with asymptotic power spectrum*. Sov. Math. Dokl. 10, 134–137, ISSN 0197-6788, translation from Dokl. Akad. Nauk SSSR 184, 546–549 (1969), Zbl 0181.20704, MR0242247.

Mrázek, M., Pospíšil, J., and Sobotka, T. (2016), *On calibration of stochastic and fractional stochastic volatility models*. European J. Oper. Res. 254(3), 1036–1046, ISSN 0377-2217, DOI 10.1016/j.ejor.2016.04.033, Zbl 1346.91238, MR3508893.

Pospíšil, J., Sobotka, T., and Ziegler, P. (2019), *Robustness and sensitivity analyses for stochastic volatility models under uncertain data structure*. Empir. Econ. 57(6), 1935–1958, ISSN 0377-7332, DOI 10.1007/s00181-018-1535-3.

Saltelli, A., Ratto, M., Andres, T., Campolongo, F., Cariboni, J., Gatelli, D., Saisana, M., and Tarantola, S. (2008), Global Sensitivity Analysis: The Primer. Chichester: Wiley, ISBN 9780470725177, DOI 10.1002/9780470725184, Zbl 1161.00304, MR2382923.

Chapter 4

Thesis attachment

On the attached CD, we created the following file structure:

- 01_data
- 02_simulation
- 03_pricing
- 04_calibration
- 05_sensitivity
- 06_significance_testing
- 07_results_bootcalibrations
- DP_text.pdf
- README.txt

In the first six folders, there are tagged mfiles[1] and in the seventh folder there are all the results from bootcalibrations that we present in this thesis. The pdf file DP_text.pdf is the text of this thesis. The last file README.txt contains general information about the content of the CD. There is also a separate README.txt file in each folder with more information about the content in detail.

[1] MATLAB codes.

Appendices

Moments Matching the Theoretical Moments of fBm

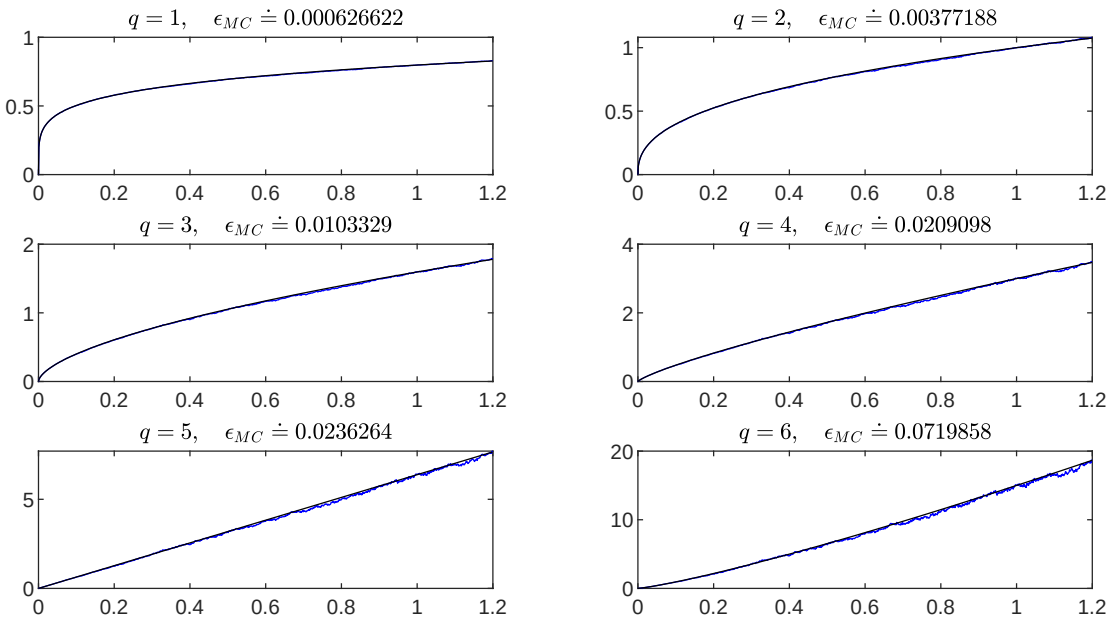

Figure 1: Sample absolute moments (blue) matching the corresponding theoretical values $\mathbb{E}\left[\left|B_t^H\right|^q\right]$ (black), see (2.14), of fBm $\{B_t^H, 0 \leq t \leq 1.2\}$ for $H = 0.20$. There were simulated $P = 100,000$ paths, with granularity $n = 4 \times 252$ steps, using the Hybrid scheme. We denote ϵ_{MC} the absolute error of the end end value.

Complete results of the robustness analysis

The following figures present the complete results of the robustness analysis.

1 RFSV-4-01

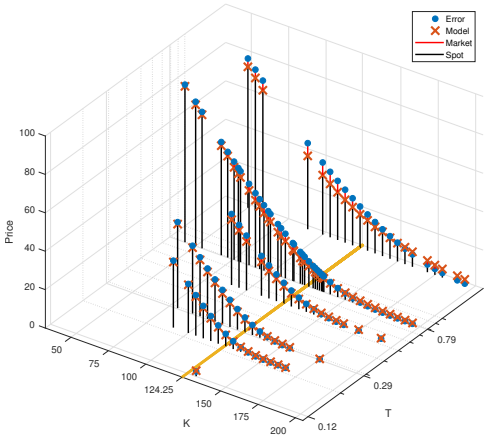
Error
Model
Market
Spot
Price
K
T

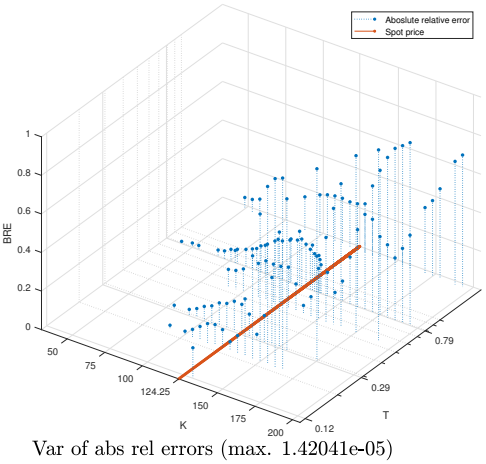
Aboslute relative error
Spot price
BRE
K
T

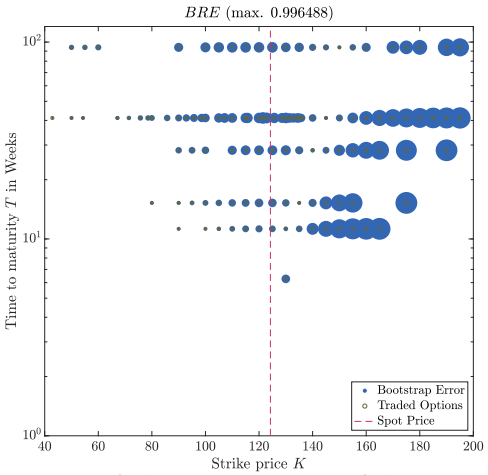
BRE (max. 0.996488)
Time to maturity T in Weeks
Strike price K
Bootstrap Error
Traded Options
Spot Price

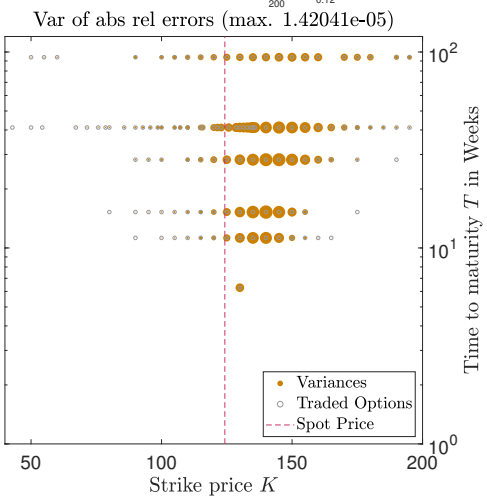
Var of abs rel errors (max. 1.42041e-05)
Time to maturity T in Weeks
Strike price K
Variances
Traded Options
Spot Price

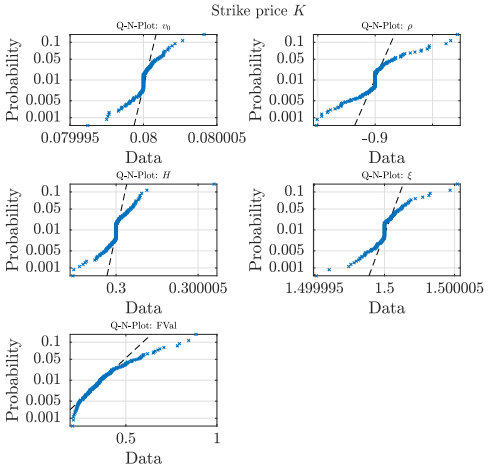
Q-N-Plot: v_0
Q-N-Plot: ρ
Q-N-Plot: H
Q-N-Plot: ξ
Q-N-Plot: FVal
Probability
Data

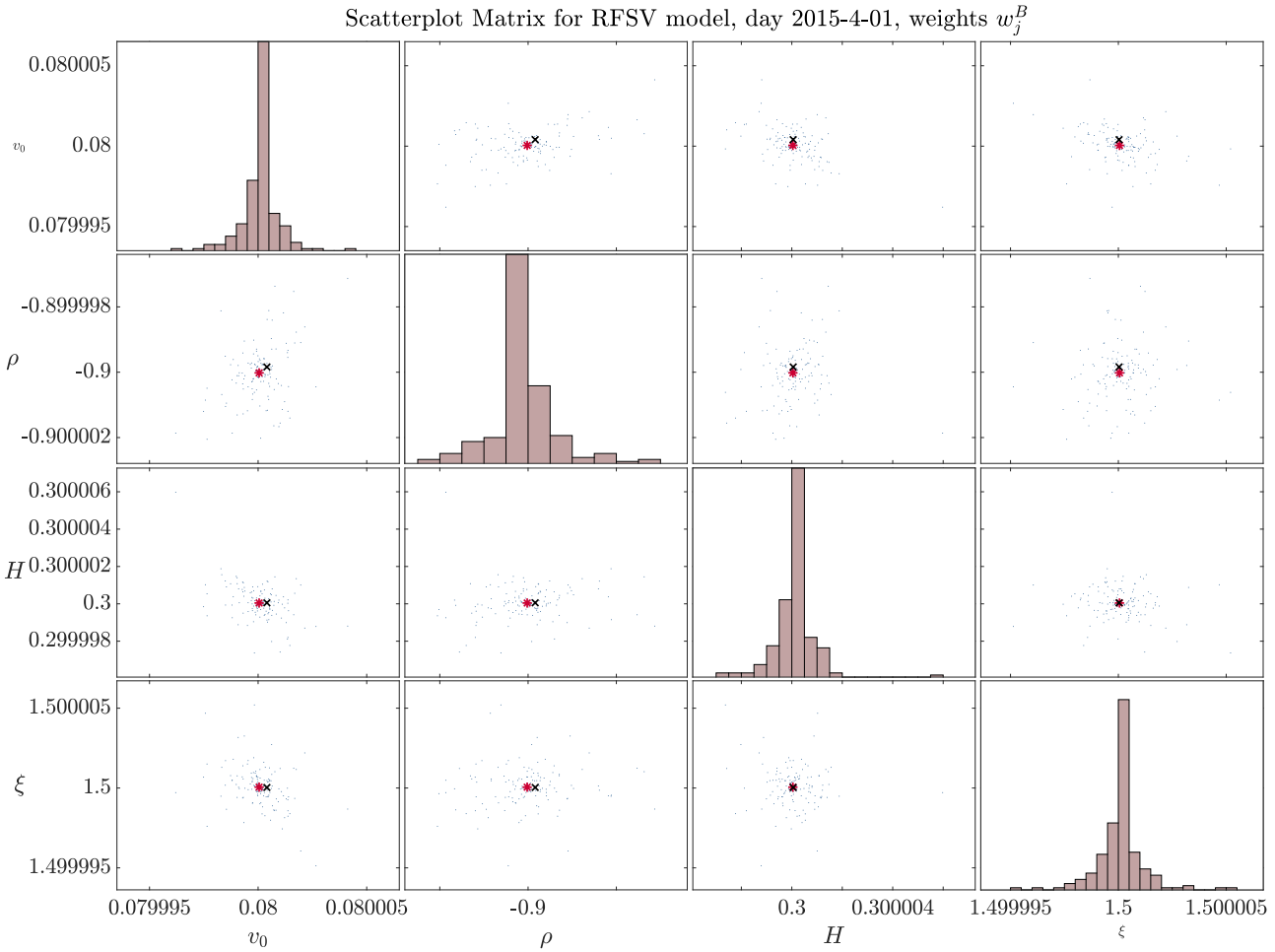
Scatterplot Matrix for RFSV model, day 2015-4-01, weights w_j^B
0.080005
0.08
0.079995
v_0
-0.899998
-0.9
-0.900002
ρ
0.300006
0.300004
0.300002
0.3
0.299998
H
1.500005
1.5
1.499995
ξ
0.079995
0.08
0.080005
v_0
-0.9
ρ
0.3
0.300004
H
1.499995
1.5
1.500005
ξ

2 aRFSV-4-01

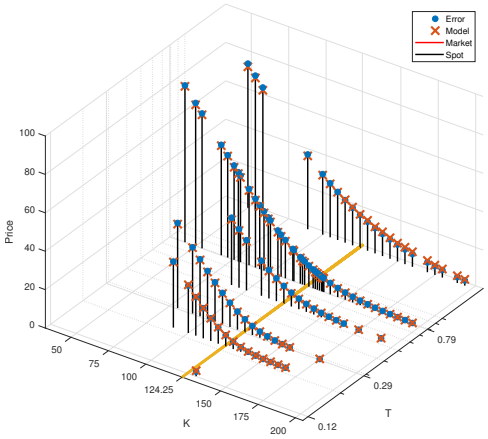
Error
Model
Market
Spot
Price
K
T

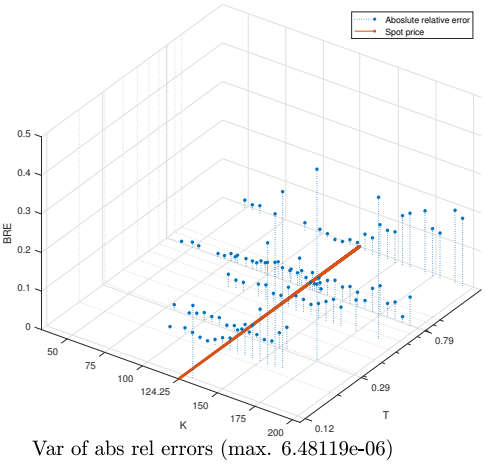
Aboslute relative error
Spot price
BRE
K
T

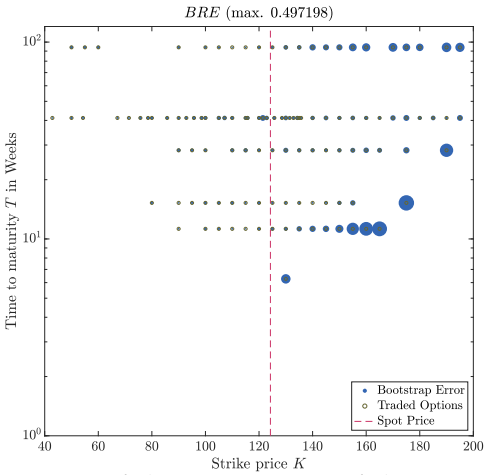
BRE (max. 0.497198)
Time to maturity T in Weeks
Strike price K
Bootstrap Error
Traded Options
Spot Price

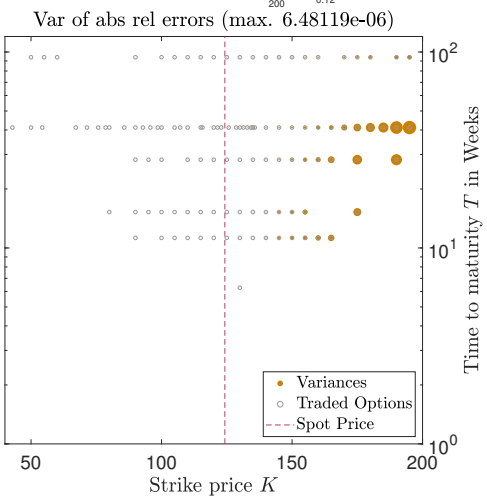
Var of abs rel errors (max. 6.48119e-06)
Time to maturity T in Weeks
Strike price K
Variances
Traded Options
Spot Price

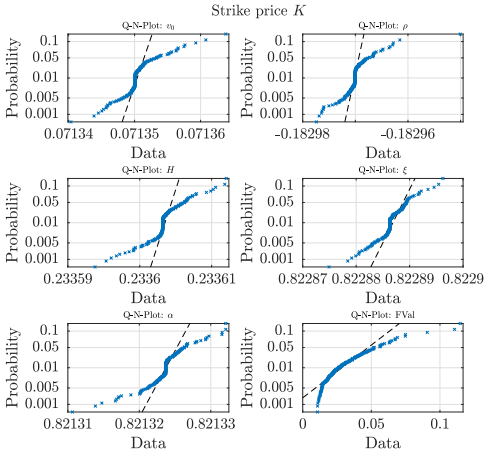
Q-N-Plot: v_0
Q-N-Plot: ρ
Q-N-Plot: H
Q-N-Plot: ξ
Q-N-Plot: α
Q-N-Plot: FVal
Probability
Data

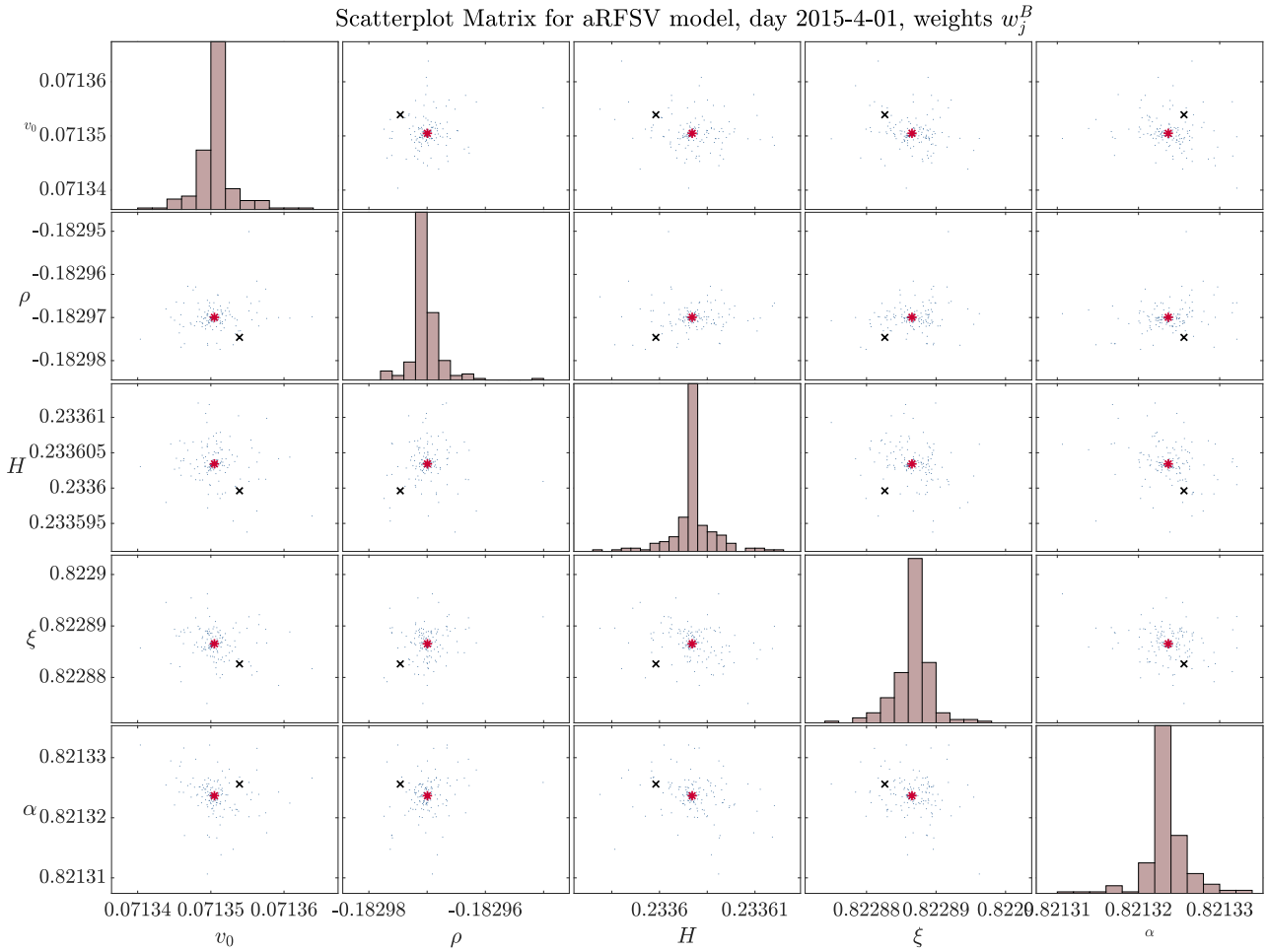
Scatterplot Matrix for aRFSV model, day 2015-4-01, weights w_j^B
v_0
ρ
H
ξ
α
0.07136
0.07135
0.07134
-0.18295
-0.18296
-0.18297
-0.18298
0.23361
0.233605
0.2336
0.233595
0.8229
0.82289
0.82288
0.82133
0.82132
0.82131
0.07134 0.07135 0.07136
-0.18298
-0.18296
0.2336
0.23361
0.82288 0.82289 0.8229
0.82131 0.82132 0.82133

3 rBergomi-4-01

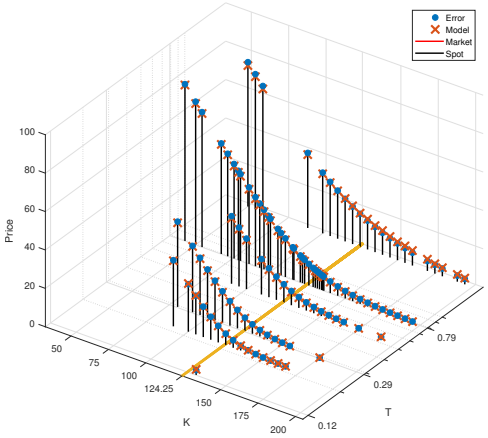

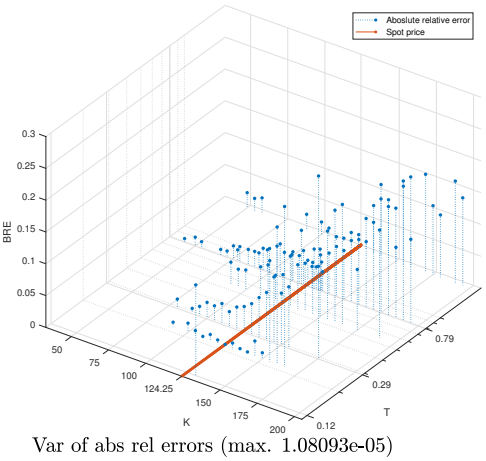

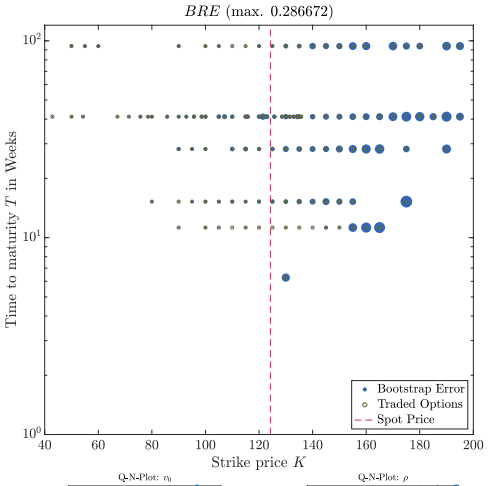

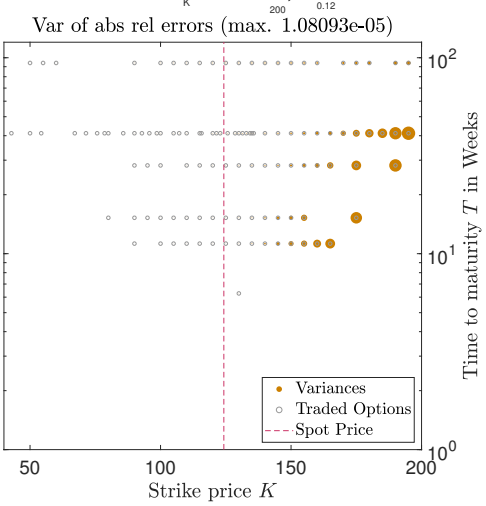

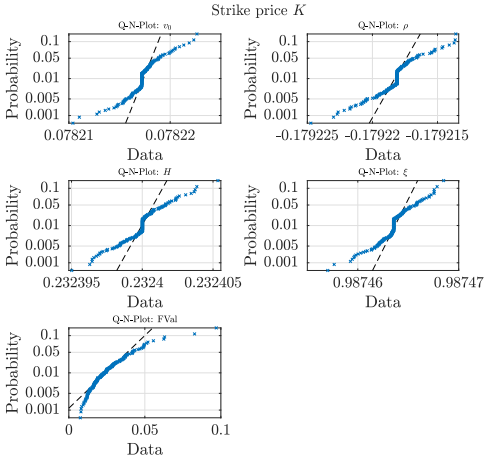

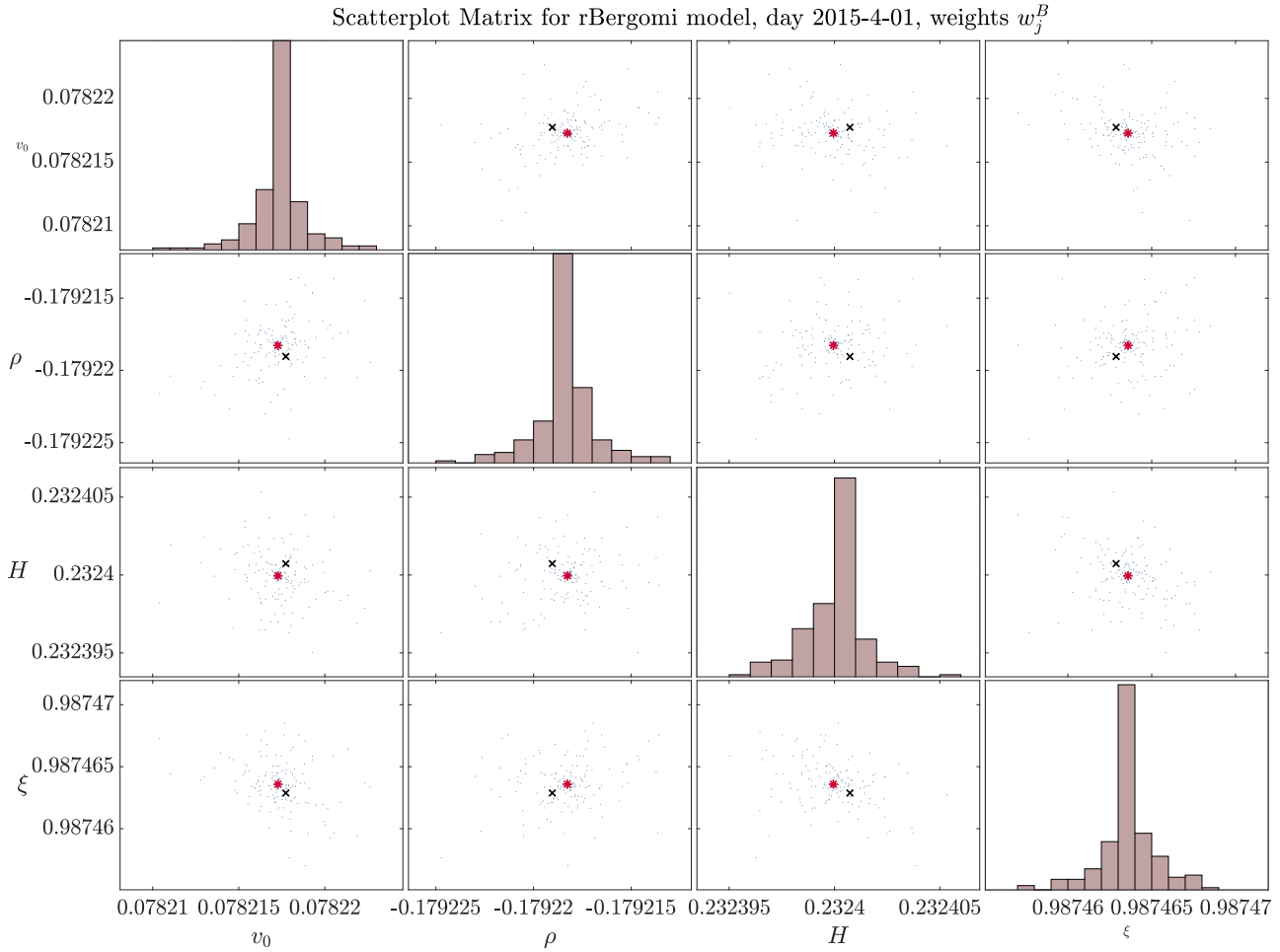
Scatterplot Matrix for rBergomi model, day 2015-4-01, weights w_j^B
v_0
0.07822
0.078215
0.07821
ρ
-0.179215
-0.17922
-0.179225
H
0.232405
0.2324
0.232395
ξ
0.98747
0.987465
0.98746
0.07821 0.078215 0.07822
v_0
-0.179225 -0.17922 -0.179215
ρ
0.232395 0.2324 0.232405
H
0.98746 0.987465 0.98747
ξ

4 RFSV-4-15

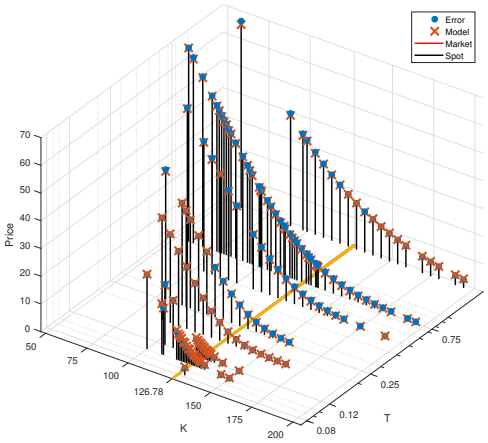
Error
Model
Market
Spot
Price
K
T

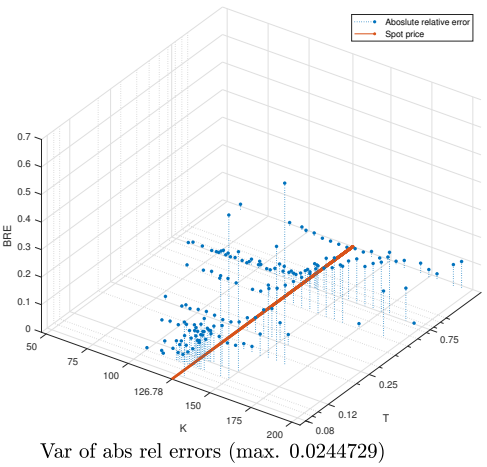
Aboslute relative error
Spot price
BRE
K
T

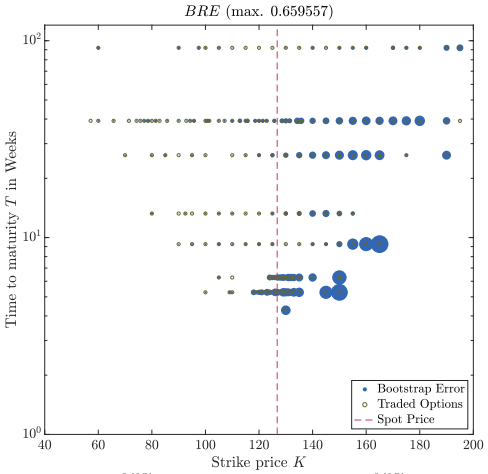
BRE (max. 0.659557)
Time to maturity T in Weeks
Strike price K
Bootstrap Error
Traded Options
Spot Price

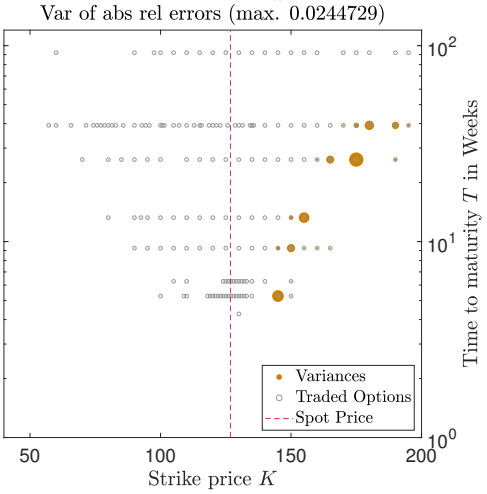
Var of abs rel errors (max. 0.0244729)
Time to maturity T in Weeks
Strike price K
Variances
Traded Options
Spot Price

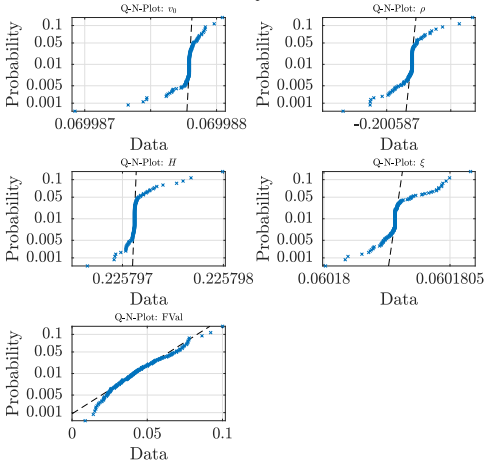
Q-N-Plot: ν_0
Q-N-Plot: ρ
Q-N-Plot: H
Q-N-Plot: ξ
Q-N-Plot: FVal
Probability
Data

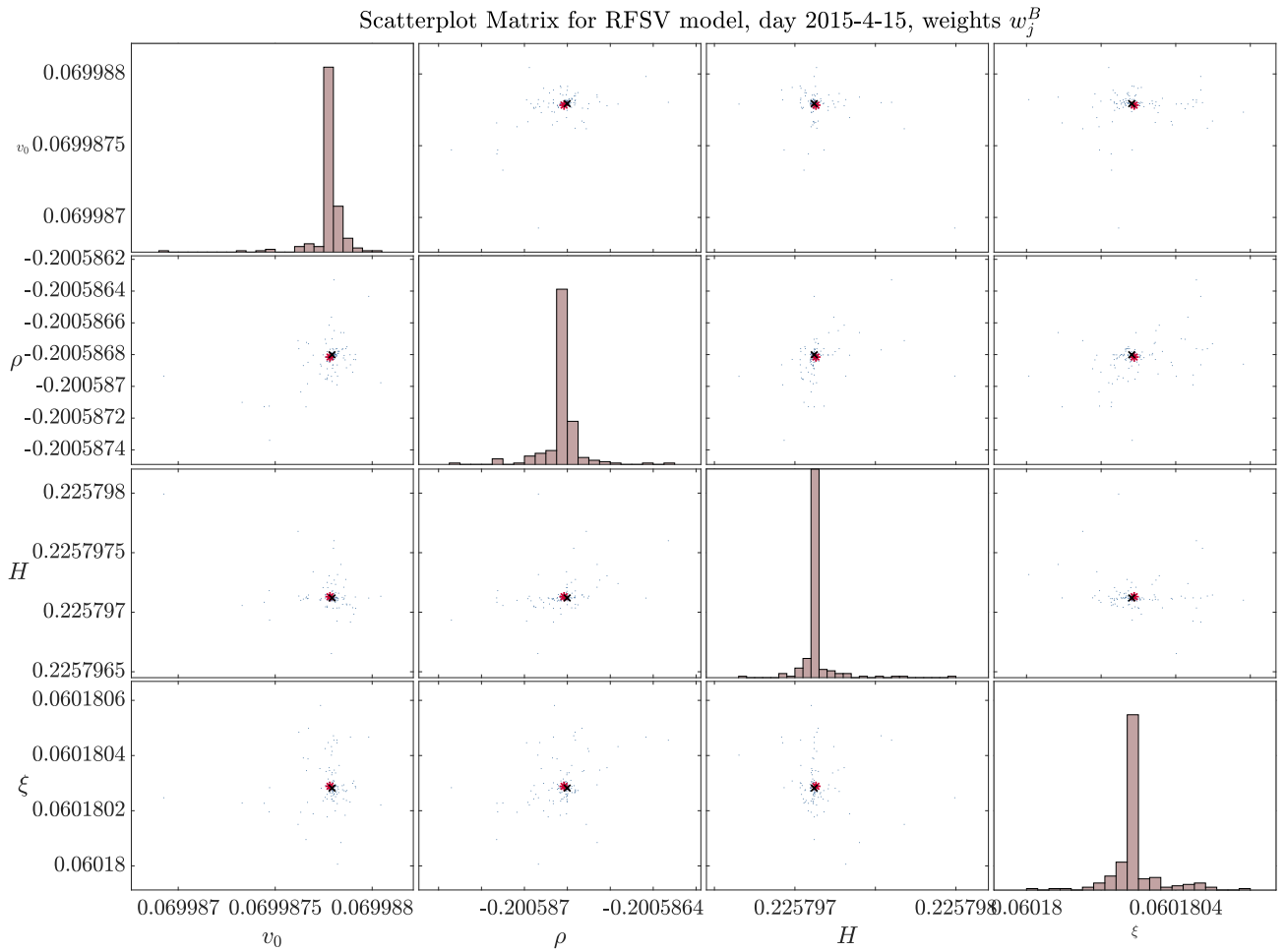
Scatterplot Matrix for RFSV model, day 2015-4-15, weights w_j^B
v_0
ρ
H
ξ
0.069988
0.0699875
0.069987
-0.2005862
-0.2005864
-0.2005866
-0.2005868
-0.200587
-0.2005872
-0.2005874
0.225798
0.2257975
0.225797
0.2257965
0.0601806
0.0601804
0.0601802
0.06018
0.069987 0.0699875 0.069988
-0.200587 -0.2005864
0.225797 0.225798
0.06018 0.0601804

5 aRFSV-4-15

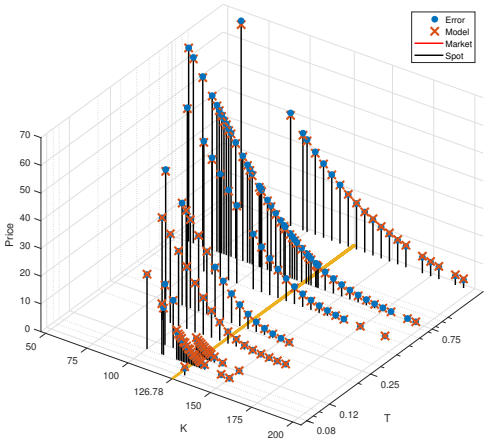
Error
Model
Market
Spot
Price
K
T

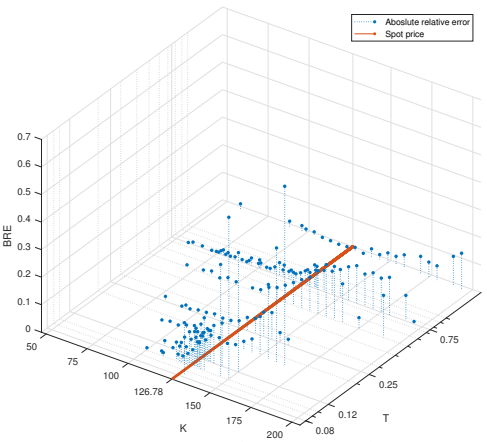
Aboslute relative error
Spot price
BRE
K
T

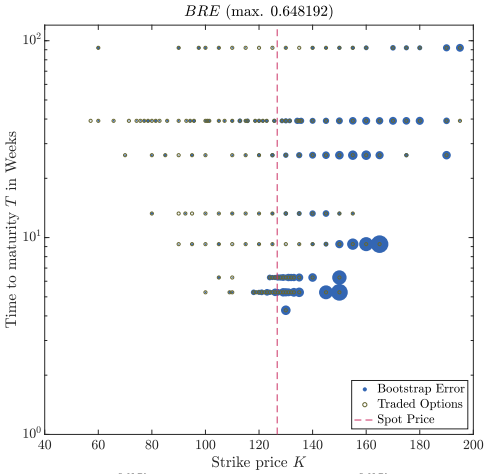
BRE (max. 0.648192)
Time to maturity T in Weeks
Strike price K
Bootstrap Error
Traded Options
Spot Price

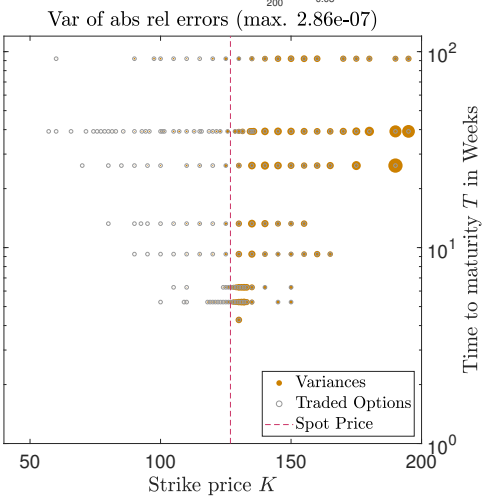
Var of abs rel errors (max. 2.86e-07)
Time to maturity T in Weeks
Strike price K
Variances
Traded Options
Spot Price

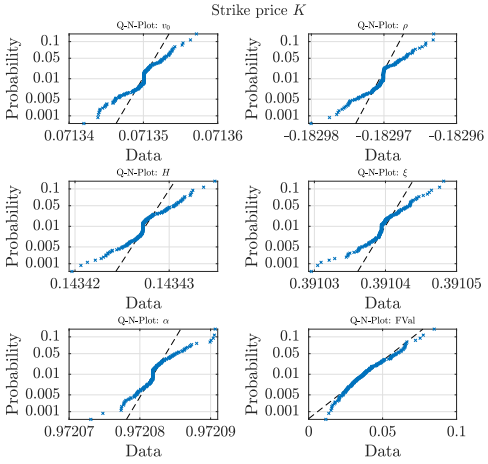
Q-N-Plot: v_0
Q-N-Plot: ρ
Q-N-Plot: H
Q-N-Plot: ξ
Q-N-Plot: α
Q-N-Plot: FVal
Probability
Data

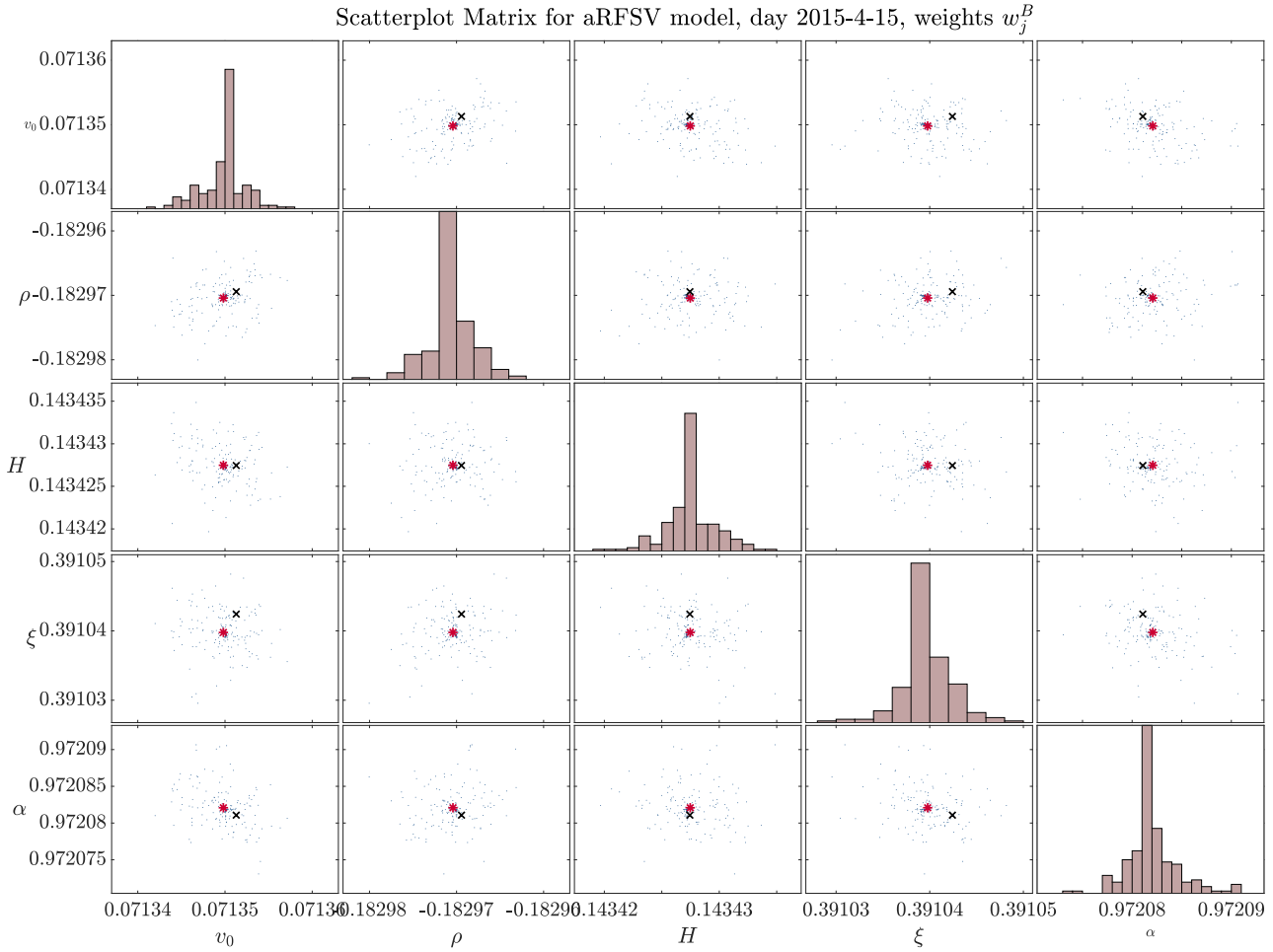
Scatterplot Matrix for aRFSV model, day 2015-4-15, weights w_j^B
v_0
ρ
H
ξ
α
0.07136
0.07135
0.07134
-0.18296
-0.18297
-0.18298
0.143435
0.14343
0.143425
0.14342
0.39105
0.39104
0.39103
0.97209
0.972085
0.97208
0.972075

6 rBergomi-4-15

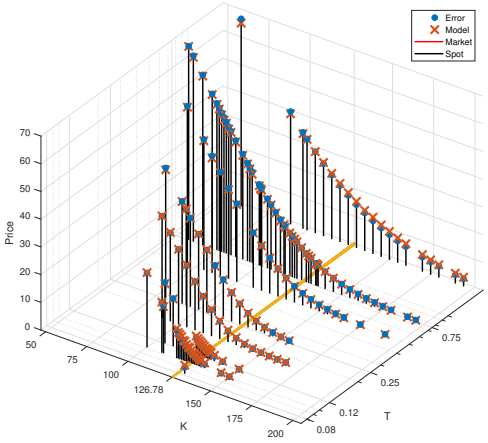

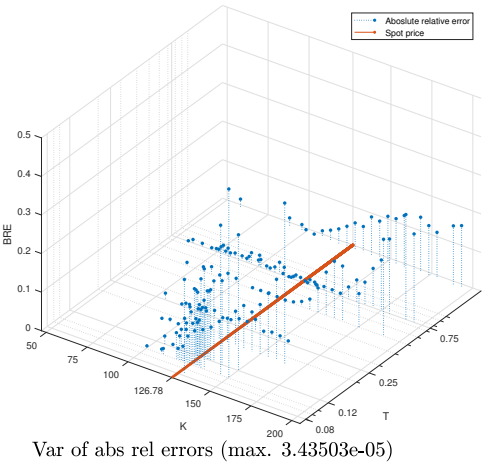

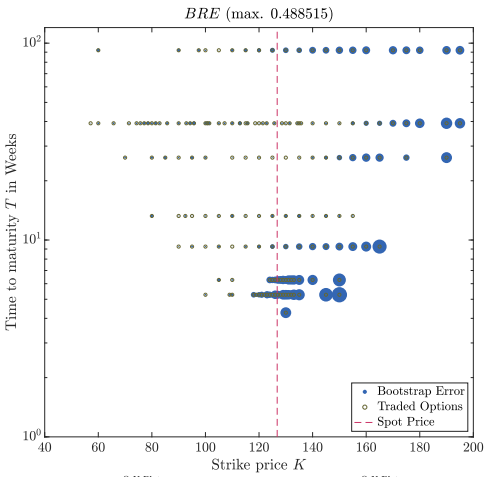

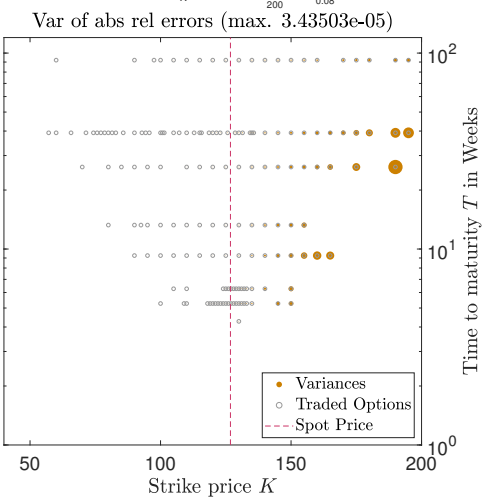

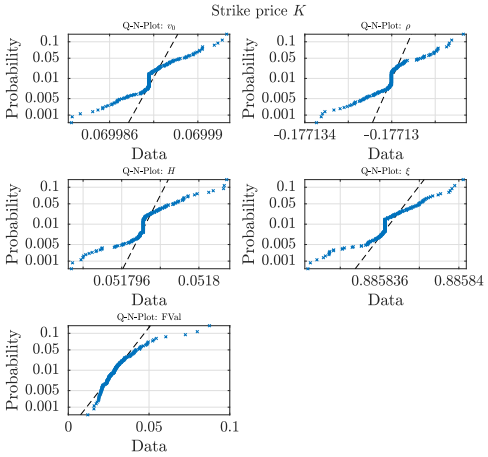

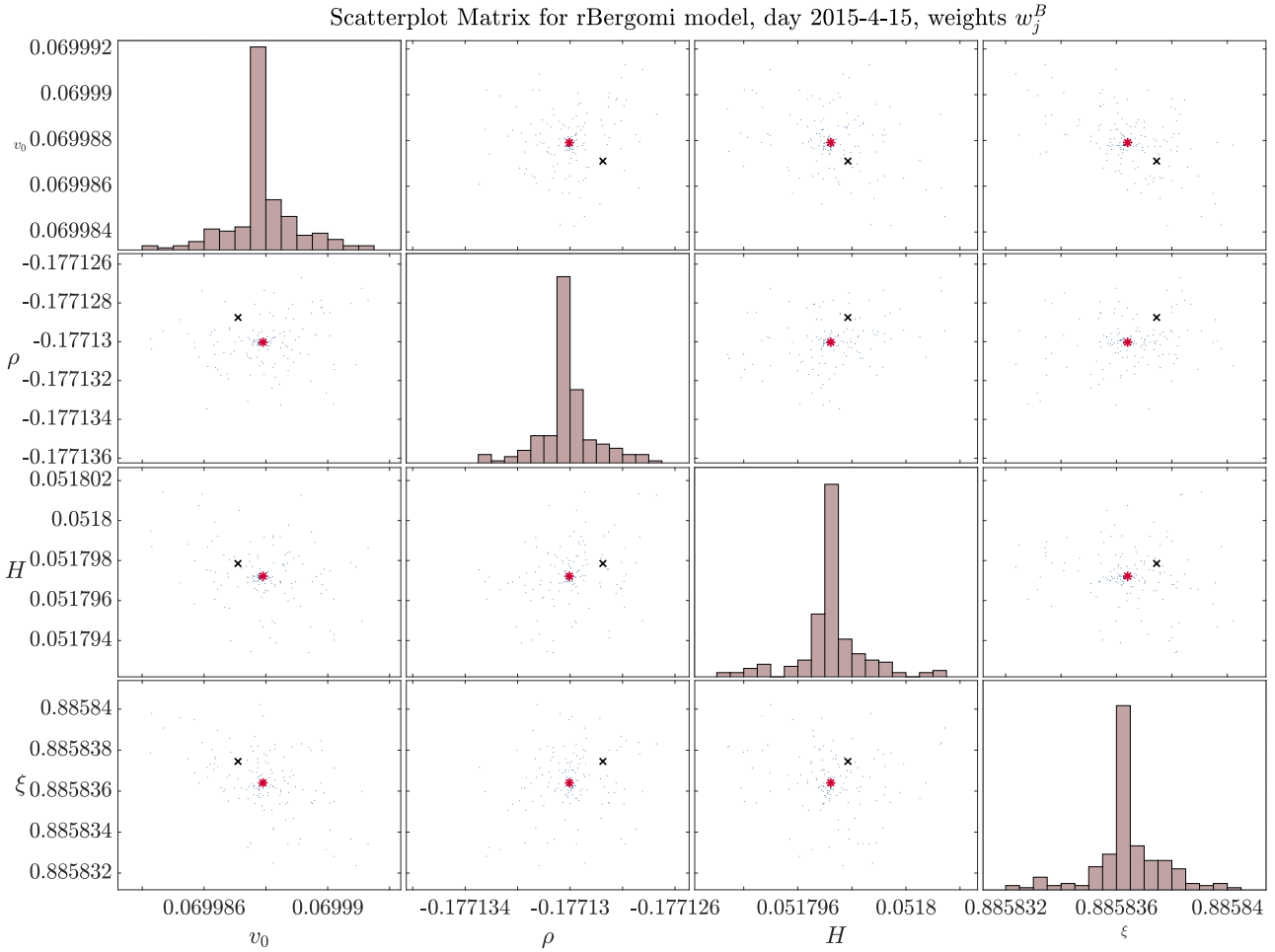
Scatterplot Matrix for rBergomi model, day 2015-4-15, weights w_j^B
v_0
ρ
H
ξ
0.069992
0.06999
0.069988
0.069986
0.069984
-0.177126
-0.177128
-0.17713
-0.177132
-0.177134
-0.177136
0.051802
0.0518
0.051798
0.051796
0.051794
0.88584
0.885838
0.885836
0.885834
0.885832
0.069986
0.06999
-0.177134
-0.17713
-0.177126
0.051796
0.0518
0.885832
0.885836
0.88584

7 RFSV-5-01

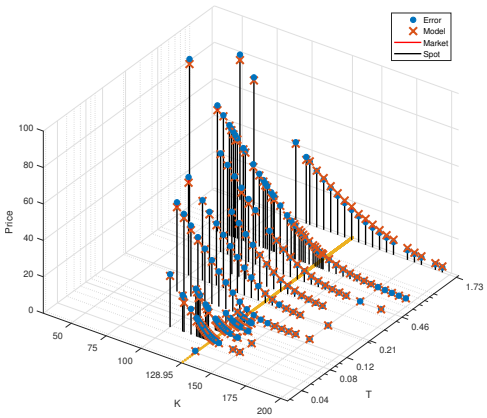

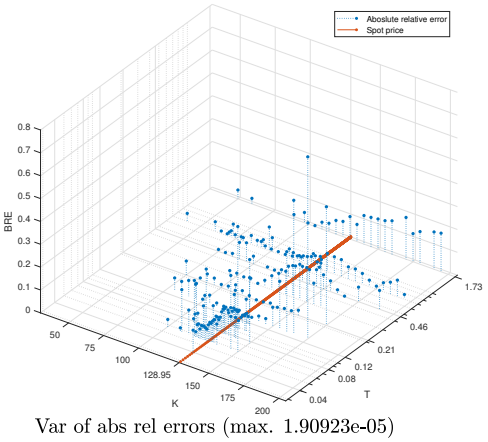

BRE (max. 0.796403)

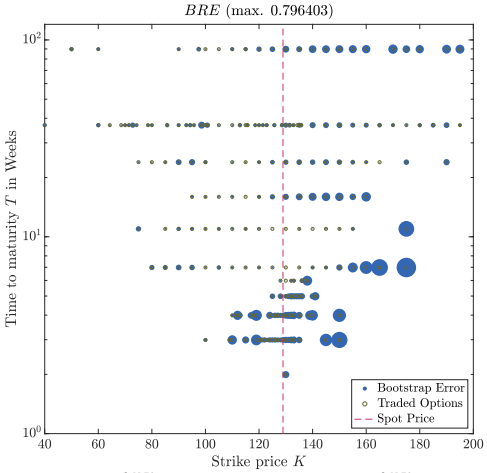

Var of abs rel errors (max. 1.90923e-05)

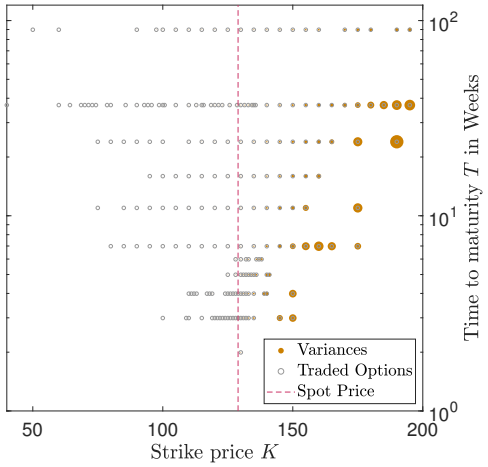

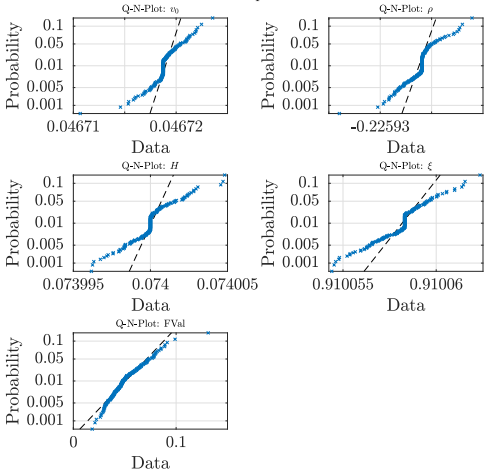

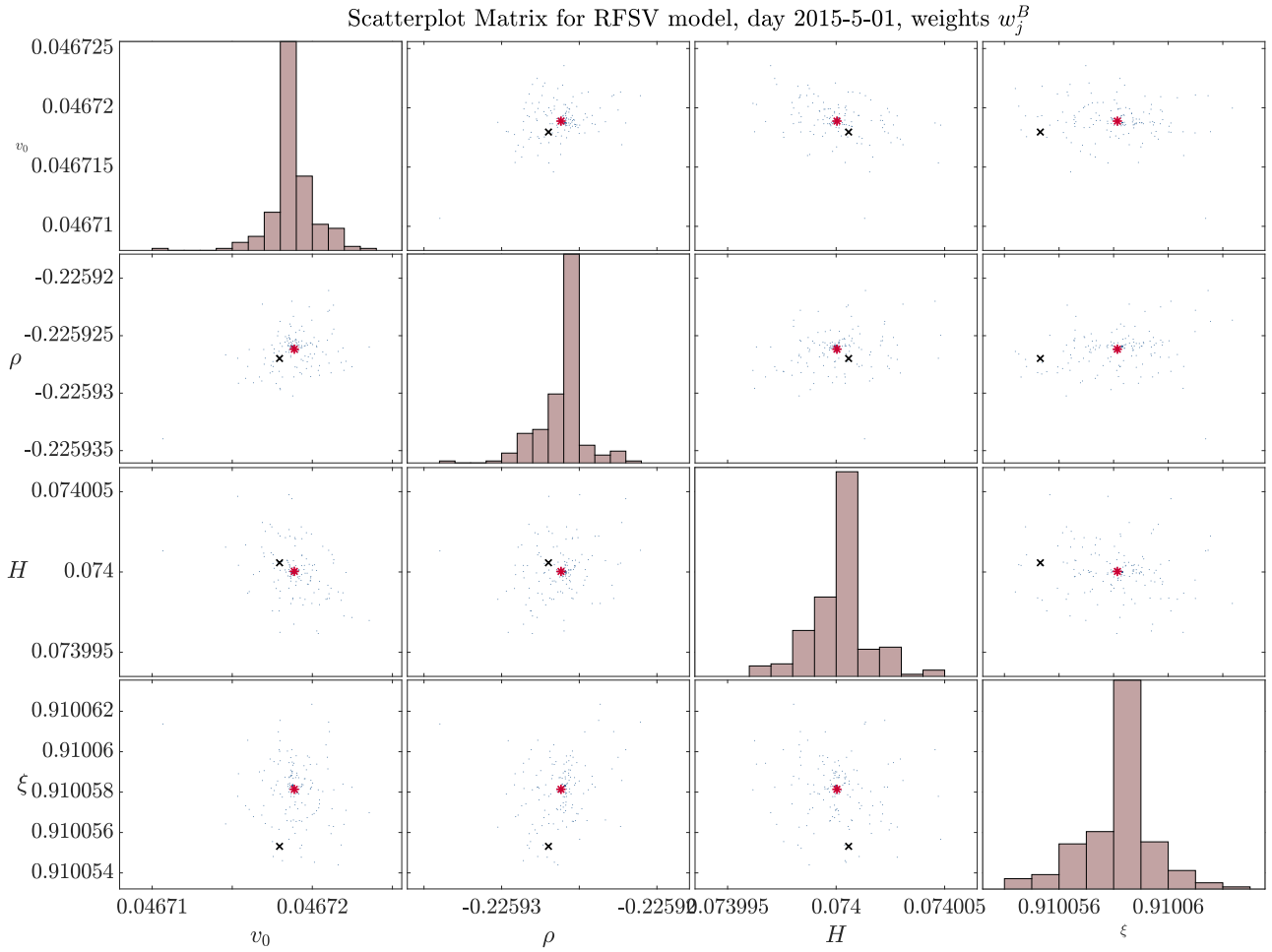
Scatterplot Matrix for RFSV model, day 2015-5-01, weights w_j^B
0.046725
0.04672
0.046715
0.04671
v_0
-0.22592
-0.225925
-0.22593
-0.225935
ρ
0.074005
0.074
0.073995
H
0.910062
0.91006
0.910058
0.910056
0.910054
ξ
0.04671
0.04672
v_0
-0.22593
-0.22592
ρ
0.073995
0.074
0.074005
H
0.910056
0.91006
ξ

8 aRFSV-5-01

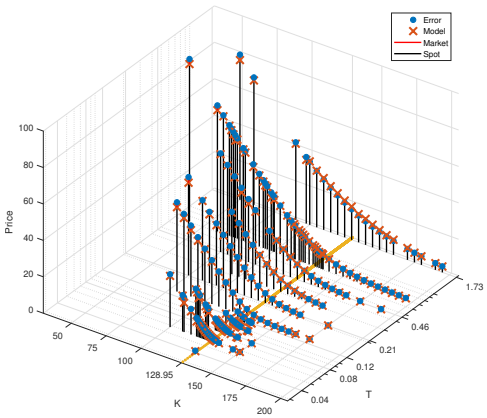
Error
Model
Market
Spot
Price
K
T

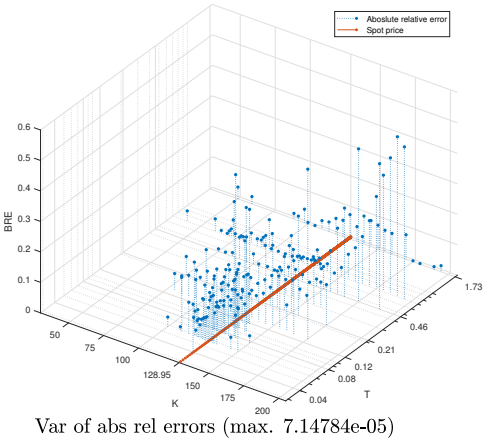
Aboslute relative error
Spot price
BRE
K
T

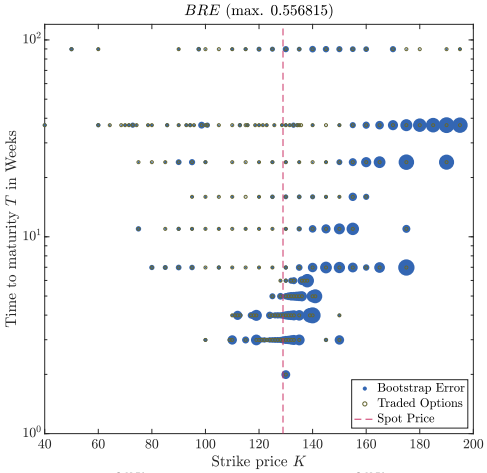
BRE (max. 0.556815)
Time to maturity T in Weeks
Strike price K
Bootstrap Error
Traded Options
Spot Price

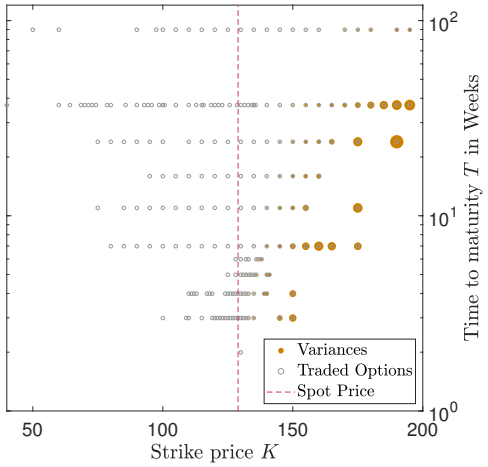
Var of abs rel errors (max. 7.14784e-05)
Time to maturity T in Weeks
Strike price K
Variances
Traded Options
Spot Price

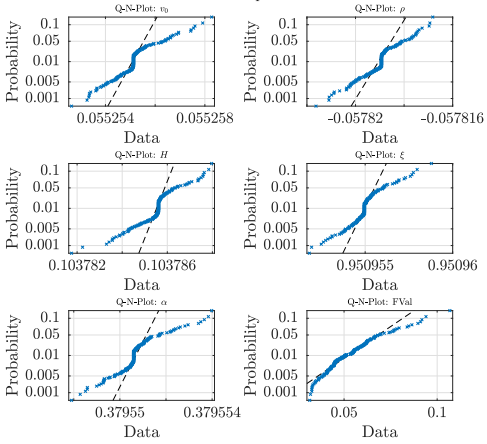
Q-N-Plot: v0
Q-N-Plot: ρ
Q-N-Plot: H
Q-N-Plot: ξ
Q-N-Plot: α
Q-N-Plot: FVal
Probability
Data

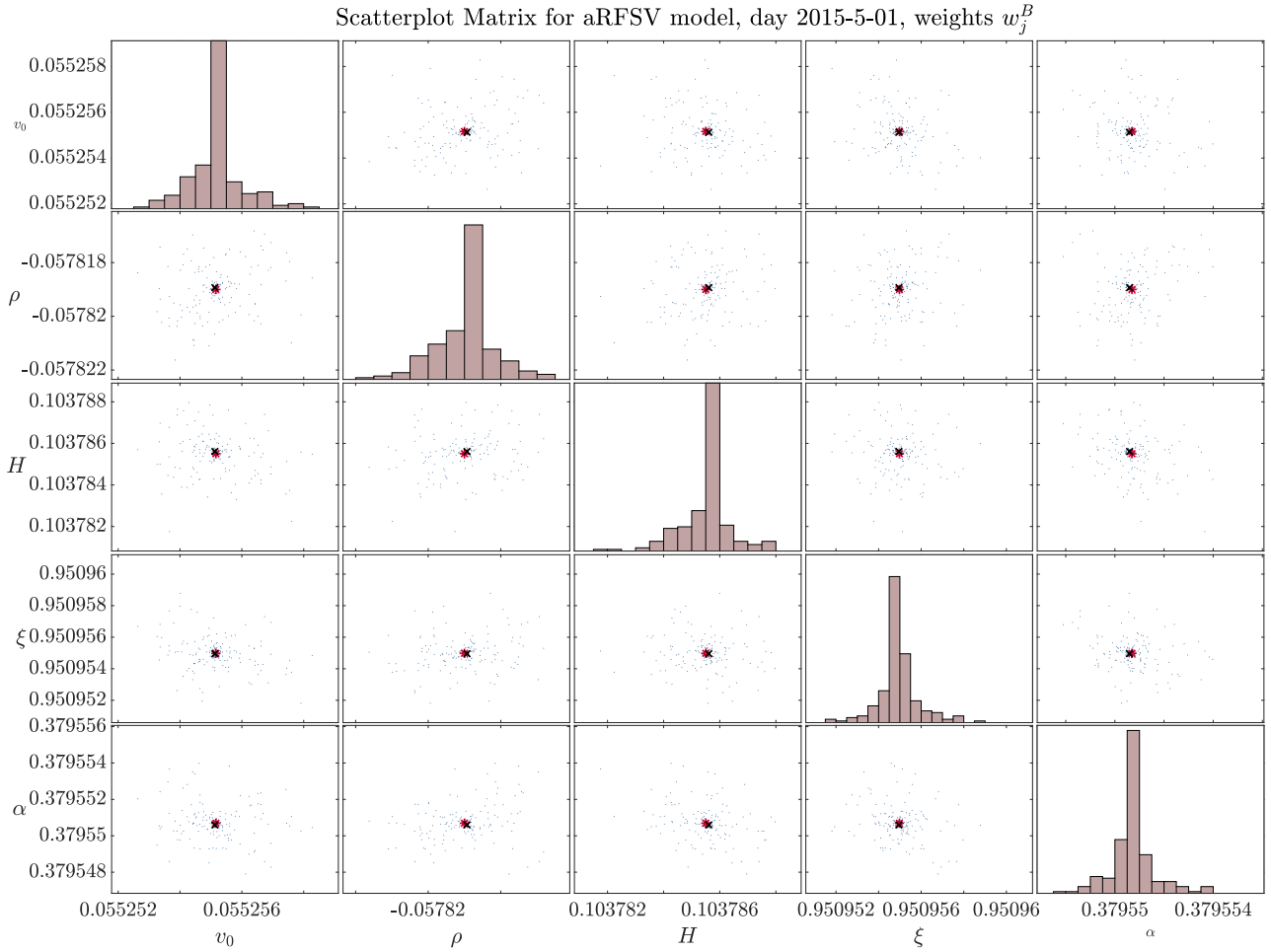
Scatterplot Matrix for aRFSV model, day 2015-5-01, weights w_j^B
v_0
ρ
H
ξ
α
0.055258
0.055256
0.055254
0.055252
-0.057818
-0.05782
-0.057822
0.103788
0.103786
0.103784
0.103782
0.95096
0.950958
0.950956
0.950954
0.950952
0.379556
0.379554
0.379552
0.37955
0.379548
0.055252
0.055256
-0.05782
0.103782
0.103786
0.950952
0.950956
0.95096
0.37955
0.379554

9 rBergomi-5-01

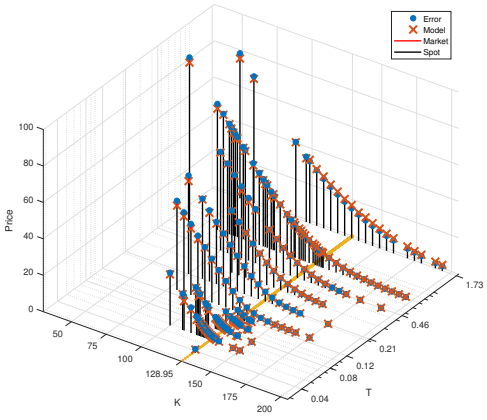

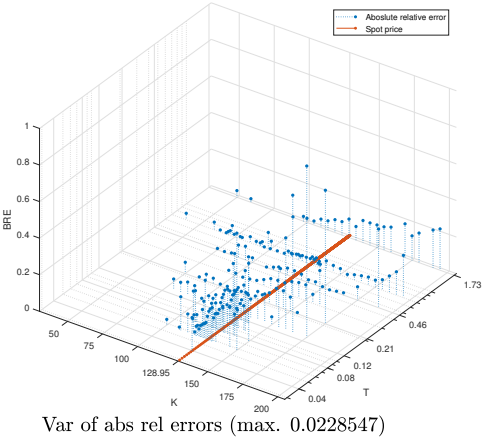

BRE (max. 0.936744)

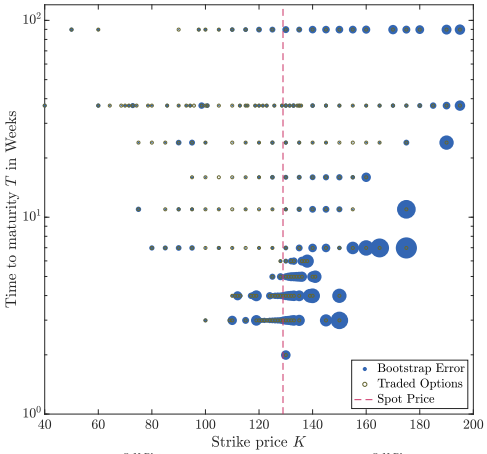

Var of abs rel errors (max. 0.0228547)

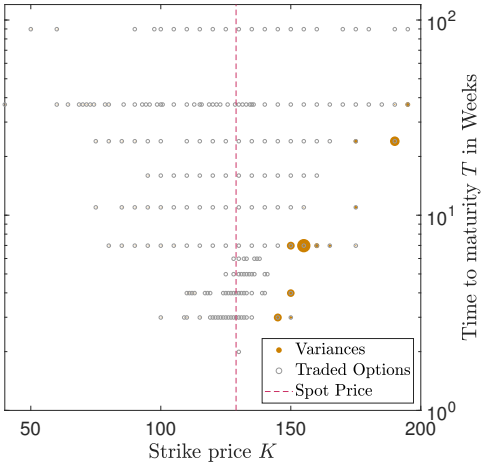

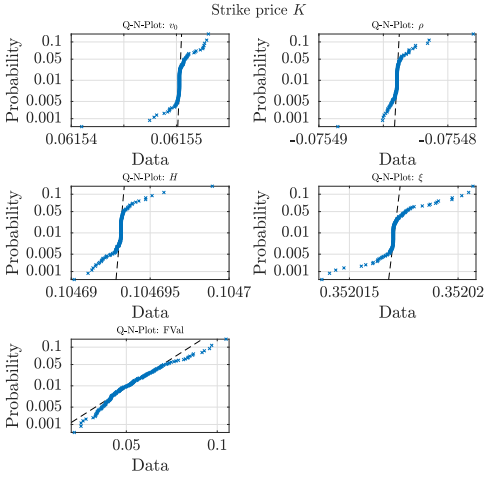

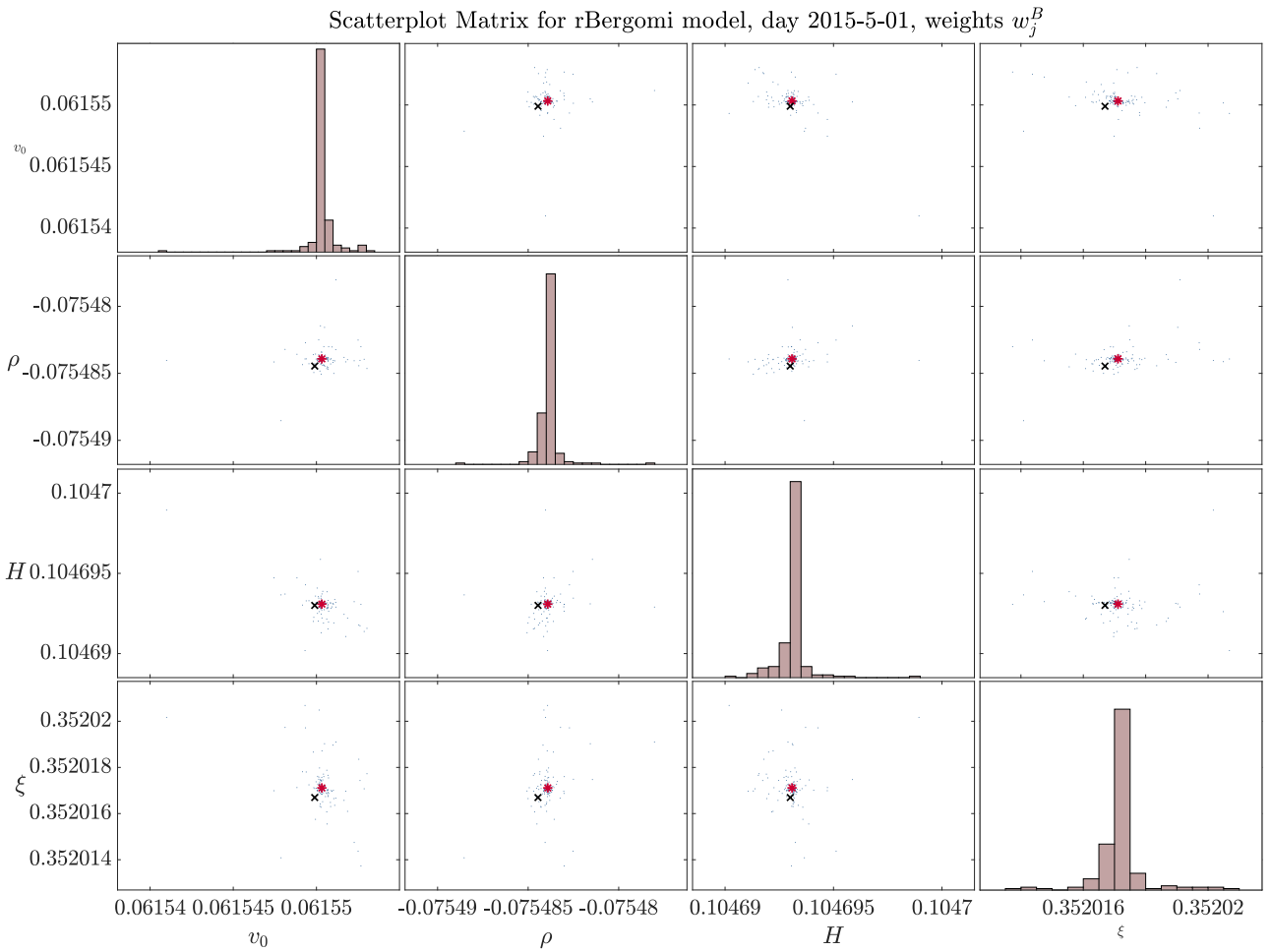
Scatterplot Matrix for rBergomi model, day 2015-5-01, weights w_j^B
v_0
0.06155
0.061545
0.06154
ρ
-0.07548
-0.075485
-0.07549
H
0.1047
0.104695
0.10469
ξ
0.35202
0.352018
0.352016
0.352014
0.06154 0.061545 0.06155
v_0
-0.07549 -0.075485 -0.07548
ρ
0.10469 0.104695 0.1047
H
0.352016 0.35202
ξ

10 RFSV-5-15

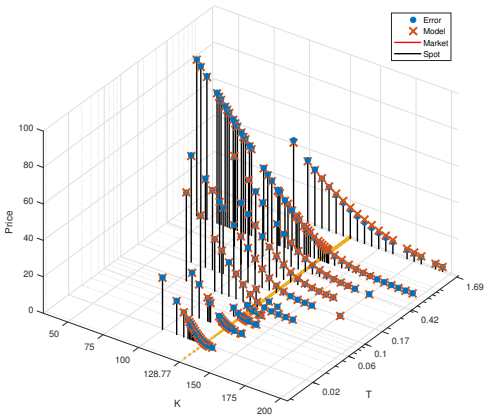
Error
Model
Market
Spot
Price
K
T

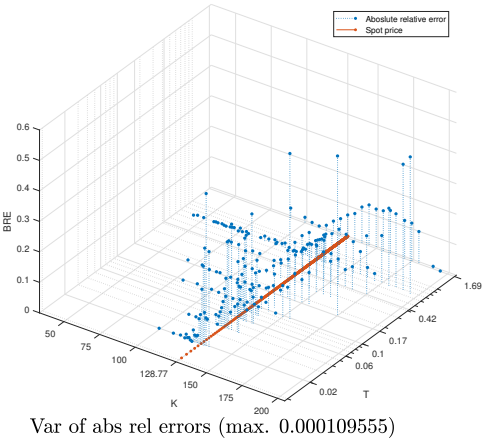
Aboslute relative error
Spot price
BRE
K
T

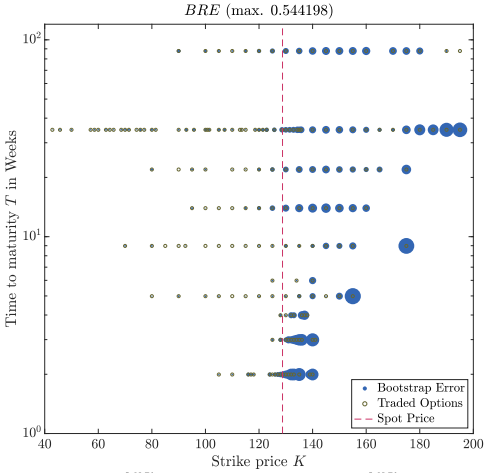
BRE (max. 0.544198)
Bootstrap Error
Traded Options
Spot Price
Time to maturity T in Weeks
Strike price K

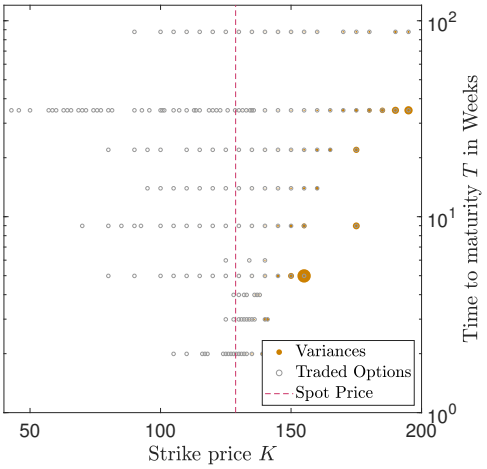
Var of abs rel errors (max. 0.000109555)
Variances
Traded Options
Spot Price
Time to maturity T in Weeks
Strike price K

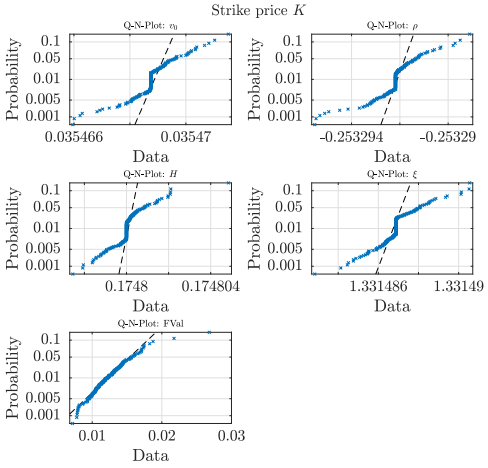
Q-N-Plot: v0
Q-N-Plot: ρ
Q-N-Plot: H
Q-N-Plot: ξ
Q-N-Plot: FVal
Probability
Data

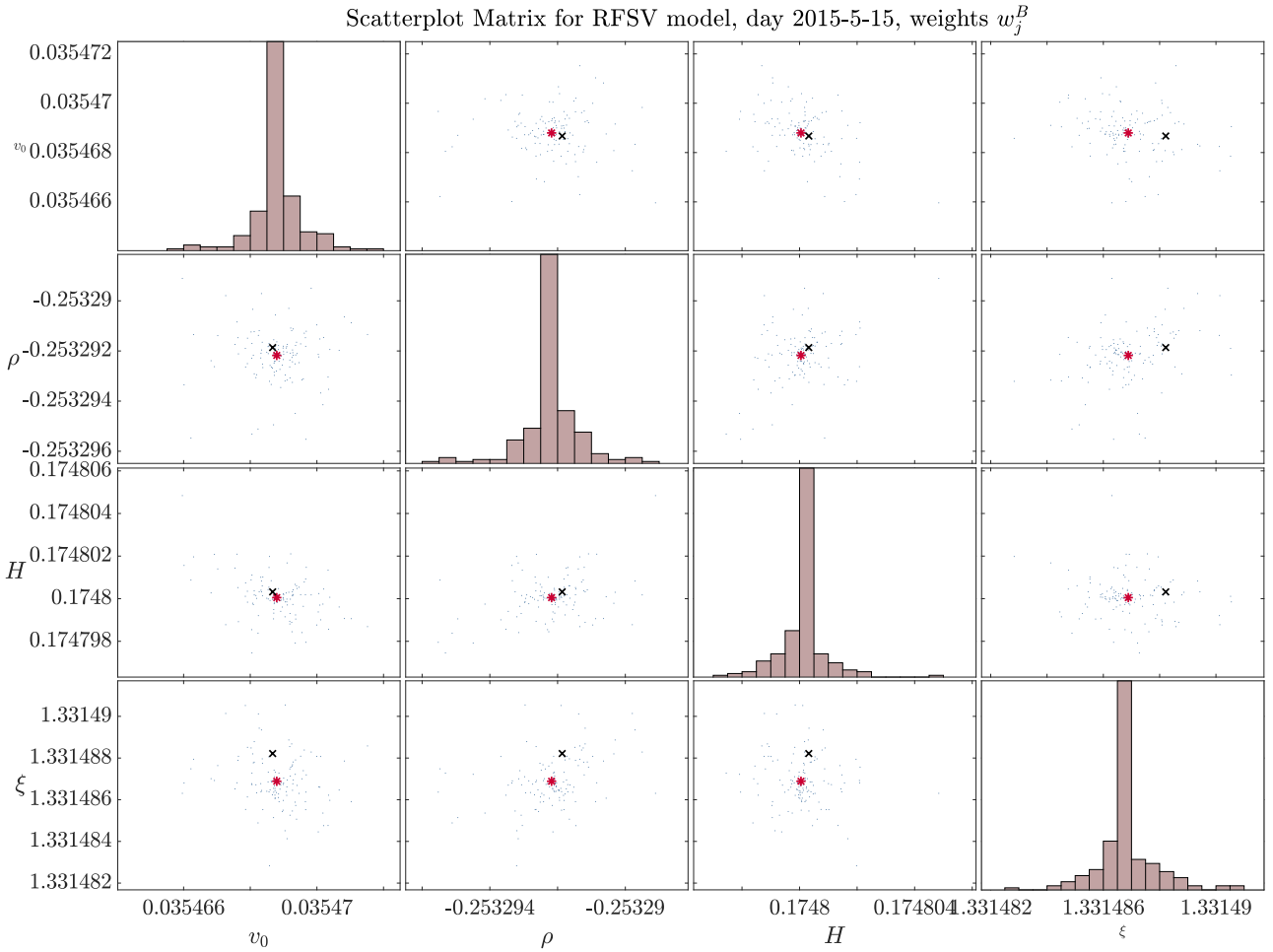
Scatterplot Matrix for RFSV model, day 2015-5-15, weights w_j^B
0.035472
0.03547
v_0 0.035468
0.035466
-0.25329
ρ -0.253292
-0.253294
-0.253296
0.174806
0.174804
H 0.174802
0.1748
0.174798
1.33149
1.331488
ξ 1.331486
1.331484
1.331482
0.035466
0.03547
v_0
-0.253294
-0.25329
ρ
0.1748
0.174804
H
1.331482
1.331486
1.33149
ξ

11 aRFSV-5-15

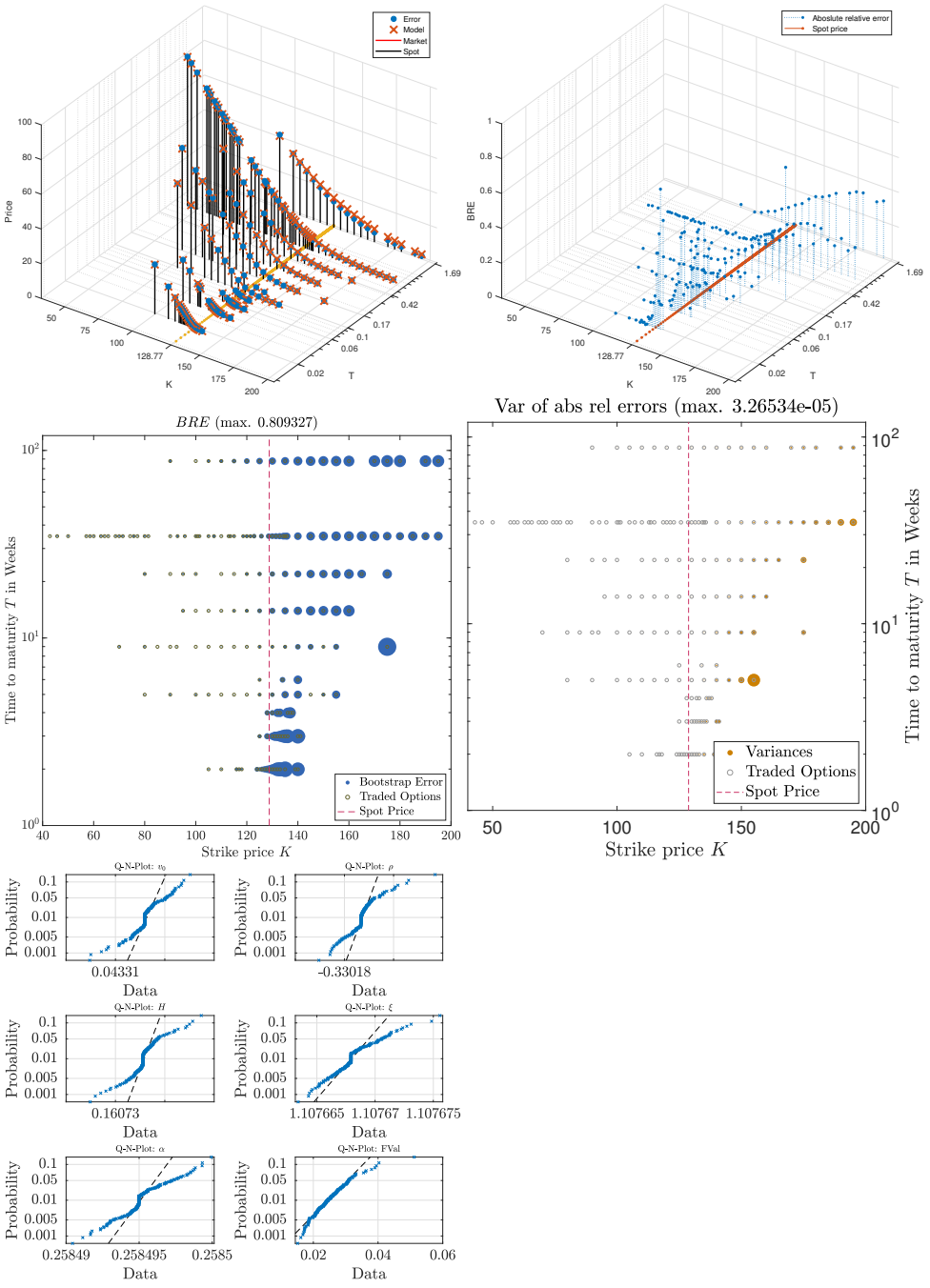
Error
Model
Market
Spot
Price
K
T
Aboslute relative error
Spot price
BRE
Var of abs rel errors (max. 3.26534e-05)
BRE (max. 0.809327)
Time to maturity T in Weeks
Strike price K
Bootstrap Error
Traded Options
Spot Price
Variances
Traded Options
Spot Price
Q-N-Plot: v_0
Q-N-Plot: ρ
Q-N-Plot: H
Q-N-Plot: ξ
Q-N-Plot: α
Q-N-Plot: FVal
Probability
Data
0.04331
-0.33018
0.16073
1.107665 1.10767 1.107675
0.25849 0.258495 0.2585
0.02 0.04 0.06

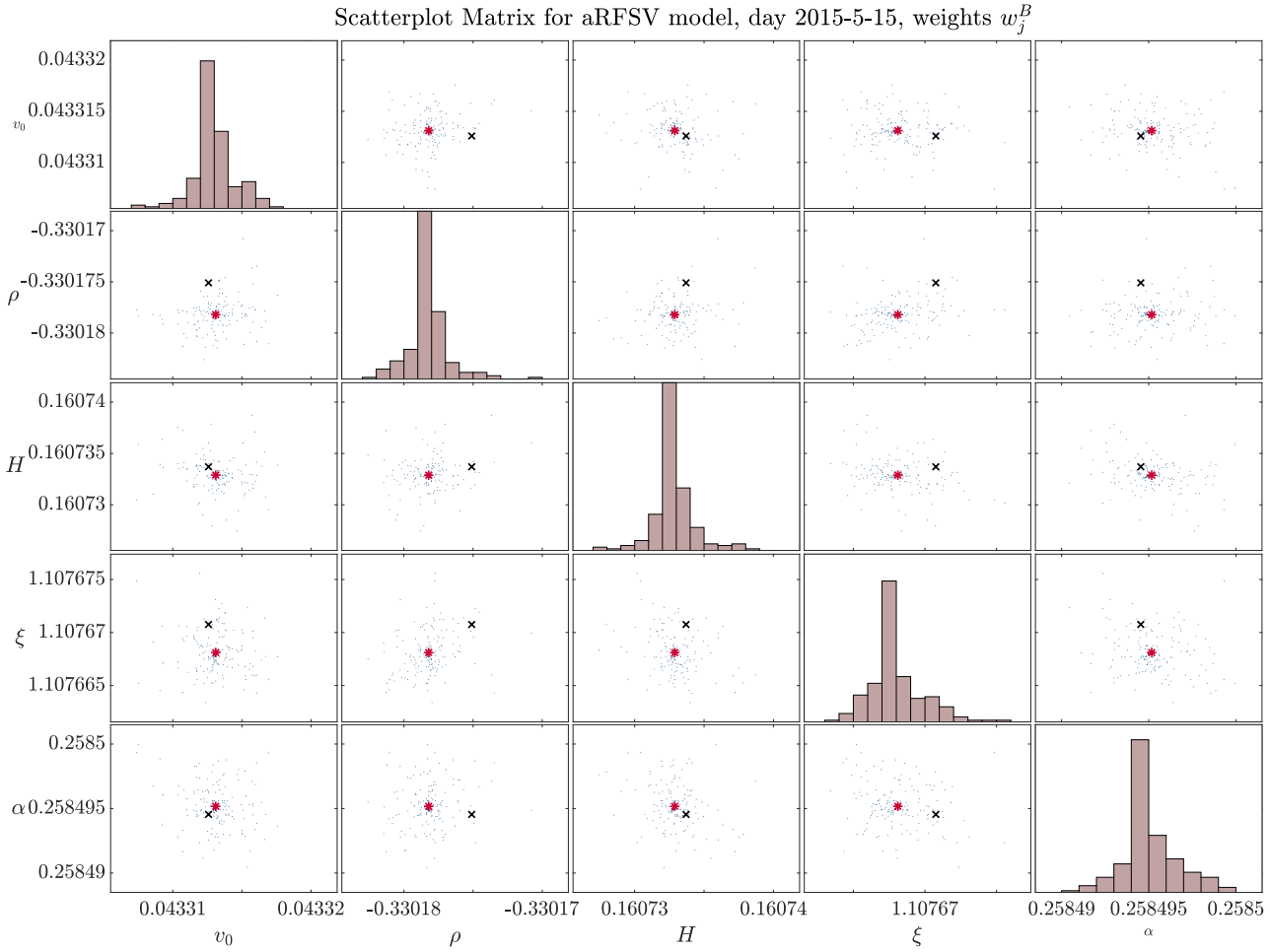
Scatterplot Matrix for aRFSV model, day 2015-5-15, weights w_j^B
v_0
ρ
H
ξ
α
0.04332
0.043315
0.04331
-0.33017
-0.330175
-0.33018
0.16074
0.160735
0.16073
1.107675
1.10767
1.107665
0.2585
0.258495
0.25849
0.04331
0.04332
-0.33018
-0.33017
0.16073
0.16074
1.10767
0.25849
0.258495
0.2585

12 rBergomi-5-15

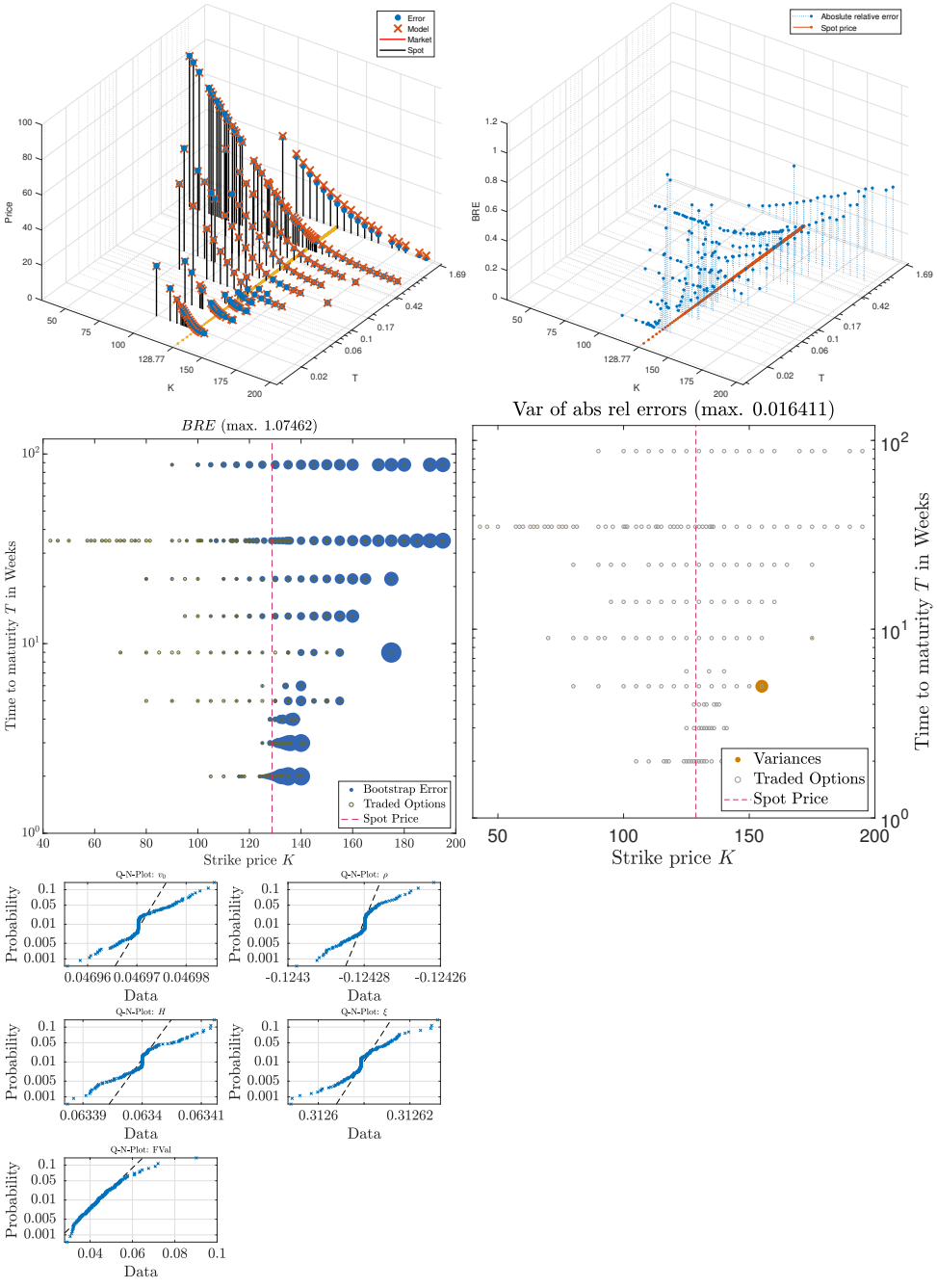

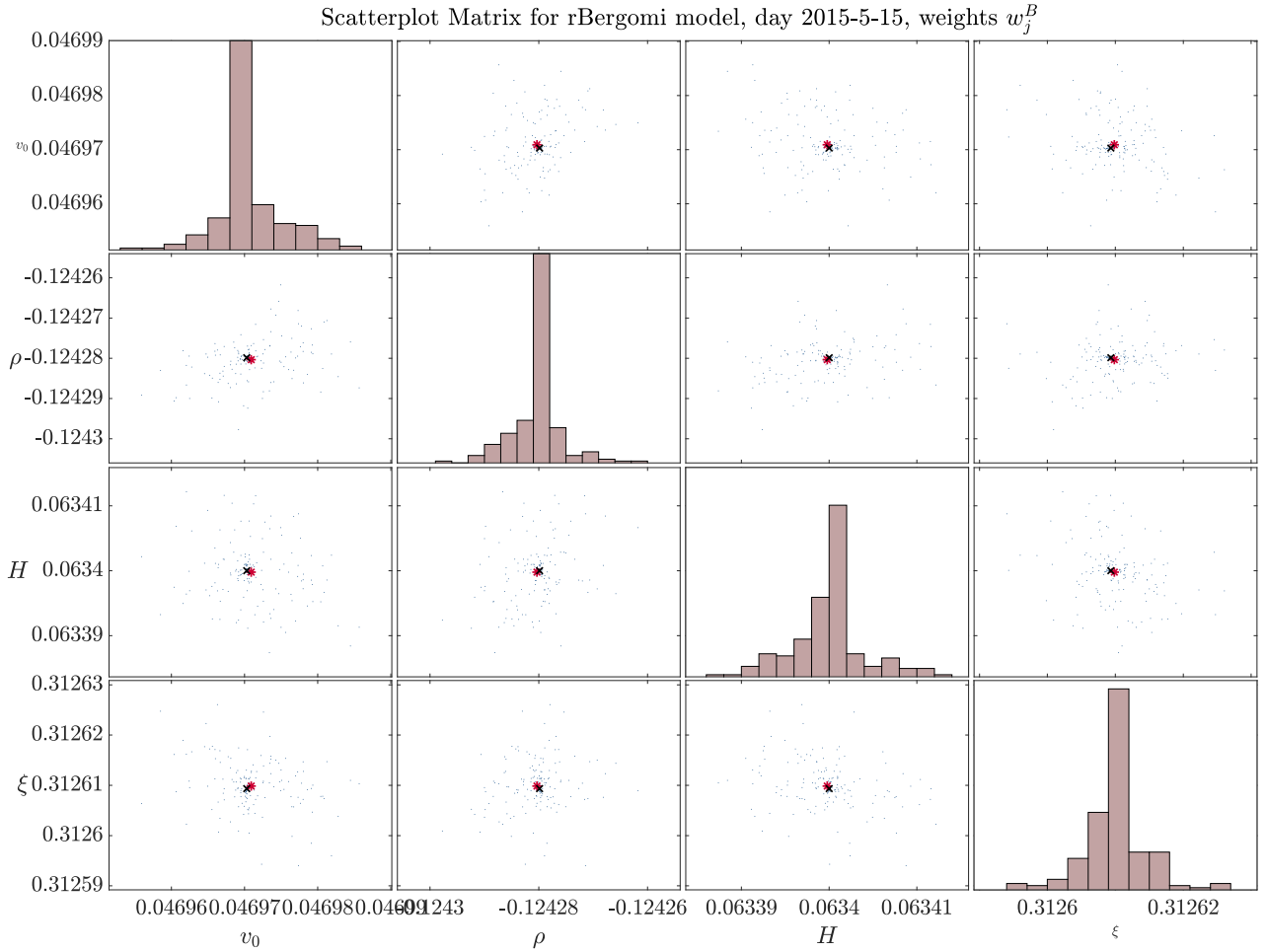
Scatterplot Matrix for rBergomi model, day 2015-5-15, weights w_j^B
0.04699
0.04698
v_0 0.04697
0.04696
-0.12426
-0.12427
ρ -0.12428
-0.12429
-0.1243
0.06341
H 0.0634
0.06339
0.31263
0.31262
ξ 0.31261
0.3126
0.31259
0.04696 0.04697 0.04698 0.04699
-0.1243 -0.12428 -0.12426
0.06339 0.0634 0.06341
0.3126 0.31262
v_0
ρ
H
ξ